UNIVERSITÀ DEGLI STUDI DI MILANO

SCUOLA DI DOTTORATO
TERRA, AMBIENTE E BIODIVERSITÀ

DIPARTIMENTO DI SCIENZE BIOMEDICHE PER LA SALUTE

Dottorato di Ricerca in Scienze Naturalistiche e Ambientali
Ciclo XXVI-BIO/08

NUOVE TECNOLOGIE NELL'AMBITO DELL'ANTROPOLOGIA FISICA E FORENSE:

IMAGING E MODELLAZIONE 3D

Ph.D. Thesis

Daniel Angelo Gaudio
Matricola: R09007

Tutor:
Prof.ssa Cristina Cattaneo

Coordinatore:
Prof. Nicola Saino

Anno Accademico 2012/2013

INDICE

CAPITOLO 1

Introduzione generale

1.1 Antropologia fisica e forense, definizione e prospettive d'indagine.

Quatrefages de *Bréau* (Vallerange, *1810* - Parigi *1892*) fu un naturalista francese che si occupò, tra l'altro, della dentatura dei roditori, dell'anatomia degli anellidi, di molluschi bivalvi e perfino della fecondazione artificiale del pesce. Era un naturalista a tutto campo, uno dei più importanti del diciannovesimo secolo. La ragione per cui egli introduce questa tesi di dottorato è però dovuto al fatto che Quatrefages s'interessò anche alla specie umana, al cui studio dedicò buona parte della sua vita. Egli fece chiamare "cattedra di antropologia" quella di "anatomia e storia naturale dell'Uomo" di cui era titolare; si può dire che la sua fu la prima cattedra ufficiale di antropologia (1855). Definì l'antropologia come "la storia naturale dell'uomo". Tale definizione è sostanzialmente valida anche oggi: secondo l'American Association of Physical Anthropology, l'Antropologia fisica (o biologica) è definibile come "(...) *biological science that deals with the adaptations, variability, and evolution of human beings and their living and fossil relatives. Because it studies human biology in the context of human culture and behavior, physical anthropology is also a social science*." (http://physanth.org/). L'antropologia fisica è una disciplina con più sotto settori: si parla di **paleontologia umana**, o paleoantropologia, per indicare lo studio dell'evoluzione umana: dalle scimmie antropomorfe, alle prime specie umane fino all'unica specie del genere Homo attualmente esistente, l'Homo Sapiens. Con Genetica e **antropologia delle popolazioni** s'intende lo studio delle differenze genetiche nelle popolazioni umane. Si parla di **antropologia fisica applicata all'archeologia** (o osteoarcheologia, o anche bioarcheologia) quando ci si riferisce allo studio dei resti umani rinvenuti in siti e contesti archeologici. L'**antropologia forense**, infine, è l'applicazione dell'antropologia fisica ai casi giudiziari e a quelli riferibili a violazioni dei diritti umani.

L'antropologia forense si occupa, tra l'altro, dell'identificazione di resti umani scheletrizzati, gravemente compromessi dalla putrefazione o comunque non identificabili (Cattaneo, 2004).

Questa tesi di dottorato si occuperà di tematiche e metodiche relative all'antropologia fisica e forense.

In antropologia fisica e forense il complesso degli strumenti "in dotazione" all'antropologo permettono di ottenere un'identificazione generica del soggetto (il suo profilo biologico: sesso, età, statura, etnia) e informazioni circa le patologie di cui il soggetto soffriva. Lo studio di lesività permette di valutare le lesioni perimortem che possono dare indicazioni circa la modalità e la causa di morte. Tali informazioni contribuiscono, in osteoarcheologia, a raccogliere dati circa le caratteristiche, lo stile di vita e lo stato di salute di una popolazione antica. In antropologia forense l'analisi dello scheletro fornisce informazioni fondamentali nelle indagini giudiziarie: l'antropologo, ove possibile, non si limita all'identificazione generica ma fornisce informazioni utili circa l'identificazione personale del soggetto.

Le operazioni preliminari che l'antropologo compie in laboratorio sono il lavaggio delle ossa, il loro restauro (qualora necessario) e quindi lo studio vero e proprio.

Pare opportuno indicare quali sono "gli strumenti" metodologici che l'antropologo utilizza nel corso delle indagini. L'antropologo studia lo scheletro umano sia macroscopicamente sia microscopicamente. Le metodiche macroscopiche prevedono analisi quantitative (si parla di antropometria, da condurre tramite appositi strumenti di misurazione) e qualitative (metodiche antroposcopiche), che si basano prevalentemente sull'osservazione delle ossa. Le analisi microscopiche prevedono l'utilizzo di microscopi ottici, stereo microscopi e microscopi elettronici al fine di valutare caratteri o condurre misure non visibili e praticabili a occhio nudo. Lo studio radiologico permette all'antropologo di visualizzare dettagli intrinseci agli elementi ossei e dentari. Come vedremo tali dettagli possono essere utili sia per ricavare informazioni circa le affezioni delle ossa, sia per raccogliere informazioni generali relative al soggetto a cui appartiene l'osso in esame.

Vi sono infine metodiche biomolecolari che si basano sullo studio delle proteine e, naturalmente, del DNA (Cattaneo 2004). All'enorme sviluppo in questi decenni delle metodiche biomolecolari, grazie alle recenti innovazioni tecniche (PCR, AMS, Proteomica) e le sempre più efficaci metodologie di estrazione del DNA, sono affiancate nuove forme di tecnologia relative agli altri campi dell'antropologia fisica (Kuzminsky, 2012) che, altrettanto velocemente, anche se in maniera meno eclatante, stanno innovando il modo di documentare e d'indagare dell'antropologo.

1.2 Nuovi tipi di tecnologie al servizio dell'antropologo

I metodi di imaging tridimensionale (3D), o diagnostica per immagini tridimensionali, hanno conosciuto un enorme sviluppo in differenti campi negli ultimi decenni; l'antropologia fisica (e forense) è una disciplina che si sta giovando di tale sviluppo sia sul piano documentativo, sia sul piano diagnostico. Negli ultimi anni molti laboratori di antropologia hanno iniziato a costituire partnership con scienziati operanti in altri campi, in particolare quello biomedico, al fine di poter utilizzare tecnologie molto costose (ad esempio Tomografia Assiale Computerizzata (TAC), risonanza magnetica (MRI), terahertz imaging (THz), etc.) (Allam et al., 2011; Buikstra, 2010; Conlogue et al., 2008; Faccia and Williams, 2008; Öhrström et al., 2010; Panagiotopoulou, 2009; Saitou et al., 2011) ma di altissimo potenziale ai fini delle indagini antropologiche.

Il primo tentativo di imaging su materiale "antropologico" risale al 1896 (si trattava di uno studio radiografico su mummie umane; Chhem, 2008) ma è con l'invenzione delle Tomografia Assiale Computerizzata (nel corso degli anni'70) che si ha il passaggio da una dimensione delle RX alle tre dimensioni dei file DICOM, con la conseguente possibilità di una ricostruzione tridimensionale dei reperti anatomici, una migliore visualizzazione delle superfici e l'opportunità di poter condurre analisi accurate anche su corpi non scheletrizzati, difficilmente indagabili se non con metodiche destruenti. Quest'ultima possibilità ha dato un decisivo impulso allo studio dei corpi mummificati permettendo di ottenere ricostruzioni virtuali tridimensionali di ossa, tessuti e organi di qualunque epoca, tanto da divenire prassi in questo tipo di indagini antropologiche.

Tali strumentazioni, essendo fisse, d'altro canto prevedono lo spostamento del materiale d'indagine presso le strutture dotate di tali macchine. L'antropologo non può condurre le indagini in maniera indipendente, essendo legato a un servizio e al personale tecnico "prestato" temporaneamente all'antropologia, ma la cui funzione originale è prettamente clinico/ospedaliera.

L'antropologia può tuttavia attingere ad altre tecnologie, fino a qualche anno fa costosissime, ma che stanno divenendo accessibili grazie all'abbassamento dei costi e delle dimensioni delle strumentazioni, alla crescente facilità d'utilizzo e alla disponibilità di Personal Computer sempre più potenti (in termini di Gigabyte delle schede grafiche, di memoria RAM, di disponibilità di memoria su disco fisso, etc.). Ci si riferisce in particolare alla tecnologia Laser Scanner 3D.

Tale tecnologia si è sviluppata in ambito industriale ma ha trovato applicazioni in numerosissimi campi: dall'architettura al rilievo dei beni artistici, in ambito archeologico e nelle scienze naturali (ad esempio nei rilievi geologici e paleontologici) fino appunto all'antropologia fisica. La scansione laser 3D viene effettuata mediante i Laser Scanners, digitalizzatori ottici che permettono il rilevamento di oggetti e superfici a scale diverse riproducendo dei modelli tridimensionali in

ambiente virtuale (e del cui principio di funzionamento si accennerà nel secondo capitolo). Il prodotto di una scansione condotta con Laser Scanner è una nuvola di punti georeferenziati (dotati quindi delle tre coordinate spaziali x,y,z) che "formano" il reperto scansionato. Il modello 3D può anche essere costituito da una griglia (*mesh*), la quale non è altro che il prodotto dell'unione dei punti, che formano quindi una rete di poligoni. La struttura del modello può dipendere dalla tipologia di Laser usata o dal software di elaborazione scelto, è possibile comunque passare da una nuvola di punti a una mesh (e viceversa) mediante un qualunque software di elaborazione 3D.

La scansione può essere condotta direttamente in sede di scavo, questo permette di documentare le ossa nel loro contesto originale e acquisire tutte le informazioni morfometriche che caratterizza il luogo di giacenza originale. Si avranno in questo caso nuvole di punti composti da milioni di punti, che dovranno essere opportunamente filtrati ed elaborati.

I modelli 3D di reperti ossei sono stati al centro di progetti in ambito paleoantropologici e paleopatologico, dal NESPOS (progetto internazionale di ricostruzione virtuale dei fossili di ominidi), ai progetti "Digitized Diseases" (http://barc.sls.brad.ac.uk/digitiseddiseases/index.php) e "From Cemetery to Clinic" (http://www.barc.brad.ac.uk/FromCemeterytoClinic) e, inoltre, nella digitalizzazione 3D dei reperti ossei della collezione dello Smithsonian Museum. Tra il 2006 e il 2009 la Comunità Europea ha finanziato il progetto EVAN (European Virtual Anthropology Network) con lo scopo di incrementare le metodologie di studio in ambito morfometrico e di varianza anatomica nell'antropologia fisica (Sholts et al., 2011).

Qualunque sia lo strumento utilizzato per scansionare un reperto scheletrico, una volta ottenuto un modello 3D si può procedere, tramite opportune procedure di conversioni di formati, anche alla stampa tridimensionale del reperto. Si tratta della Stereolitografia, una tecnica che permette di realizzare singoli oggetti (in resina, o materiale termoplastico) a partire direttamente da dati digitali (in termini pratici vi è la concreta possibilità di scansionare un reperto a Tokyo, condividere il file tramite Web, e ottenerne una copia in resina a Milano nel giro di poche ore).

Il tema della documentazione e della ripetibilità delle indagini risulta certamente importante in ambito archeologico (e più in generale in ogni ambito scientifico) ma è cruciale nel delicato ambito dell'antropologia forense dove, per essere in linea con i dettami relativi agli accertamenti giudiziari, le indagini devono essere non invasive, ripetibili, non modificabili e il più possibile oggettive (Cattaneo, 2004). Appaiono quindi fondamentali tutte quelle tecniche che permettono la documentazione meno invasiva e meno "distruttiva" possibile dei reperti.

Come si accennava, le innovazioni tecnologiche stanno contribuendo al forte sviluppo metodologico nell'antropologia, e appare scontato che tali innovazioni possono avere risvolti

importanti nei diversi ambiti antropologici; sarebbe tuttavia forviante pensare che esse possano sostituire le metodiche classiche e il giudizio critico dell'operatore. Nell'ottica dell'indagine oggettiva relativa alle potenzialità e ai limiti dell'apporto di tale tecnologie, si fonda l'approccio con cui è stata condotta questa ricerca.

1.3 Scopo della ricerca

Scopo di questa ricerca è quindi quello di indagare le potenzialità e i limiti di nuove tecnologie 3D da utilizzare per la documentazione, l'archiviazione e la diagnostica nell'ambito dell'antropologia fisica e forense.

Verificare inoltre l'effettivo vantaggio dell'informazione che può essere estratta dai dati 3D rispetto alla tipologia di informazioni e documentazione correntemente usata, non tanto per sostituire le metodiche in uso, quanto per integrarle.

La ricerca è stata volta *in primis* a valutare le tecnologie più promettenti in tema di antropologia virtuale; si è sperimentato pertanto l'uso di un Laser Scanner 3D di proprietà del Laboratorio di Antropologia e Odontologia Forense (LabAnOF) del Dipartimento di Morfologia Umana dell'Università di Milano. In base ai risultati ottenuti e agli ambiti di ricerca indagati si è altresì optato per ulteriori strumentazioni non disponibili presso il LabAnOF; sono state quindi condotte collaborazioni con laboratori e strutture dotate della strumentazione utile allo svolgimento di questa ricerca.

Allo scopo di indagare le potenzialità documentative e di archiviazione virtuale 3D è stata acquisita digitalmente la più ampia varietà di materiale antropologico possibile: da reperti ossei sullo scavo, ai singoli elementi scheletrici acquisiti in laboratorio, fino a soggetti viventi. Si è cercato inoltre di studiare le più efficaci modalità "tecniche" di acquisizione per i diversi tipi di materiali e soggetti, verificando le problematiche legate a limiti di scansione in base alle caratteristiche intrinseche del materiale acquisito e al tipo di strumento utilizzato. Sono state valutate quindi le procedure di elaborazione digitale dei modelli ottenuti sia ai fini forensi, sia a quelli osteoarcheologici. Sono stati infine studiati e applicati numerosi software per l'elaborazione digitale, ricercando inoltre i formati digitali più idonei all'archiviazione dei dati al loro trasferimento su più programmi.

Sono state poi selezionate alcune problematiche di antropologia fisica e forense che da un lato necessitano di miglioramento metodologico e diagnostico, da ricercare anche mediante l'utilizzo delle nuove tecniche d'acquisizione e modellazione tridimensionale, dall'altro che rispondono alle concrete esigenze investigative di un laboratorio di Antropologia Forense impegnato nella soluzione di casi di natura giudiziaria.

La **documentazione, acquisizione e archiviazione dei dati tridimensionali**, ha reso possibile, tramite l'utilizzo delle tecnologie 3D, un'indagine relativa alla diagnosi d'età e alla ricostruzione facciale, argomenti che rientrano, in antropologia, nella **stesura del profilo biologico**. L'uso del modello 3D è stato applicato alla tecnica di sovrapposizione cranio-facciale (che rientra nei metodi d'**identificazione personale).**

Si è inoltre affrontato il tema della **lesività scheletrica,** verificando la capacità documentativa e diagnostica delle lesioni antemortem (calli ossei) e della lesività perimortem mediante metodologie di esplorazione e ricostruzione delle lesioni in ambiente virtuale.

1.4 Campi d'applicazione

1.4.1 Documentazione, profilo biologico, identificazione.

Una delle operazioni fondamentali nell'indagine antropologica è la documentazione dei reperti che si stanno indagando. Fondamentale nell'ambito archeologico, sia in sede di scavo, per l'appropriata documentazione dello stesso, sia dei singoli reperti poiché una volta studiati solitamente sono archiviati e/o restituiti al committente dello studio. Il materiale oggetto di indagine deve quindi essere ben documentato sia per offrire un efficace supporto alla relazione antropologica, sia perché potrebbe non essere più a disposizione dell'operatore una volta concluso lo studio. In ambito forense, oltre alle motivazioni appena esposte, l'adeguata documentazione è cruciale poiché, se non condotta sotto il corretto profilo giudiziario, può non solo inficiare l'indagine ma anche un intero processo (Cattaneo, 2004).

L'avvento della fotografia digitale ha rivoluzionato il mondo del rilievo fotografico, rendendo possibile la produzione di enormi quantità di fotografie ad alta risoluzione scaricabili su un qualunque disco, fisso o removibile, a sua volta sempre più capiente. Erano solo i primi anni novanta quando i modelli di fotocamera digitale più all'avanguardia raggiungevano la risoluzione di 1,5 MP (MegaPixel). Un modello della Kodak (DCS200) con tali caratteristiche costava circa 10.000 dollari (Reis, 2008).

Oggi per meno di 30 euro ognuno di noi può acquistare una fotocamera digitale a 3 MP. Un laboratorio può investire circa 100 euro per comprare una fotocamera da 12 MP, dotata di funzione "Macro", che permette di fotografare oggetti a pochi centimetri di distanza dall'obiettivo (ideale per ritrarre i dettagli), ottenendo immagini di qualità impensabile fino a pochi anni fa.

Le fotografie e il rilievo fotografico in genere hanno tuttavia delle difettosità "intrinseche":

- Bidimensionalità: una fotografia rappresenta quanto catturato su un asse X e un asse Y. Questa caratteristica rappresenta il principale limite; una foto non consente di discernere perfettamente i livelli di profondità di un dettaglio (ad esempio di una lesione).
- Difficoltà nel legare il generale al particolare: in altri termini se una foto a forte ingrandimento rende bene i particolari, il particolare perde parzialmente la sua collocazione nel contesto generale (principio di indeterminazione).
- Impossibilità di misurazione: una foto bidimensionale non consente la misura tra due punti, ma solo la "stima" in base all'inserimento nel campo fotografico di un repere metrico di riferimento (il classico righello o meglio la scala ABFO).

Tali difettosità intrinseche delle immagini 2D rendono ragione della differenza tra visione diretta e resa fotografica, infatti il nostro occhio è strutturato per la visione tridimensionale e i livelli di profondità contribuiscono in modo fondamentale alla definizione della visione.

Il contributo della tecnologia 3D alla documentazione volge appunto al superamento di questi limiti. Il processo di digitalizzazione di un oggetto fisico per l'analisi o la rimodellazione computerizzata di superfici geometriche, mediante apposite attrezzature e rielaborazioni, si sviluppa in **due fasi:** la prima è denominata **fase di acquisizione dei dati**; la seconda è la fase di elaborazione degli stessi.

I sensori tridimensionali (Laser Scanner) sono strumenti che permettono di generare un'immagine 3D dell'oggetto che inquadrano. A differenza della tradizionale fotografia, sono in grado di descrivere l'oggetto rilevato nelle sue tre dimensioni spaziali riuscendone a restituire una misura oggettivizzata. In generale, si distinguono due principali famiglie di scanner: i *ranging scanners* (*scanner* a misura diretta dalle distanza, tra cui quelli a tempo di volo) ed i *triangulation scanners* (*scanner* a triangolazione). Nei primi, la posizione dell'emettitore *laser* e del ricevitore coincidono. Nei secondi, emettitore e ricevitore sono separati da una distanza nota a priori (*base line*) sulla quale si basa il principio della triangolazione. Possono acquisire la superficie esterna della scena e dell'oggetto, ma non possono penetrare sotto le superfici. (Sgrenzaroli 2013).

La tomografia assiale computerizzata, nata dall'esigenza di indagare le strutture interne di un elemento anatomico, restituisce anch'essa un modello tridimensionale dell'oggetto acquisito. **Un modello 3D è una rappresentazione digitale, fedele e misurabile, dell'oggetto in esame**, ottenuta mediante la rappresentazione esplicita delle sue caratteristiche morfometriche.

Alcuni autori hanno confrontato metodi diversi per la produzione di modelli tridimensionali e valutato l'accuratezza nelle misure condotte sui modelli ottenuti. Fourie (2011) ha testato l'accuratezza del Laser Scanner Minolta Vivid 900 rispetto a una Tac Cone Beam, scansionando dei volti e rilevando l'estrema accuratezza (sub millimetrica) di entrambi gli strumenti.

Il presente studio ha altresì indagato i vantaggi e gli svantaggi dell'utilizzo del Laser Scanner rispetto alle TAC di nuova generazione (in particolare CBCT e pQCT) nel tentativo di individuare lo strumento più adatto da utilizzare in relazione alle caratteristiche del reperto, al tipo di documentazione da condurre, e all'obiettivo della documentazione stessa.

All'acquisizione del modello, come si diceva, segue una fase di elaborazione del dato 3D tramite appositi software; l'elaborazione prevede l'importazione del dato 3D all'interno del software, eventualmente il filtraggio dei dati ridondanti (rumore), l'editing dei dati, il mashing (l'eventuale creazione di una rete poligonale dei dati), e infine l'esportazione del dato 3D attraverso la conversione nel formato che si ritiene più idoneo.

Nel presente studio si è verificato la capacità documentativa di un Laser Scanner a tempo di volo nel documentare uno scavo archeologico, in particolare una fossa comune risalente alla Grande Guerra **(Capitolo 2)**.

Spostandosi dallo scavo al laboratorio si è testata la riproducibilità di superfici articolari di sinfisi pubiche e superfici auricolari dell'ileo, acquisite con tre differenti laser scanners a triangolazione ottica (adatti quindi a reperti di piccolo e medie dimensioni) **(Capitolo 3).**

In conseguenza dell'ottenimento di un modello tridimensionale è possibile procedere in diversi ambiti dell'antropologia fisica e forense, nel corso di questo studio si è indagato in particolare:

- La stesura del profilo biologico: consiste nella raccolta, da parte dell'antropologo, di tutti i dati informativi che possono essere desunti dallo studio dei resti scheletrici relativamente al sesso, l'età, la razza, la statura e, eventualmente, le possibili caratteristiche fisiognomiche del soggetto. In ambito osteoarcheologico la stesura del profilo biologico permette non solo la raccolta dei caratteri di uno scheletro ma anche di raccogliere informazioni utili a definire la struttura biodemografica della popolazione antica cui appartiene (Canci 2005). In ambito forense la stesura del profilo biologico di un soggetto può circoscrivere la cerchia dei "sospetti d'identità" nel caso di un individuo non identificato, oppure avvalorare o smentire l'ipotesi identificativa su un soggetto rinvenuto in un contesto critico (si pensi ad esempio a un soggetto carbonizzato in auto). Il profilo biologico risulta inoltre fondamentale per distinguere persone diverse in contesti di ossa commiste (Adams and Byrd 2006) e nei disastri di massa.

In particolare è stata condotto uno studio circa l'utilizzo dell'imaging 3D per la **diagnosi** d'età a partire dall'estrazione di volumi dentari **(capitolo 8.1)**: la valutazione dell'età biologica è una disciplina in continua evoluzione che trova le sue principali applicazioni in ambito clinico (diagnosi, prognosi e terapia auxologiche e odontoiatriche) e in ambito forense relativamente alla stima dell'età cronologica a essa correlata sia su cadaveri sia su viventi.

Ci si è inoltre rivolti al tema della **ricostruzione facciale (capitolo 8.2)**, anch'esso rientrante nella ricostruzione del profilo biologico. La ricostruzione facciale è l'operazione di riproduzione di un volto a partire da un cranio. Nel corso di questa ricerca si è valutato l'utilizzo del Laser Scanner 3D rispetto alla TAC tradizionale nell'acquisizione di crani sui cui condurre la ricostruzione facciale; si è inoltre operata la ricostruzione facciale utilizzando un nuovo software per la ricostruzione facciale (AFA 3D TIVMI) che opera applicando automaticamente un numero molto elevato di spessori tissutali (78), con origine in altrettanti punti craniometrici, ottenuti mediante una ricerca di valori tissutali condotti su una vastissima popolazione europea (500 individui).

Ci si è poi rivolti a un particolare e delicato ambito dell'antropologia, quello dell'**identificazione personale**. Accertare l'identità da cadaveri o resti umani o resti scheletrici consiste nel riconoscere i caratteri individuali che differenziano inconfondibilmente un determinato individuo da qualsiasi altro individuo (Cattaneo 2004). È un argomento che inserito nelle ricerche antropologiche riguarda prevalentemente (ma non esclusivamente) l'antropologia forense. L'identificazione personale, per definirsi tale, viene basata sulla cosiddetta "physical evidence", che si può ottenere attraverso indagini genetiche, dattiloscopiche, odontologiche e osteologiche. Vi possono essere casi in cui le tecniche più diffuse d'identificazione non possono essere condotte: si pensi ad esempio al rinvenimento di resti umani di immigrati, di cui non si ha notizia di parenti (cosa che purtroppo accade spesso) e in cui non è possibile avere confronti digitali per compromissione dei polpastrelli a causa dei fenomeni decompositivi. Si devono allora utilizzare altri metodi d'identificazione. Le tecniche osteologiche prevedono l'utilizzo di confronti radiografici dei dati ante/post-mortem, è pertanto necessario poter disporre di documentazione radiografica del soggetto in vita. Oltre alla difficoltà di reperimento del materiale radiografico, l'identificazione osteologica è difficilmente quantificabile (al contrario di quella dattiloscopica e genetica) e in letteratura vi è ancora un certo dibattito su come considerare un carattere o forma unica e specifica.
In assenza di altre opzioni rimane un'ultima tecnica, la **sovrapposizione cranio facciale**. A patto di possedere una qualunque immagine del soggetto in vita.
Tale metodica confronta la morfologia del cranio con la foto del volto di un soggetto scomparso, valutandone la corrispondenza secondo specifici caratteri. Si è condotto uno studio **(capitolo 4)** per valutare i vantaggi e l'affidabilità della tecnica a partire da un modello 3D ottenuto da un cranio scansionato con Laser Scanner.

1.4.2 Lesività scheletrica

Particolare importanza assume la possibilità di documentare lesioni, anche sub millimetriche, presenti nel tessuto osseo. Attraverso le tecniche d'acquisizione tridimensionale delle lesioni, la "documentazione" può divenire metodo che consente "l'esplorazione" delle stesse, e avere, in altre parole, valenze diagnostiche. Sono stati condotti studi relativamente alle lesioni perimortem e antemortem.

- Lesività perimortem

Di particolare importanza, in antropologia forense, sono le lesioni perimortem, cioè quelle lesioni che hanno causato la morte del soggetto o sono dovute a un trauma verificatosi immediatamente prima o dopo la morte del soggetto.

A seconda della modalità traumatica si distingue principalmente (si riporta qui solo la lesività che interessa la presente ricerca) una lesività da arma bianca, da arma da fuoco, contusiva e lacero-contusiva.

Lesività da arma bianca (Cattaneo, 2004; Arbarelo,1999): a seconda del tipo di arma bianca avremo differenti tipi di lesione:

- lesioni da punta: nell'osso e nella cartilagine, data la poca elasticità di questi tessuti, sono caratterizzate da fori, a fondo cieco o trapassanti, che conservano la forma e le dimensioni della punta feritrice.

- lesioni da taglio: raramente sono penetranti (interessano prevalentemente parti molli); si possono però avere intaccature delle ossa, di regola superficiali ma talora anche resecanti. Quando il filo della lama scorre sull'osso produce fessurazioni che si presentano con conformazione a V; agli estremi della lesione possiamo rinvenire le cosiddette "codette", segni prodotti dal filo della lama che via via si riporta verso la superficie.

- lesioni da punta e taglio: ferite di questo tipo vengono generate quando la lama presenta un estremo acuminato e uno o più spigoli affilati taglienti; variano di aspetto a seconda che la lama sia monotagliente, bitagliente, tritagliente o tetratagliente.

Le ferite d'arma da taglio, e in particolare da coltello, sono fra le più frequenti cause di morte nei casi di omicidio (Martin 1999).Gli studi qui presentati **(capitoli 5 e 6**) si sono in particolare focalizzati alla documentazione e analisi di questo tipo di lesività.

- Lesività antemortem

Quando un trauma genera lesioni dell'osso sulla persona in vita, provocando una frattura parziale o totale dell'osso stesso ma non la morte dell'individuo, il processo di guarigione comporta la formazione di un callo osseo che è conseguenza di una risposta di tipo proliferativo da parte dell'osso leso; in seguito avviene il rimodellamento e l'arrotondamento con formazione di osso lamellare nel tratto danneggiato. Il callo osseo costituisce la fase ultima del processo di guarigione di una frattura, con la fusione dei due monconi ossei dovuta alla deposizione di osso neoformato. La guarigione può essere completa o, a seconda del trauma subito, portare a una menomazione residua del segmento scheletrico.

In antropologia fisica riconoscere lesioni *ante mortem* e individuarne le caratteristiche può fornire informazioni utili circa l'occupazione e gli stress meccanici a cui l'individuo era sottoposto. In ambito forense la possibilità di avere più informazioni circa l'epoca di cagione e lo stadio di guarigione di una frattura può supportare le indagini identificative. Se un incremento delle informazioni utili alla datazione dei calli ossei può essere ricavato dalle nuove tecnologie digitali viene indagato e discusso nel **capitolo 7.**

Bibliografia

- http://www.barc.brad.ac.uk/FromCemeterytoClinic.
- http://barc.sls.brad.ac.uk/digitiseddiseases/index.php.
- http://physanth.org
- Adams BJ, Byrd JE, (2006). Resolution of small-scale commingling: A case report from the Vietnam War', *Forensic Science International*, **156**, 63-69.
- Allam AH, Thompson RC, Wann LS, Miyamoto MI, el-Halim Nur el-Din A, el-Maksoud GA, Al-Tohamy Soliman M, Badr I, el-Rahman Amer HA, Sutherland ML, Sutherland JD, Thomas GS, (2011). Atherosclerosis in ancient Egyptian mummies: the Horus study. *Journal of the American College of Cardiology* **4**: 315-327.
- Arbarelo P, (1999). Compendio di medicina legale, Minerva Medica, Torino.
- Buikstra, JE, (2010). Paleopathology: a contemporary perspective. In: Larsen, C.S.n A Companion to Biological Anthropology. Wiley-Blackwell, Chinchester.
- Canci A, Minozzi S, (2006). Archeologia dei resti umani. Carocci, Roma.
- Cattaneo C, Grandi M,(2004). Antropologia e Odontologia Forense. Guida allo studio dei resti umani. Testo atlante. Monduzzi Editore, Bologna.
- Chhem RK, (2008). Paleoradiology: History and New Developments. In: Brothwell R, Chhem RK, Paleoradiology, Springer-Verlag Berlin, Heidelberg.
- Conlogue G, Beckett R, Bailey Y, Posh J, Henderson D, Double G, King, T, (2008). Paleoimaging: the use of radiography, magnetic resonance, and endoscopy to examine mummified remains. *Journal of Radiology Nursing* **27**: 5-13.
- Faccia KJ, Williams RC, (2008). Schmorl's nodes: clinical significance and implications for the bioarchaeological record. *International Journal of Osteoarchaeology* **18**: 28-44.
- Fourie Z, Damstra J, Gerrits PO, Ren Y, (2011). Evaluation of anthropometric accuracy and reliability using different three-dimensional scanning systems.
- *Forensic Science International* **207**: 127–134
- Martin JR, (1999). Identifying Osseous Cut Mark Morphology for Common Serrated Knives. Thesis presented for the Master of Art degree, Department of Anthropology, University of Tennessee Knoxville

- Kuzminsky SC, Gardiner MS, (2012). Three-dimensional laser scanning: potential uses for museum conservation and scientific research. *Journal of Archaeological Science* **39**: 2744-2751.
- Öhrström L, Bitzer A, Walther M, Rühli FJ, (2010). Technical note: terahertz imaging of ancient mummies and bone. *American Journal of Physical Anthropology* **142:** 497-500.
- Panagiotopoulou O, (2009). Finite element analysis (FEA): applying an engineering method to functional morphology in anthropology and human biology. *Annals of Human Biology* **36**: 609-623.
- Quatrehomme G., Iscan MY (1999). Characteristics of gunshot wounds in the skull. *Journal of Forensic Science* **44**: 568-576.
- Reis G., (2007). Analisi Forense con Photoshop. Apogeo, Lavis (Trento).
- Saitou N, Kimura R, Fukase H, Yogi A, Murayama S, Ishida H, (2011). Advanced CT images reveal nonmetric cranial variations in living humans. *Anthropological Science* **119**: 231-237.
- Sgrenzaroli M, Vassena G, Galassi A, Gaudio D, Martini P, (2013). La rappresentazione della scena del crimine: dalla descrizione narrativa ai rilievi tridimensionali. In: Curtotti D, Saravo L, Manuale delle investigazioni sulla scena del crimine. Giappichelli Editore, Torino.
- Sholts SB, Flores L, Walker PL, Warmlander SKTS, (2011). Comparison of Coordinate Measurement Precision of Different Landmark Types on Human Crania Using a 3D Laser Scanner and a 3D Digitiser: Implications for Applications of Digital Morphometrics. *International Journal of Osteoarchaeology*. **21(5):**535-43.

CAPITOLO 2

Excavation and study of skeletal remains from a World War I Mass Grave.

Gaudio D, Betto A, Vanin S, De Guio A, Galassi A, Cattaneo C.

Article first published online: 8 AUG 2013

DOI: 10.1002/oa.2333

International Journal of Osteoarchaeology
Int. J. Osteoarchaeol. (2013)
Published online in Wiley Online Library
(wileyonlinelibrary.com) DOI: 10.1002/oa.2333

SHORT REPORT

Excavation and Study of Skeletal Remains from a World War I Mass Grave

D. GAUDIO,[a,b]* A. BETTO,[c] S. VANIN,[d] A. DE GUIO,[c] A. GALASSI[b] AND **C. CATTANEO[a]**

[a] *LABANOF, Laboratorio di Antropologia e Odontologia Forense Sezione di Medicina Legale e delle Assicurazioni DMU–Dipartimento di Morfologia Umana e Scienze Biomediche, Università degli Studi di Milano, Italy*

[b] *U.O.S di Medicina Legale, ULSS N. 6 Ospedale Civile San Bortolo, Vicenza, Italy*

[c] *Dipartimento di Archeologia, Università Di Padova, Italy*

[d] *Department of Chemical and Biological Sciences, School of Applied Sciences, University of Huddersfield, UK*

ABSTRACT This study presents the excavation and multidisciplinary analysis of seven skeletons recovered in a World War I Mass Grave on the mountains of the Veneto Region, Italy. While it is not a rare phenomenon to these mountainous areas involved in the First Conflict, it is exceptional, on these mountains, to find a mass grave with soldiers in primary burials. Stratigraphic excavation was the mean used for recovery, along with 3D laser scanning documentation. Every skeleton but one was found complete and in anatomical connection. Four soldiers lay in the prone position; two subjects were lying on their side. Identification of the nationality was performed for two of the subjects, who both of whom had personal effects such as a badge for military vaccinations and religious medals. What remained of their uniforms gave clues about their Italian nationality. The entomological analysis conducted on fly puparia discovered close to the bones revealed that the bodies had not been buried immediately.

The skeletons were biologically profiled by sex, age, height and ancestry. An accurate study of pathology and stress markers was carried on, as well as on skeletal trauma in order to establish the type of trauma and ammunition involved. The remains belonged altogether to seven Italian male soldiers ages between 18 and 35. Various kinds of stress markers revealed occupational (enthesopathies) and metabolic stress: several signs of cribra cranii and of cribra orbitalia were registered. The study of the injuries revealed a surprising variety of types of lesions, mostly lethal: a few subjects were struck by a shrapnel grenade; one soldier was killed by a grenade explosion. Two of the soldiers were probably executed, instead: this conclusion reached on the basis of gunshot holes (9 mm) in their skulls, and by the position of the injuries. Copyright © 2013 John Wiley & Sons, Ltd.

Key words: Archaeology of War; Laser Scanner; Mass Grave; Physical Anthropology

Introduction

The study presents the excavation and the multidisciplinary analysis of seven skeletons recovered in a World War I Mass Grave on the mountains of the Veneto Region (Site of Soglio Melegnon di Arsiero, Vicenza, Italy). Although the finding of skeletal remains from to World War I is not such a rare phenomenon on the mountainous areas which had been involved in the First Conflict, it is rather exceptional to find a mass grave with soldiers in primary burials. In Europe, a limited number of archaeological excavations involving skeletal remains of fallen soldiers during the Great War have been conducted in recent years (Jacques, 1997; Desfossès *et al.*, 2003; Fraser, 2005). In Italy, however, these kinds of archaeological excavations were not conducted until 2006. Furthermore, anthropological studies regarding skeletal remains of soldiers fallen during WWI are very rare in the scientific literature (Jankauskas and Palubeckaitė-Miliauskienė, 2007; Jankauskas *et al.*, 2007; Jankauskas *et al.*, 2011).

This study is part of a three year project financed by the province of Vicenza (2006–2009) to improve the recovery and the analysis of fallen soldiers of World War I. Before this project, remains were recovered

* Correspondence to: Dott. Daniel Gaudio-LABANOF, Laboratorio di Antropologia ed Odontologia Forense, Sezione di Medicina Legale Dipartimento di Scienze Biomediche per la Salute, Università degli Studi di Milano, V. Mangiagalli 37, Milan, Italy.
e-mail: daniel.gaudio@unimi.it

Received 26 March 2013
Revised 30 June 2013
Accepted 14 July 2013

without any scientific method or protocols and put into ossuaries, easily mixing different individuals, in absolute anonymity.

The project was conducted during the years 2006–2009 through the direct recovery of remains through archaeological diggings. More than 40 skeletons were recovered, and pathologies and injuries typical of troopers were found (Gaudio *et al.*, 2009). Regarding this case, recovery and anthropological studies were commissioned by judicial authorities, following hikers' reports of visible bones on the ground. The emergence of bones was probably due to the effects of a clandestine excavation conducted by collector in search of object dating from WWI.

The site where the mass grave was found is in Veneto region of Italy. Veneto Mountains became a site of critical battles during 1916, as the Austro-Hungarian army tried to break through the Pianura Padana (also known as 'Strafexpedition'). The Italian army fought to restore the 'Sette Comuni' uplands, and along the Coni Zugna-Pasubio line. The mass grave is located on the Tonezza Upland: this territory, hardly contended during May 1916, became the last bastion to prevent the Imperial Army from conquering the plains around the city of Vicenza.

Skeletal remains were recovered where an Italian battalion of 87 B cannons had been placed. That battalion suffered several attacks by the third corps of the Austro-Hungarian troops. While the results of this battle were not well noted in official records, anthropological and archaeological science provided previously unknown information and details of this war episode.

Materials and methods

The remains were retrieved through stratigraphic excavation. Moreover the grave was documented by 3D scanning, by means of Laser Scanner Photon 20 which detects all of the points of incidence of the laser beam in a sphere having a diameter of 40 m; therefore, the entire grave was recorded by means of one scan. The 3D Laser Scanner is also equipped with a camera (Nikon D 200, fish-eye lens) that performs twelve o'clock poses according to a round angle horizontally, allowing a 'mapping' at 360° of the scenario. It is then possible to apply colour and texture to the cloud of points of the photographic mapping, obtaining a 3D colored scan (Figure 1).

Even though skeletal remains were retrieved by archaeological methods they were extremely broken and fragile, due to the environment in which they were buried.

Bone fragility can be explained by biological (i.e. plants, roots, fungi, bacteria and moulds), chemical (i.e. ground acidity, precipitates, etc) and physical factors (ground frost/defrost). For this reason, bones were restored assembling skeletal fragments, and total reconstruction was achieved in some areas (particularly skulls).

Subsequently, a biological profile of every individual was drawn up, by identifying sex, height and age.

Sex was determined on the basis of morphological criteria (morphology of pelvis and cranium, Bass, 1987; Ubelaker, 1999) and metrical criteria (maximum diameters of the heads of femur, humerus and radius, Ubelaker, 1999); stature by Trotter and Gleser (1977) and Simmons' formulae (Simmons *et al.*, 1990). Age was determined by the evaluation of union of epiphyses of long bones (Black and Scheuer, 2000), morphology of the pubic symphysis (Brooks and Suchey, 1990), auricular surface (Lovejoy *et al.*, 1985) and on the teeth, whenever possible, by means of Mincer *et al.* (1993) and Lamendin *et al.* (1992) aging methods.

A study of pathologies of the skeletons was conducted in order to recognize, describe and analyse effects of any disease and trauma 'registered' in the bones.

In the present study, the following pathologies were classified: degenerative pathologies (due to occupational stress and similar causes); dental pathologies, infections, stress markers due to metabolic problems or to nutritional deficiencies and antemortem trauma effects.

The analysis of lesions was particularly focused on the distinction between *perimortem* and *postmortem* lesions, moreover, the recognition of injuries due to war weapons.

To distinguish *peri-* and *post*mortem lesions, the following criteria were used: analysis of the colour of the fracture rims; signs of elasticity on the rims themselves and morphology of rims (surface, angle, etc.) (Wieberg and Wescott, 2008). Injury mechanism, strictly connected to the war context, was subdivided into the following categories: primary blast injury, secondary blast injury, gunfire injury, resulting from light artillery (Kimmerle and Baraybar, 2008).

Finally, the grave soil was examined with the aim to recover any entomological element of possible relevance to this investigation. This search was performed with a Leica M60 stereomicroscope.

Results

The goal was to recover what was still in situ of the skeletal remains and the personal effects of the soldiers and investigate the archaeological context of the deposition. The remains were buried near a tabular area

Figure 1. Graphic rendering of the mass grave (individuals: A = GM 19; B = GM 14; C = GM 18; D = GM 17; E = GM 16; F = GM 20; G = GM 15; 10 = SU 10: bedrock; 4 = SU 4: layer of clay soil; −5 = SU −5: cut for the excavation of the pit). On the left mosaic of ortho-photos of the mass grave at the end of the excavation. Below, the image is not a picture but a 3D reproduction of the grave. This figure is available in colour online at wileyonlinelibrary.com/journal/oa.

placed at the head of a canyon of karstic origin. The mode of burial of the bodies was carried out as a result of an excavation that had impacted even ethno-archaeological structures (remains of charcoal burning) located upstream of the pit. The lateral limits of the pit appeared to be those of the natural gully, while the downstream boundary was represented by the sudden increase in the slope of the gully. The coverage of the bodies was completed after the deposition: the grave was filled with (from bottom to top) soil, selected sub-decimetric and centimetric limestone lithoids and soil with centimetric calcareous lithoids. The passage of time had allowed the complete grassing of the area, making the site virtually unidentifiable in relation to grass-marks.

Thanks to the procedures of stratigraphic excavation, other human remains were exposed, for a total of five people in anatomical and primary deposition, to which were added the partial remains of another individual in primary deposition, in addition to the remains affected by the excavation of the rescuer. A total of seven individuals were excavated.

Four soldiers lay prone, whereas two subjects were put down on their sides (Figure 1). Nothing could be said about the position of the individual excavated by the hiker.

Identification of the nationality was performed for two of the subjects, who still had personal effects consisting of a badge for military vaccinations (GM 20 F) and religious medals (GM 17 D, Figure 2). What remained of their uniforms gave clues about their Italian nationality and of the period.

Most of the skeletons were very well preserved in every portion, except for GM 15 G, which, though lying in a primary burial, was largely incomplete.

Using the Laser Scanner permitted us to gain a 3D model geometrically fitting the grave. The resulting model, coloured by means of digital photos, rendered it possible to take measurements and sections, and to conduct virtual explorations of the grave itself.

The seven individuals were between 18 and 35 years of age. Stature was between 162 and 175 cm.

From a pathological perspective, they present quite a homogeneous situation. Degenerative and occupational stress diseases prevail (for example disc herniation).

Figure 2. Religious medals of subject GM 17 D. This figure is available in colour online at wileyonlinelibrary.com/journal/oa.

The presence of three cases of osteochondritis dissecans was observed (GM 14, GM 18 C and GM 19 A) and, a single subject (GM 14 B), exhibited signs of nutritional deficiency, probably anemia (cribra orbitalia). Biological and pathological profiles of the seven skeletons are reported in Table 1.

The study of injuries revealed a variety of types of lesions: on GM 14 B, an entry wound of 12 mm diameter in the right parietal was found, with bevelling on the inner bony table. No exit hole was noted, and the projectile was not found in the grave. The skull base showed heavily fragmented fractures; thus, the projectile might have come out from the base itself.

GM 17 D (Figure 3) presented several comminuted fractures on his seventh cervical vertebra, right humerus, right ulna and a circular projectile lesion on the second left rib, as well as projectile defects on the left femur (roughly 12 mm of diameter). The entry hole is surrounded by three radial fracture lines, Y shaped; on the dorsal side of the bone, an exit hole was found that presented irregular margins. GM 19 A showed projectile defects in the right scapula (roughly 12 mm of diameter) that presented smooth surface margins and three fracture lines that departed from projectile defects. There are fractures on the fourth and fifth cervical vertebrae, on two right ribs (comminuted fractures), and one oblique fracture on the diaphysis of the right fibula. All fracture surfaces present a homogeneous colour with the external cortical bone. The three subjects described (GM 14 A, GM 17 D and GM 19 A) had probably been struck by a shrapnel grenade. GM 15 G showed many comminuted skeletal fractures and traumatic amputations. Comminuted fractures were recovered on several vertebrae and ribs, on the left clavicle, left scapula, left humerus, right coxal bone and both femora; fracture surfaces present a

Table 1. Biological profile of the seven soldiers

Subject	Sex	Age	Heights (cm)	Pathologies/stress markers
GM. 14 B	M	18–23	165–171	Dental diseases, nutritional stress markers (cribra orbitalia cribra and cranii), degenerative diseases (pitting on carpus and metacarpus, left clavicular enthesopathy), osteochondritis dissecans on the joint surface in femur (posterior–lateral surface of lateral condyles) and tibia right (articular surface of lateral condyles).
GM. 15 G	M	23–29	165–177	Degenerative diseases (disc herniation).
GM. 16 E	M	26–34	174–180	Degenerative diseases (disc herniation), obturator foramen osteophyte.
GM. 17 D	M	18–23	160–166	Dental diseases, degenerative diseases (disc herniation).
GM. 18 C	M	18–23	168–173	Degenerative diseases (right clavicular enthesopathy), osteochondritis dissecans on right femur (patellar surface).
GM 19 A	M	26–34	163–169	Degenerative diseases (clavicular enthesopathy, enthesopathy left and right femur), osteochondritis dissecans on the left humerus (articular surfaces of trochlea).
GM 20 F	M	26–35	165–171	Dental disease, degenerative diseases (right clavicular enthesopathy)

Figure 3. Combination of different types of injury in the same subject (GM17 D): on the left blast trauma of a cervical vertebra, on the right entry perforation (femur) probably caused by Shrapnel bullet. This figure is available in colour online at wileyonlinelibrary.com/journal/oa.

homogeneous colour with external cortical bone. GM 18 C had comminuted fractures and traumatic amputations of the left tibia and fibula, the fractures presented smooth surface margins. These two soldiers (GM 15 G, GM 18 C) had sustained extreme fragmentation maybe by a grenade explosion.

GM 16 E showed an entry wound (approximately 9 mm diameter) in his right parietal bone; an exit wound was present, situated on the squamosal suture, between the left parietal and left temporal bones (Figure 4). The entry wound is clearly circular, but the fracture rim of the hole is not complete; the exit hole is irregularly shaped, and the wound track has a right–left direction with downward inclination.

GM 20 F had a semicircular entry wound (roughly 9 mm diameter) on the right supraorbital margin and an exit hole in the occipital bone; the wound track has antero–posterior direction with upward inclination. Again, projectile defects (of highly irregular shape, more than 12 mm in diameter) were found on his left tibia, four fracture lines (two upper and two lower) departed from the fracture margin.

The analysis of the grave soil allowed the identification of fly puparia belonging to two different species. Four puparia belonging to a species in the family Phoridae were isolated from the left coxal bone of GM14 B and from foot of GM14 B. Members of the family Phoridae are known as coffin flies, and they are able to reach deeply buried cadavers. Mainly active during the warmer season, they can be found as well in spring and autumn, and they have been described to be present on buried remains about one year after the burial or 4–8 months after death in exposed bodies (Smith, 1986; Campobasso *et al.*, 2004). The most important species of this family able to colonize a body belong to the genera *Anevrina*, *Conicera*, *Diploneura*, *Dohiphora*, *Metopina*, *Triphleba* and *Megaselia* (Smith, 1986).

Fragments of a puparium belonging to *Protophormia terranovae*, a species in the family Calliphoridae, were present on GM14 B coxal bone. The identification of these insect remains was possible because the presence of the posterior spiracles, typical of the member of Calliphoridae and the particular shape and disposition of the papillae around the posterior region of the pupae diagnostic of this species (Szpila, 2010) (Figure 5). Blowflies (Calliphoridae) are among the first insects that colonize a body after death, and usually they exhibit a limited ability to colonize buried remains (Gunn and Bird, 2011). *Protophormia terraenovae*, which overwinter mainly as adults is one of the first flies to appear in spring and has been already reported from archaeological cases related with the WWI in Northern Italy (Vanin *et al.*, 2009). The larvae of this species have the tendency to pupate on the cadaver, and they could

Figure 4. The wound track of a probably gunshot (about 9 mm) in subject GM 16 E. This figure is available in colour online at wileyonlinelibrary.com/journal/oa.

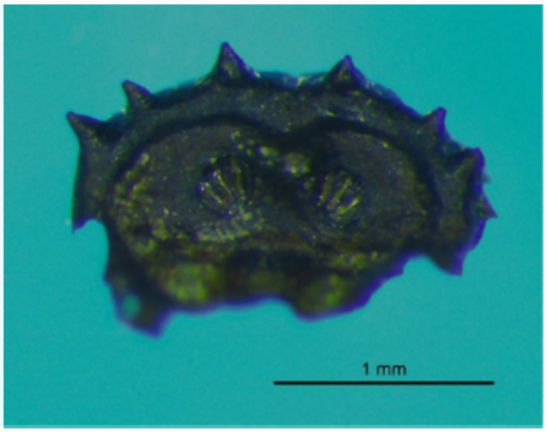

Figure 5. Fragments of the puparium of Protophormia terranovae (Diptera, Calliphoridae), collected from cox/sx GM 14 B, after being cleaned in a warm solution of NaOH. Spiracles with three radial slits are typical of the Calliphoridae family, whereas the particular shape and disposition of the papillae are a diagnostic character for this species. This figure is available in colour online at wileyonlinelibrary.com/journal/oa.

complete development following burial and emerge from the soil as adults (Balme *et al.*, 2012) but, to the author's knowledge, has never been reported from buried bodies: this finding suggests a spring colonization of an exposed body or partially exposed body with a later burying.

Discussion

Thanks to the stratigraphic excavation, it was possible to understand the order in which the bodies were laid: the first body to be put down was individual GM 19 A, partially covered by the individual GM 18 C. Then, they set down individual GM 17 D, partially covered by the individual GM 16 E, and then individual GM 14 B, whose head was covered by the feet of individual GM 20 F. Individual GM 15 G largely incomplete and covering individual GM 16 E must have been put down in the moment right before filling the grave.

One question needs to be answered: who dug the grave. Either Italian soldiers who buried the fallen companions, or Austro-Hungarians, who, once they had conquered their position, had to dispose of the enemies' corpses. Some useful information can be drawn by what emerged from the archaeological dig: as already discussed, except for one individual (GM 20 F), subjects lay in primary burial. The only element by which the question can find a solution can therefore be extrapolated from the position of the skeletons: as can be observed in Figure 1, at least four individuals were prone during their burial, the others on one side. It seems evident that the soldiers were put into the grave with no particular care and with no ceremony. That seems to point to a quick burial performed by Austro-Hungarian soldiers. An Italian origin of the grave cannot however be excluded, of course. In an emergency situation of danger, they could have been pushed to bury their companions in a rush. The last hypothesis seems to be less probable, given the care put in the covering of the grave, invisible for almost a century. Regardless, the entomological analysis reveals that the bodies have not been buried immediately.

These subjects showed extremely high evidence of degenerative pathologies and stress markers on all skeletons, i.e. several cases of enthesopathy of the clavicle at the attachment site of costo-clavicular ligament. They were probably caused by the carrying of heavy loads, which usually weigh on the rim-clavicle ligaments (Capasso *et al.*, 1999). Three individuals had vertebrae marked by Schmorl nodules, a consequence of degenerative arthrosis caused by disc herniation (Ortner and Putschar, 1985). These kinds of lesions are typical of old people or of individuals who suffer from stress to the spine, e.g. multiple flexions of the rachis and the carrying of heavy loads (Capasso *et al.*, 1999). Presumably, these pathologies are connected to repetitive movements of the ostheoarticular complex; these types of lesion were particularly frequent among lower socio-economic classes and poor people, overall among countryside workers (De Sèze and Ryckewaert, 1979). For this reason, it is not surprising to find a subject (GM 14 B) showing cribra cranii and cribra orbitalia, an indicator of a chronic anaemic status (Fornaciari and Giuffra, 2009) which could be connected to nutritional deficiencies. Also, the high evidence of osteochondritis dissecans found in three of the seven individuals is generally caused by micro trauma correlated with repeated stress and can be put in connection with a physically straining lifestyle.

The study of injuries revealed a surprising variety of causes of death (Figures 3 and 6). In GM 14 B, GM 17 D and GM 19 A were observed the contemporary presence of bullet wounds of about 12/13 mm diameter, and of bones severely damaged by comminuted fractures. Characteristic holes of 12/13 mm diameter were observed in previous cases (Gaudio *et al.*, 2009) in which a shrapnel projectile was found close or inside the bones and at the same time comminuted fractures were observed in other parts of the skeleton.

In cases of GM 14 B, GM 17 D and GM 19 A, it is conceivable that the injuries described can be attributed to the effect of shrapnel grenades, which can cause damage both by the explosion effects and by the projectiles they contained (12 mm caliber).

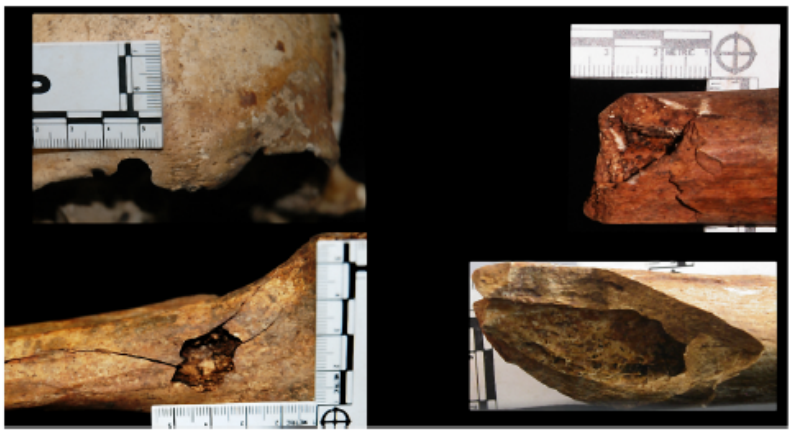

Figure 6. The study revealed high variety of types of lesions: on the top to the left, a semicircular entry wound (roughly 9 mm diameter) on the GM 20 F skull. Below on the left, an entry hole of highly irregular shape, more than 12 mm in diameter, was found on GM 20 F's left tibia. On the right, the fractures sustained to the shafts on both GM 15 G femora, probably caused by a grenade explosion. This figure is available in colour online at wileyonlinelibrary.com/journal/oa.

One soldier (Gm 15 G) with extremely serious fractures (Figure 6) and largely incomplete skeleton was lying below the other remains; the most trustworthy hypothesis is that the soldier was heavily dismembered, likely due to a very near explosion of a grenade during an artillery bombing. Another subject (GM 18 C) presents traumatic amputation of the left tibia and fibula, which can indicate an amputation caused by a grenade (his left foot was completely bent on the relative tibia, when retrieved). The individual does not show perimortem lesions; nevertheless, such a heavy wound on his left leg can be considered to be responsible for his death, because of a consequent hemorrhagic shock. Obviously, many other scenarios can be hypothesized.

Two subjects (GM 16 E and GM 20 F) showed gunshot injures (roughly 9 mm) on the skull (Figures 4 and 6): determining bullet caliber is problematic; in some cases, the general caliber of the bullet may be estimated according to the diameter (Kimmerle and Baraybar, 2008): defect size is used to eliminate possible ammunition classes (Di Maio, 1999); the dimension of the hole in bones may be of that projectile or larger (Dodd, 2006). Kimmerle and Baraybar (2008) assert that if the impact of the projectile occurs perpendicularly, the wound will be circular, reflecting the shape and size of the bullet. This is the case of skull wounds in subjects GM 16 E and GM 20 F. In case of GM 16 E, the fracture rim of the hole is not complete but however it is possible to observe the cross section of the hole. In GM 20 F, the impact occurs perfectly perpendicularly and the cross section is clear. The diameter is in both cases about 9 mm.

As both the Austro-Hungarian Army and the Italian were equipped with 9 mm caliber pistols (models generally used were the Steyr Model 1912 to the Austro-Hungarian Army and Glisenti Beretta Model 1910 or Model 1915 for Italian Army), it is not possible, in the absence of the bullet, to determine the type and the nationality of the weapon that caused the injury. Soldier GM 20 F revealed several aspects that were difficult to interpret. Gunshot 9 mm caliber (frontal entry) was not the only injury found: a projectile lesion on left tibia, very irregular and wide, 12 mm at least. Although speculative, this individual was probably hit by a shrapnel projectile and later moved and shots by hand pistol because of the severity of his injuries. Obviously, it is only one of many possible scenarios that resulted in the death of this soldier.

As discussed, it was not possible to verify the nationality of the weapons, based solely on the only diameter of the holes in the bones. Only the caliber could roughly be determined; therefore, it could not be established whether the victims had been shot by enemies or allies. Even though the first hypothesis may sound most reasonable, there are no elements to exclude the second one, from the point of view of an act of mercy towards injured comrades-in-arms (particularly in the GM 20 F case).

Conclusions

The study carried out on this rare case of a mass grave from to World War I allowed the recovery of a piece of buried history; by means of a multi-disciplinary approach, it has been possible to reconstruct an unknown episode of WWI, giving a historiographic contribution where official documents are lacking.

References

Balme GR, Denning SS, Cammack JA, Watson DW. 2012. Blow flies (Diptera: Calliphoridae) survive burial: Evidence of ascending vertical dispersal. *Forensic Science International* 216: e1–4.

Bass W. 1987. *Human Osteology. A laboratory and field manual*. Missouri Archaeological Society: Columbia.

Black S, Scheuer L. 2000. *Developmental Juvenile Osteology*. Academic Press: Londra.

Brooks S, Suchey JM. 1990. Skeletal Age determination based on the os pubis: a comparison of the Acsadi-Nemeskeri and Suchey-Brooks methods. *Human Evolution* 5: 227–38.

Campobasso CP, Disney RHL, Introna F. 2004. A case of Megaselia scalaris (Loew)(Dipt, Phoridae) breeding in a human corpse. *Internat J. Forensic Med. Toxicol.* 5: 3–5.

Capasso L, Kennedy AR, Wilczak AC. 1999. *Atlas of occupational markers on Human Remains*. Edigrafital SPA: Teramo.

De Sèze S, Ryckewaert A. 1979. *Malattie delle ossa e delle articolazioni*. Gaggi Editore: Bologna.

Desfossès Y, Jacques A, Prilaux G. 2003. Arras «Actiparc», les oubliés du «Point du Jour». *Sucellus, Dossers Archéologiques Historiques et Culturels du Nord Pas Calais* 54: 84–100.

Di Maio VJM. 1999. *Gunshot Wound: Practical Aspects of Firearms, Ballistics, and Forensic Techniques*. CRC Press: New York.

Dodd MJ. 2006. *Terminal Ballistics: A text and Atlas of Gunshot Wounds*. CRC Press: New York.

Fornaciari G, Giuffra V. 2009. *Lezioni di paleopatologia*. ECIG: Genova.

Fraser A 2005. Finding Jakob. *Battlefields Archaeological Review* 1: 29–40.

Gaudio D, Galassi A, Poppa P, Cattaneo C. 2009. Studio antropologico dei resti scheletrici risalenti alla grande guerra: tra storia, medicina e antropologia. *Medicina nei Secoli* 21: 1037–1058.

Gunn A, Bird J. 2011. The ability of the blowflies Calliphora vomitoria (Linnaeus), Calliphora vicina (Rob-Desvoidy) and Lucilia sericata (Meigen) (Diptera: Calliphoridae) and the muscid flies Muscina stabulans (Fallén) and Muscina prolapsa (Harris) (Diptera: Muscidae) to colonise buried remains. *Forensic Science International* 207: 198–204.

Jacques A. 1997. La bataille d'Arras, avril-mai 1917. Guerre 1914-1918. *Documents d'Archéologie et d'Histoire du XXéme siécle* 5.

Jankauskas R, Palubeckaitė-Miliauskienė Ž. 2007. Dental status of two military samples: soldiers of Napoleon's Great Army and German soldiers in World War. *Papers on Anthropology* 16: 222–236.

Jankauskas R, Barkus A, Urbanavičius A, Palubeckaitė-Miliauskienė Ž. 2007 a. Stature variation during the 19th century: Napoleonic versus German soldiers of World War. *Papers on Anthropology* 16: 122–131.

Jankauskas R, Palubeckaitė-Miliauskienė Ž, Stankevičiūtė D, Kuncevičius A. 2011. Im Osten etwas Neues: Anthropological analysis of remains of German soldiers from 1915-1918. *Anthropologischer Anzeiger* 68: 393–414.

Kimmerle EH, Baraybar JP. 2008. *Skeletal Trauma: Identification of Injuries Resulting from Human Rights Abuse and Armed Conflict*. CRC Press: New York.

Lamendin H, Baccino E, Humbert JF, Tavernier JC, Nossintchouck RM, Zerilli A. 1992. A Simple Technic for Age Estimation in Adult Corpses: the Two Criteria Dental Method. *Journal of Forensic Sciences* 37: 1373–1379.

Lovejoy CO, Meindl RS, Pryzbeck TR, Mensforth RP. 1985. Chronological metamorphosis of the auricular surface of the ilium: a new method for determination of adult skeletal age at death. *Amer. J. Phys. Anthrop.* 68: 15–21.

Mincer HH, Harris EF, Berryman HE. 1993.The A.B.F.O. Study of Third Molar Development and Its Use As an Estimator of Chronological Age. *Journal of Forensic Sciences*. 38(2): 379–390.

Ortner DJ, Putschar WGJ. 1985. *Identification of Pathological conditions in human skeletal remains*. Smithsonian Institution Press: Londra.

Simmons T, Jantz RL, Bass W. 1990. Stature estimation from fragmentary femora: a revision of the Steele method. *Journal of Forensic Sciences* 35 (3): 628–36.

Smith KGV. 1986. *A manual of forensic entomology*. London Trustees of the British Museum: London.

Szpila K. 2010. Key for the Identification of Third Instars of European Blowflies (Diptera: Calliphoridae) of Forensic Importance. In *Current Concept in Forensic Entomology*, Amendt, J, Goff ML, Grassberger M, Campobasso CP (ed.). Springer: Verlag, 43–56.

Trotter G, Gleser C. 1977. Corrigenda to Estimation of Stature based on Measurements of Stature Estimation of stature from long bones of Long-Limb Bones of American Whites and Negroes. *American Journal of Physical Anthropology* 10: 463–514.

Ubelaker DH. 1999. *Human Skeletal Remains. Excavation, analysis, interpretation*. Taraxacum: Washington.

Vanin S, Turchetto M, Galassi A, Cattaneo C. 2009. Forensic Entomology and Archaeology of War. *Journal of Conflict Archaeology* 50: 127–139.

Wieberg D, Wescott DJ. 2008. Estimating the Timing of Long Bone Fractures: Correlation Between the Postmortem Interval, Bone Moisture Content, and Blunt Force. *Journal of Forensic Sciences* 53: 1028–1034.

CAPITOLO 3

Surface curvature of pelvic joints from three laser scanners: separating anatomy from measurement error.

Villa C, Gaudio D, Cattaneo C, Buckberry J, Wilson AW, Lynnerup N.

Submitted to Journal of Forensic Science

Surface curvature of pelvic joints from three laser scanners: separating anatomy from measurement error.

Chiara Villa[1*], Daniel Gaudio[2], Cristina Cattaneo[2], Jo Buckberry[3], Andrew S.Wilson[3], Niels Lynnerup[1]

[1]Laboratory of Biological Anthropology, Department of Forensic Medicine, University of Copenhagen, Denmark;
[2]LABANOF, Forensic Anthropology and Odontology Laboratory, Department of Human Morphology, University of Milan, Italy.
[3]Biological Anthropology Research Centre, Archaeological Sciences, University of Bradford, UK;

Keywords: forensic science, forensic anthropology, pubic symphysis, auricular surface, curvature, laser scanner, surface area, distance deviation, 3D models

Abstract

Recent studies have reported that quantifying symphyseal and auricular surfaces curvature changes on 3D models acquired by laser scanners have a potential for age-at-death estimation. However, no tests have been carried out to evaluate the repeatability of the results between different laser scanners. We calculated and compared the surface curvature of 3D models of symphyseal and auricular surfaces generated from three different laser scanners. The surface area and the distance between co-registered meshes were also investigated. Close results were found for surface areas (differences between 0.3% and 2.4%) and for distance deviations (average < 20 μm, SD < 200 μm). The curvature values were found to be systematically biased between different laser scanners, but still showing similar trends with increasing phases / scores. We filtered the 3D models to separate anatomy from the measurement error of each instrument, so that similar curvature values could be obtained ($p < 0.05$) irrespective of the specific laser scanner.

Introduction

Recent studies have shown the benefits of quantitative methods using 3D laser scanner models in addressing fundamental issues in physical and forensic anthropology. Sexual dimorphism and population and ancestry variation have been investigated quantifying surface areas or extracting curves [1-5]. The morphological features of the symphyseal and the auricular surfaces used for age estimation have been examined looking at the surface curvature changes [6-8]. Laser scanners have also been used to investigate cranial facial variation and for facial identification [9-13].

In all these applications, the precision and the repeatability of the measurements among different instruments are essential for the reliability of each method; in fact, there are different models of laser scanners and differences between the software used for post-processing the scans (i.e. aligning, merging and fusion of the single scans to create a 3D model). It has been demonstrated that the surface areas were reproduced with high precision and the measurement errors of the extracted information varied from 0.2% to about 1% [5, 14]; it has been also shown that the location of points on the surface (landmarks) and the measurements of length could be accurately repeated on 3D models [11, 12, 15]. When some of the parameters used for the scans made by the same laser scanner have been changed, measurement error was reported to increase slightly to 2% [14]. However, all these studies have tested the repeatability of measurements made by the same instrument.

Laser surface scanning (and CT-scanning) of bones is proposed as a method to make osteological data more widely and easily available, e.g. the Smithsonian 3D collection [16], "Digitised Diseases" [17] and "From Cemetery to Clinic" [18]. It is thus important to investigate whether 3D models acquired by different laser scanners may exhibit larger differences than those acquired by the same scanner. Irrespective of the

performance of each laser scanner, the nodes of the resulting 3D model surfaces represent the true anatomical shape, plus some error due to measurement uncertainty. The formal expression of this uncertainty is difficult, as it requires full knowledge not only of the instrument and object properties, but also of operational details which may not always be available, such as calibration steps followed and the exact distance between object and scanner [19, 20]. A simple but general approach to assess measurement error that does not rely on any external knowledge beyond the scanned 3D mesh would therefore be particularly convenient. We assumed the measurement uncertainty manifests itself exclusively as independent random error in the position of mesh nodes, which can be effectively reduced by a smoothing operation over neighboring nodes. If this assumption is appropriate, the use of an adequate amount of smoothing would filter out the measurement error while preserving the overall anatomical shape of the bone surface, and homogenize 3D models from different instruments. The aim of this paper was to experimentally verify the validity of our assumption by using 3D models of symphyseal and auricular surfaces generated with three different laser scanners, three different kinds of post-processing software, and the same algorithm used in Villa et al. [6]. To approximate the conditions of an independent replication of this experiment, only the final 3D models were compared, excluding other influences such as the resolution of the instrument, the operational conditions or type of algorithm used to merge the scans.

Materials and methods

Sample

The sample consisted of the 24 Suchey-Brooks pubic bone casts (12 females, 12 males) [21] and 19 archeological auricular surfaces of the "recording kit" collected by Buckberry and Chamberlain as illustrative of the different scores of the features described in their method [22]. We selected only the central area of the pubic symphyseal face

inside the margins and the internal area of the auricular surface, i.e. the area delimitated by the contour of the joint, as described in [6].

Laser scanning

Three different laser scanners were used in this study (Table 1): FaroArm Quantum with V3 Laser Line Probe - FARO Singapore Pte. Ltd (abbreviated Faro), property of the University of Bradford (UK); Minolta VI-910 - Konica Minolta Sensing, Inc. Osaka-Japan (abbreviated Minolta), property of the University of Milan (Italy); and a custom laser scanner (abbreviated Custom) property of the University of Copenhagen (Denmark) [6]. The Faro is equipped with an articulated arm, thus the object to scan was kept fixed during the scanning process; for the other two laser scanners, the scanning system was fixed while the object was moved. In order to capture as much detail as possible, the object was located as close as the laser scanner allowed.

Three different software applications were used for the post-processing: PolyWorks [23] was the software accompanying the Faro instrument, Geomagic Studio [24] was used for the scans from Minolta and David-laser scanner software [25] for those from Custom. In each software, the followed steps were carried out: first, each mesh was visually inspected, and occasional spikes were removed and small holes were filled; second, the individual meshes were aligned (the Faro roughly aligned the individual scans during the scan processing, so a second alignment was performed in this case); third, the aligned meshes were merged for generating the final mesh and removing redundant data; finally, a slight smoothing (the lowest possible smooth allowed by each software) was applied at the merged mesh. The final model was saved in STL format (Standard Triangulation Language) and used in all analysis.

Many factors can have an effect on the scans and are difficult to control and reproduce. First, the performance of the different laser scanners rarely can be

compared since there are no protocols and the precision and accuracy specified by different manufacturers are measured and expressed in different ways [26]. Furthermore, the quality of the resulting 3D models depends not only on the nominal resolution of the laser scanner, but also, among other factors, on the ambient light, the manual skill of the operator (more evident in Faro), surface color and the geometry of the object, the distance of the scanner to the object and the instantaneous incident angle of the laser and the line of sight of the camera [19, 20]. We were only interested on the differences among the final 3D, so the scans were acquired under optimal conditions by qualified operators. While this may not be the most formally rigorous experimental protocol, it can be argued that it provides the most relevant common ground for comparison among instruments under operational circumstances as close as possible to the real world application of these instruments. As we are only concerned with the practical usability of the typical scans a user will obtain, we have focused on comparing the final 3D models, without emphasizing these other factors further.

	Portability	**Weight**	**Texture**	**Velocity of scan (*)**	**Type of laser scanner system**	**Accuracy**	**Type of mesh**	**Range of price (€)**
FARO	Yes	~10 kg	No	Fast (less than 5)	Mobile (object fixes)	0.023 mm (a)	Triangle, unstructured	>50 000
MINOLTA	Yes	~11 kg	Yes, color	Fast (less than 5)	Fixed (object moves)	[b]X: ±0.22mm Y: ±0.16mm Z: ±0.10mm (b)	Triangle, structured	>50 000
CUSTOM	Yes	~5 kg	Yes, grey scale	Very slow (~15 min)	Fixed (object moves)	0.025- 0.04 mm (c)	Triangle, structured	<5 000

Table 1: Performance parameters of the laser scanners. The accuracy values are taken from the available manufacturers literature. They are not always comparable across instruments and with the actual measurement conditions used in this work (* to scan a pubic bone, (a) volumetric maximum deviation at 1.8m , (b) to the Z reference plane -Conditions: TELE/FINE mode, Konica Minolta's standard, (c) calculated as 0.5% of the object size)

Surface curvatures, surface areas and distances.

For each specimen scanned by each laser scanner, we calculated the mean of the curvature values (as in [6]): therefore, we calculated the curvature of 57 three-dimensional models of auricular surfaces (19 specimens scanned three times) and 72 three-dimensional models of pubic bones, (24 casts scanned three times). The differences between the 3D models of the same specimen were calculated and expressed in percent. The curvature values of 3D models from Custom laser scanner were used as reference models. To reduce the total curvature differences to a maximum of 2%, we applied a smoothing factor, i.e. we modified the algorithm for calculating curvature to eliminate the measurement error of the lasers.

To enable a comparison with other studies reported in the literature, we quantified the surface areas (reported in cm^2); we also calculated the differences of surface area (expressed in cm^2 and percent) between the 3D models of the different instruments. In additional, we calculated the distance deviation (reported in μm), i.e. the distance between the points of a 3D model of one laser and corresponding ones of second laser scanner. We used a function of Geomagic Studio Software, called "deviation", that returned for each two-by-two comparison the "Average distance and the "Standard Deviation distance"; furthermore this function generated color-coded mapping of the differences, highlighting the areas and the specimens with problems.

Statistical analyses

All descriptive statistics (means, standard deviations (SD), and differences) were calculated using SPSS software, version 20. We used scatter plots to undertake a visual evaluation of the distances between 3D models from different laser scanners. Each scatter plot shows the comparison between two laser scanners: 1) Faro versus Minolta; 2) Custom versus Faro; 3) Custom versus Minolta. To highlight any variation with increasing age, we ordered the auricular surface features based on increasing score; the features were used in the following order: TO= transverse organization, ST= surface texture, MA= macroporosity, MI= microporosity, AC= apical change. In the same way, we ordered the pubic bones based on increasing phase; two values were present for each phase, representing the early (E) and the advanced (A) patters. The scatter plots were also used to investigate the curvature values, with the same organization described above; in this case, each series represented a laser scanner: Faro, Minolta and Custom. Finally, we performed Kruskal-Wallis ANOVA to compare the revised curvature values, after the use of the smoothing.

Results

Surface curvature

The curvature values of the auricular surface and the pubic bone (male and females separately) are shown in Figure 1. The scatter plots in the column "a" (on the left) show the results obtained using the unmodified algorithm used in Villa et al. [6], with the same smoothing factor for all laser scanners. The curvature values show similar trends with increasing phases and scores: the curvature increases and decreases in the same manner in all three laser scanners, but with a systematic difference among the models of laser scanners. Faro shows the highest curvature values in all samples, both for the pubic bones and the auricular surfaces. Minolta and Custom have closer values, but more than 50% of the curvature values of Minolta are higher than those from Custom, especially in

the auricular surfaces. In the pubic bones, differences of 28.8% (females) and 20.5% (males) were found between Faro and Custom, 0.29% (females) and 1.6% (males) between Custom and Minolta. Differences of 44.2% and 9.7% were found in the auricular surfaces, between Faro and Custom, and between Minolta and Custom respectively. To reduce these curvature differences, we modified the amount of smoothing in the curvature algorithm. The curvatures of Faro could be homogenized with Custom using a smoothing factor of 10 for the male pubic bones, of 15 for the female pubic bones, and 20 for the auricular surfaces (Fig. 1, column "b"); in this manner, the distance between the two lasers were reduced to about 1.5%. The curvature values of Minolta and Custom in the pubic bones for both sexes were already very close, with a difference lower than 2%, so no further smoothing factor was applied. A smoothing factor of 5 was required to reduce the difference between the auricular surfaces of Minolta and Custom to 1.8%. Figure 1b (scatter plots on the right) show the corrected curvature values. We found no statistically significant difference ($p > 0.05$) between the corrected curvatures values produced by the different laser scanners.

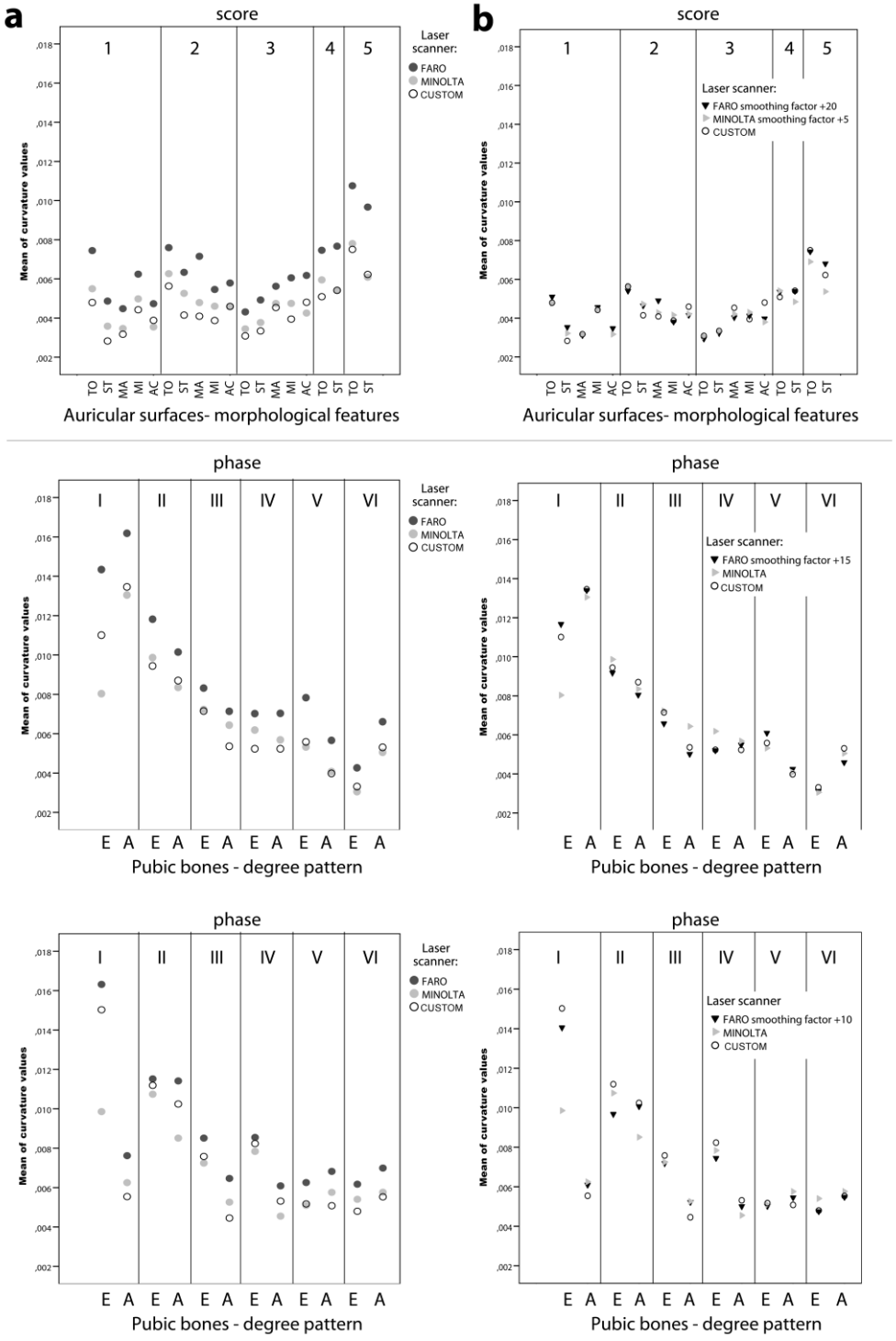

Figure 1: Curvature values of the auricular surface (top row) and of the pubic bones (middle row females, bottom row males). Column **a** shows the curvatures value with the same "smoothing factor" for 3D models by all laser scanners; Column **b** shows the curvature values with different "smoothing factor" (reported in the legends)

Surface areas

The measurements of the surface area and differences between the laser scanners for the auricular surfaces and the symphyseal surface (males and females separately) are reported in Table 2. The largest difference for the auricular surfaces was 0.15 cm^2 and was found between Faro and Minolta corresponding to 1.5%. In the symphyseal surface, Custom and Faro have the highest differences, -0.08 cm^2 (2.4 %) in females and -0.05 cm^2 (1.9%) in males.

		Surface area (cm^2)			Area difference (cm^2)					
	N	**Custom**	**Faro**	**Minolta**	**Custom-Faro**	**%**	**Custom-Minolta**	**%**	**Faro-Minolta**	**%**
Auricular surfaces	19	10.05±4.3	10.09±4.3	9.94±4.1	0.03	0.3%	0.12	1.2%	0.15	1.5%
Pubic bones Females	12	2.39±0.5	2.44±0.6	2.42±0.5	0.05	1.9%	0.03	1.1%	0.02	0.8%
Pubic bones Males	12	3.13±0.7	3.21±0.7	3.20±0.7	0.08	2.4%	0.07	2.1%	0.01	0.3%

Table 2: Mean value and standard deviation of the surface area of the auricular surfaces and the pubic bones for each laser scanner and area differences in cm and percent

Distance deviations

Figure 2 show the distributions of the "average distances" (black solid points) and average plus/ minus the SD for the auricular surfaces. It is clear that there is more variation in distances (most evident in the SD) in the last scores where the surface topography is more irregular: score 3 for AC, scores 4 and 5 for TO and ST. This is more evident in the comparison between Custom and the other two laser scanners. Faro and Minolta show the lowest "SD distance", less than 100 μm with a mean "average distance" of 1.1 μm (Table 3).

	Custom vs Minolta		Custom vs Faro		Faro vs Minolta	
	Average distance	SD distance	Average distance	SD distance	Average distance	SD distance
Auricular surfaces	0.7±2.2	66±38	3.7±4	67±36	1.1±3.6	46±17
Pubic bones Females	-2.3±14	109±81	-0.7±2.3	70±29	3.9±13.5	77±78
Pubic bones Males	-4.4±12.2	81±51	2.6±11.9	79±43	0.4±3.1	36±15

Table 3: Deviation distances: average distances and standard deviations (SD) of the auricular surfaces and the pubic bones for coupled laser scanners (all measurements in micrometers - μm)

The "average distances" are small in all comparisons, ranging from 0.7 to 3.7 μm. For the pubic bones, the "average distances" are similar between laser scanners, varying less than 10 μm (Table 2), while the standard deviations increase and reach values over 100 μm; in particular, in females for the phase I (early and advanced patterns, indicated with E and A in the Figure 3) the "average distances" are different from zero and the "SD distance" are over 200 μm. The more complicated the surface topography is (i.e. having high ridges and deep furrows, showing deep depression or porosity), the more the distance deviations increase. An example can be seen in Figure 4, where the color-coded mapping of the distance deviations between laser scanners are visible for the phase VI advanced pattern of the females: Faro and Minolta show the least difference, indeed the surface is dominated by green color indicating distance between -0.05 to 0.05 μm; the largest deviation in all three comparisons is in the big depression in the lower part of the pubic symphysis. This is an example of a scan artefact in which the camera of the laser scanner failed to record the laser beam because of the depth of the feature and overhanging edges which were obscured. Other examples, in males phase II advanced and phase IV early have obscured

areas that are very difficult to scan and result in large difference between laser scanners, most noticeable between the Custom and the other two instruments (Fig 3).

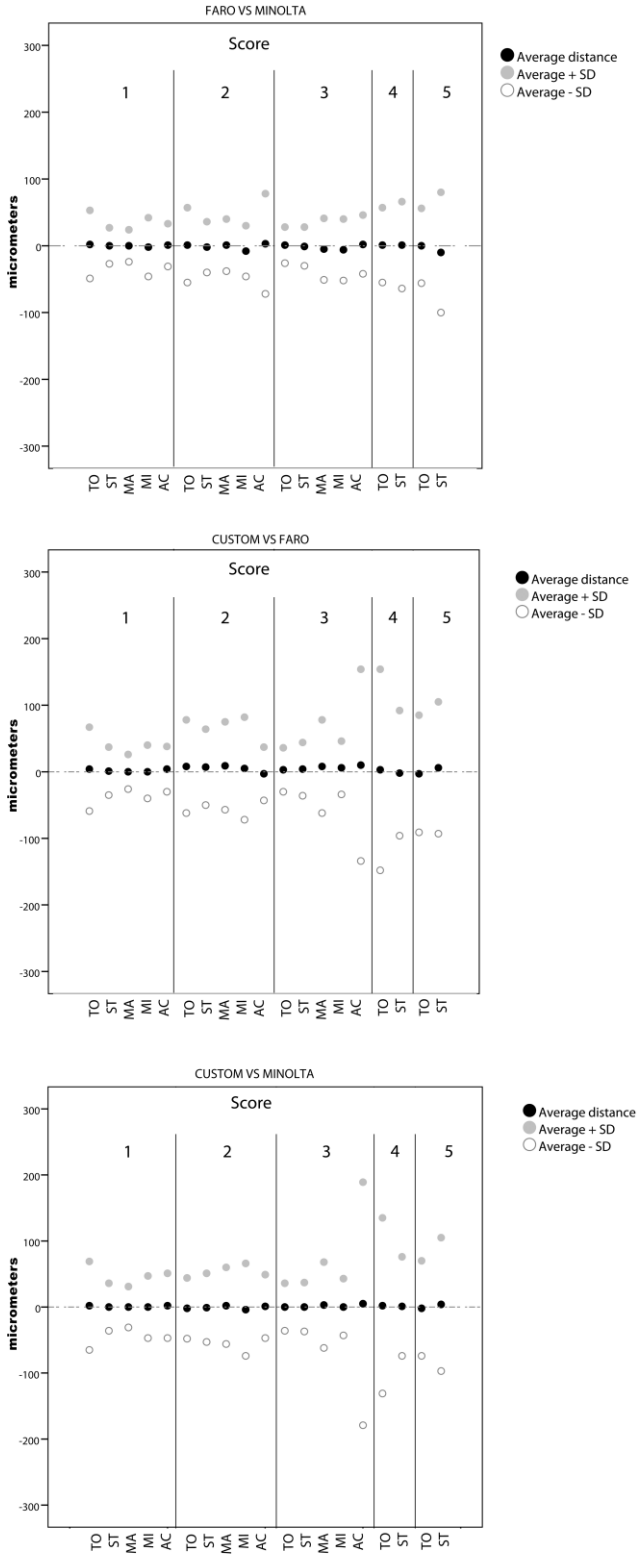

Figure 2: Auricular surface distance deviation

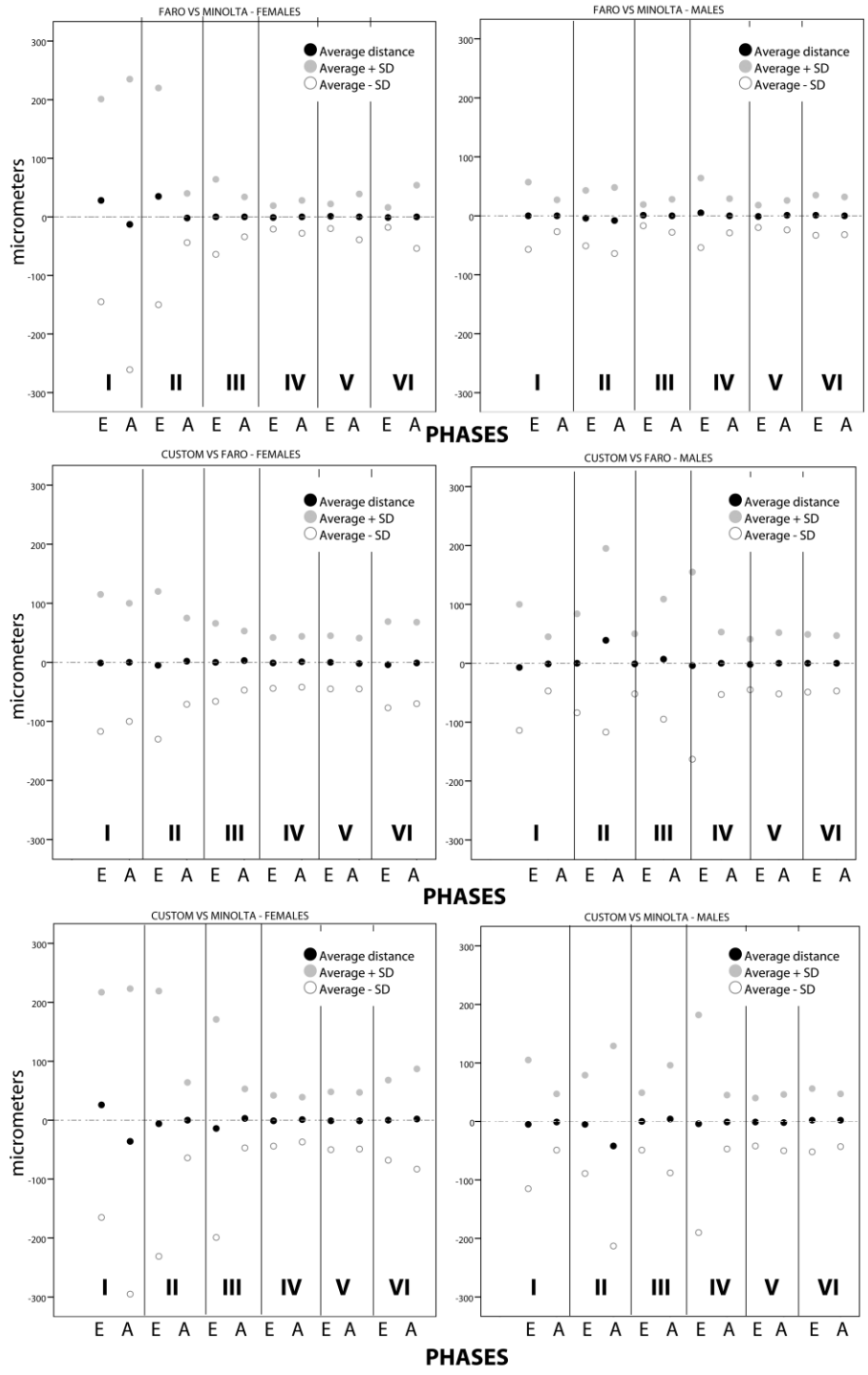

Figure 3: Pubic bone distance deviation; females (left) males (right).

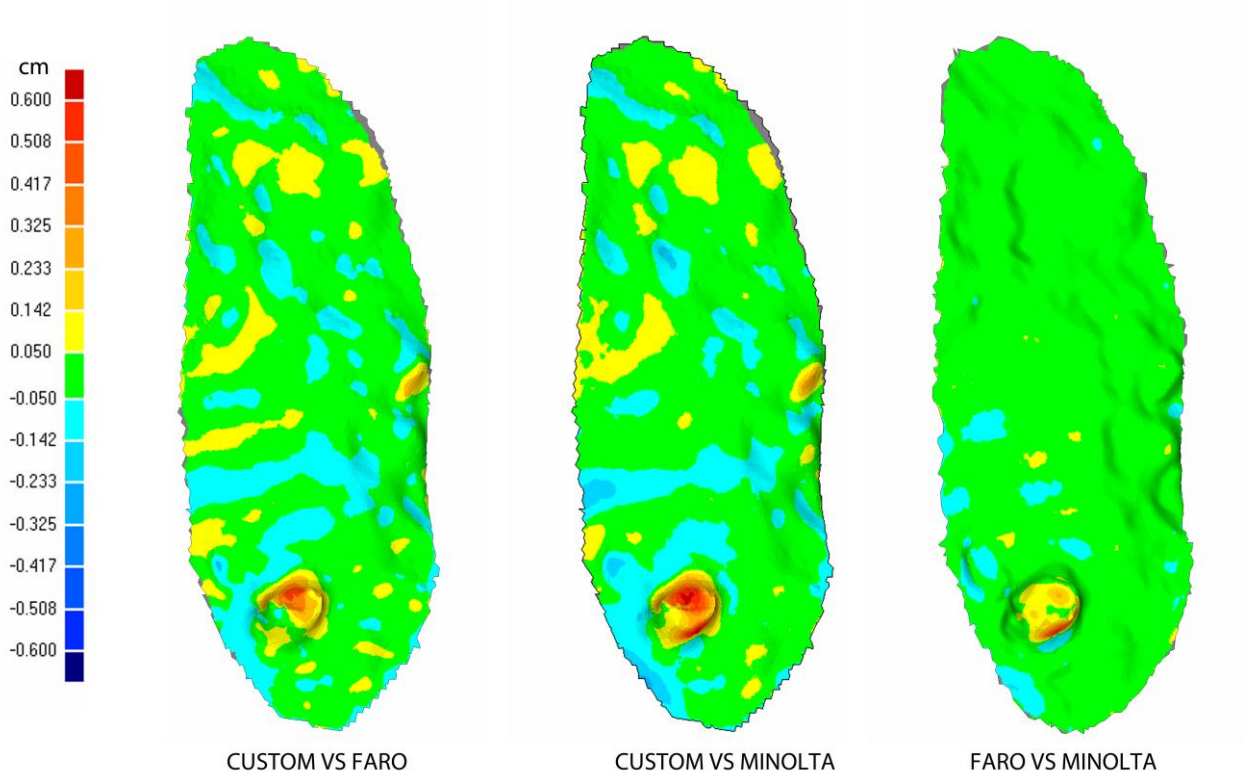

Figure 4: Color-coded mapping of the differences between laser scans for the female phase VI advanced pattern. The larger distances are marked by red and blue colors. Differences between 0.05 and -0.05 are indicated with green.

Discussion

We used 3D models of symphyseal and auricular surfaces generated with three different laser scanner systems to verify the repeatability of surface curvature analysis among instruments using the algorithm described in Villa et al. [6]. Comparing the final 3D models, we found that the overall anatomical shape of the bone surface could be represented independently from the laser scanners: we obtained very low distance deviation between 3D models and differences less than 2.5% in the surface area. The differences between the curvature values, as hypothesized in the introduction, depended on the measurement uncertainty produced by each instrument, i.e. each laser scanner introduces a specific amount of random error in the position of the points. The curvature values showed similar trends with increasing

phase or score, although they were found to be systematically biased between different laser scanners. The measurement uncertainty of each instrument could be reduced and the curvature results among laser scanners could be homogenized applying an amount of smoothing directly proportional to the differences between curvature values. We used the highest smoothing in 3D models from Faro that showed the highest differences in curvature values both in the symphyseal and auricular surfaces with respect to the other two laser scanners. These large differences might be explained by considering the organization of the mesh points: the 3D models from Faro had an unstructured grid, i.e. the points of the mesh were not distributed regularly at the same distance, but they were more concentrated and dense in the areas with more details and more distant and less numerous in the flat areas. In contrast, Custom and Minolta showed similar curvature results probably because both instruments produced 3D models with structured grid. In addition, we noticed that those cases showing the larger distance deviations (for example phase I of the symphyseal surface) still kept the larger differences in curvature values, even after the smoothing. This confirms that the smoothing operation could reduce only the independent random error, not the imprecision in the scans.

Furthermore, our tests strongly confirmed that the surface area can calculate with little error using three different laser scanners. Indeed, we obtained comparable errors to those reported by Sholts et al. [14] and Garvin and Ruff [5]. Faro and Minolta showed the smallest difference (less than 1%) in the symphyseal surfaces, while the largest one in the auricular surfaces (1.5%). The larger differences in the symphyseal surface were between Custom and the other two laser scanners, and it could be due to the optical surface properties of the specimens and ambient light, since the Suchey-Brooks pubic bone casts are white and shiny. This may have introduced more noise and imprecision in the scans [19, 20]. No correspondence between the results of distance deviations and the

difference in surface area were found: in the auricular surfaces Custom and Minolta showed the lowest distances, while in the symphyseal surfaces Custom and Faro were better in the females, Faro and Minolta in the males.

Further analysis needs to identify other factors that can reduce measurement error: process of decimation (i.e. reduction of the number of points in a mesh), or function to transform unstructured grid in structured one, and vice versa, could have a similar effect. We would underline that our results could not be generalized: applying the algorithm described in [6], we detected the features useful for age estimation in a similar way across different laser scanners. Depending on the nature of the investigation, a high resolution laser scanner can have an impact and perform better. Similarly it is also worth considering other scan technologies such as white light, otherwise known as structured light scanners. Finally, a 3D model can be appropriate for one purpose and not for another; thus the analysis needs to be tested for each specific case [27], since no standard procedures are yet defined. This is a necessary step forward towards enabling practical quantitative surface morphology analysis of 3D bone models.

Conclusions

The overall anatomical shape of the bone surface was reproduced in comparable ways using three different laser scanners, as demonstrated by the close surface areas and the low distance variation between co-registered meshes. However, each laser scanner introduces a specific amount of random error in the position of each measured point that can introduce bias to the results of curvature quantification. By applying an adequate amount of smoothing, it was possible to separate the anatomy signal from the instrumental measurement error, thus making the results of the technique developed in Villa et al. [6] irrespective of the specific laser scanner.

Acknowledgements

The authors would like to acknowledge the support of members of the Digitised Diseases team – specifically Emma L. Brown, Tom Sparrow and Andrew Holland who provided support and technical advice.

References

[1] Sholts SB, Walker PL, Kuzminsky SC, Miller KW, Warmlander SK. Identification of group affinity from cross-sectional contours of the human midfacial skeleton using digital morphometrics and 3D laser scanning technology. J Forensic Sci 2011;56(2):333-8.

[2] Sholts SB, Warmlander SK. Zygomaticomaxillary suture shape analyzed with digital morphometrics: reassessing patterns of variation in American Indian and European populations. Forensic Sci Int 2012;217(1-3):234 e1-6.

[3] Shearer BM, Sholts SB, Garvin HM, Warmlander SK. Sexual dimorphism in human browridge volume measured from 3D models of dry crania: a new digital morphometrics approach. Forensic Sci Int 2012;222(1-3):400 e1-5.

[4] Ruiz Mediavilla E, Perea Perez B, Labajo Gonzalez E, Sanchez Sanchez JA, Santiago Saez A, Dorado Fernandez E. Determining sex by bone volume from 3D images: discriminating analysis of the tali and radii in a contemporary Spanish reference collection. Int J Legal Med 2012;126(4):623-31.

[5] Garvin HM, Ruff CB. Sexual dimorphism in skeletal browridge and chin morphologies determined using a new quantitative method. Am J Phys Anthropol 2012;147(4):661-70.

[6] Villa C, Buckberry J, Cattaneo C, Frohlich B, Lynnerup N. Quantitative analysis of the morphological changes of the pubic symphyseal face and the auricular surface and implications for age at death estimation. J Forensic Sci 2013 in review;in review.

[7] Tocheri MW, Razdan A, Dupras TL, Bae M, Liu D. Three Dimensional Quantitative Analyses of Human Pubic Symphyseal Morphology: Can Current Limitations of Skeletal Aging Methods Be Resolved. Am J Phys Anthropol (Suppl.34) 2002;155.

[8] Biwasaka H, Sato K, Aoki Y, Kato H, Maeno Y, Tanijiri T, et al. Three dimensional surface analyses of pubic symphyseal faces of contemporary Japanese reconstructed with 3D digitized scanner. Leg Med (Tokyo) 2013.

[9] Cattaneo C, Cantatore A, Ciaffi R, Gibelli D, Cigada A, De Angelis D, et al. Personal identification by the comparison of facial profiles: testing the reliability of a high-resolution 3D-2D comparison model. J Forensic Sci 2012;57(1):182-7.

[10] Lynnerup N, Clausen ML, Kristoffersen AM, Steglich-Arnholm H. Facial recognition and laser surface scan: a pilot study. Forensic Sci Med Pathol 2009;5(3):167-73.

[11] Park H-K, Chung J-W, Kho H-S. Use of hand-held laser scanning in the assessment of craniometry. Forensic Sci Int 2006;160(2–3):200-6.

[12] Toma AM, Zhurov A, Playle R, Ong E, Richmond S. Reproducibility of facial soft tissue landmarks on 3D laser-scanned facial images. Orthodontics & Craniofacial Research 2009;12(1):33-42.

[13] Shahrom AW, Vanezis P, Chapman RC, Gonzales A, Blenkinsop C, Rossi ML. Techniques in facial identification: computer-aided facial reconstruction using a laser scanner and video superimposition. Int J Legal Med 1996;108(4):194-200.

[14] Sholts SB, Warmlander SK, Flores LM, Miller KW, Walker PL. Variation in the measurement of cranial volume and surface area using 3D laser scanning technology. J Forensic Sci 2010;55(4):871-6.

[15] Sholts SB, Flores L, Walker PL, Warmlander SKTS. Comparison of Coordinate Measurement Precision of Different Landmark Types on Human Crania Using a 3D Laser Scanner and a 3D Digitiser: Implications for Applications of Digital Morphometrics. International Journal of Osteoarchaeology 2011;21(5):535-43.

[16] humanorigins.si.edu/evidence/3d-collection.

[17] http://barc.sls.brad.ac.uk/digitiseddiseases/index.php.

[18] http://www.barc.brad.ac.uk/FromCemeterytoClinic/.

[19] Vukasinovic N, Bracun D, Mozina J, Duhovnik J. The influence of incident angle, object colour and distance on CNC laser scanning. International Journal of Advanced Manufacturing Technology 2010;50(1-4):265-74.

[20] Zaimovic-Uzunovic N, Lemes S. Influence of surface parameters on laser 3D scanning. 10th International Symposium on Measurement and Quality Control (ISMQC 2010)September 5-9, Osaka-Japan, 2010D4-026-01/04.

[21] Suchey JM, Brooks ST, Katz D. Instructions for use of the Suchey-Brooks system for age determination of the female os pubis. Instructional materials accompanying female pubic symphysial models of the Suchey-Brooks system. Fort Collins, Colorado: France Casting. 1988.

[22] Buckberry JL, Chamberlain AT. Age estimation from the auricular surface of the ilium: A revised method. Am J Phys Anthropol 2002;119(3):231-9.

[23] http://www.innovmetric.com/polyworks/3D-scanners/home.aspx?lang=en.

[24] http://www.geomagic.com/en/products/studio/overview/.

[25] http://www.david-3d.com/?section=Downloads.

[26] Guidi G, Russo M, Magrassi G, Bordegoni M. Performance Evaluation of Triangulation Based Range Sensors. Sensors 2010;10(8):7192-215.

[27] Friess M. Scratching the surface? The use of surface scanning in physical and paleoanthropology. Journal of Anthropological Sciences 2012;907-31.

CAPITOLO 4

Reliability of cranio-facial superimposition using 3D skull models-

Gaudio D, Olivieri L, De Angelis D, Poppa P, Galassi A, Cattaneo C.

Submitted to Journal of Forensic Science

Reliability of cranio-facial superimposition using 3D skull models

Daniel Gaudio1, B.S.c; Lara Olivieri[1]; Danilo De Angelis[1], M.D., Ph.D.; Pasquale Poppa[1], B.S.c, Ph.D.; Andrea Galassi[2] M.D.; Cristina Cattaneo[1], B.S.c, M.A., M.D., Ph.D.

[1]LABANOF, Forensic Anthropology and Odontology Laboratory, Department of Human Morphology, University of Milan, Italy.

[2]ULSS 6 Hospital of Vicenza

Abstract

Reliability of cranio-facial computer-aided non automatic superimposition technique was examined. 3D model of five skulls acquired by Laser Scanner and 10 photographs were overlapped with 2D-2D superimpositions (using image obtained from 3D skull model) and 2D-3D superimpositions (using 3D skull model). The superimposition results were evaluated using method based only on landmarks, only on morphological features and using both combined methods (17 landmarks and 12 anatomical features). Moreover, a 3D model without mandible of each skull has been produced and used for superimposition. It was evaluated also if a division of skulls by sex could effectively increase the number of correct identifications. Results show that the 2D-3D superimposition based only on landmarks is the more reliable methodology (5/5 correct identifications, 40% false positives). The persistence of a high percentage of false positives in all the methodologies indicates that this technique should not be used to identify.

Keywords: forensic science; forensic anthropology; personal identification; cranio-facial superimposition; skull-photo overlay; 3D skull model; laser scanner.

Introduction

One of the main question asked by the Authority, when skeletonized or seriously decomposed human remains are recovered, is the identification of the subject. Personal identification is done comparing antemortem and postmortem records and it can be carry out by means of four main methods of analysis: fingerprint, genetic, odontology, anthropology. The first ones are more known by the Authority because of their "quantificability", on the contrary it does not exist a specific standard for the morphologic techniques (odontology and anthropology) that establishes how many and which corresponding features are needed for a positive identification.

Among the anthropological identification techniques there is one of them which has been tested since thirty years: the cranio-facial superimposition that compares cranial morphology with facial morphology of a missing person, evaluating the correspondence according to specific features.

According to the employed devices, from 1930s to nowadays, the cranio-facial superimposition developed through three different phases [1]: with the expression of "*photographic superimposition*" [2, 3, 4, 5, 6] is meant that the superimposition is realized, with tracing paper, from the photo of the subject and from photo of the skull in the same orientation. After the introduction of video device, "*video superimposition*" was developed [5, 6, 7, 8, 9, 10, 11, 12]: skull and subject's photo are placed in front of two different cameras, and with the help of a mixer device the two images are overlapped and visualized on a screen. Finally from the second half of the 1980s superimposition has been carried out with computers and so it has been called "*computer-aided superimposition*". This last methodology is divided into 2 categories: the "non automatic" one, if the computer is used only as interface and the superimposition (sizing and orientation of the images) is manually made by the operator also with the help of some commercial software [11, 13, 14, 15, 16, 17,

18, 19, 20] and the “automatic” one if the computer itself carries out the superimposition automatically finding the best result [21].

There are different techniques for evaluating superimposition results, i.e. if there is a correspondence between the skull and the face. Austin-Smith et al. [5] propose a morphological method that visually evaluates the concordance of some morphological features in the skull and photo (i.e. width of the forehead, length of the skull, curve of the mandible, dimension of nose, etc.). Other authors [16, 22] use a technique based on specific landmarks (bony and soft landmarks) which are placed both into skull and face to evaluate the correspondence between the two images; others finally, use a combined method that employs both landmarks and morphological features [18].

According to some authors the technique can be useful to identify an unknown subject [16, 17], especially if two or more photographs, taken from different points of views, are used [5, 9], although the availability of several photos is a great limit for forensic cases. Other authors think that it should be employed exclusively to exclude identity [6, 19, 23].

Many papers describe cranio-facial superimposition as usable and used for judiciary purposes: Austin-Smith et al. [5] cite as one of the earliest and most famous cases of photographic superimposition the Ruxon murder case. Yoshino et al. [9] state that superimposition is frequently used in criminal cases to identify; Fenton et al. [6] employed it as an excluding technique in a close disaster; Birngruber et al. [17] consider cranio facial superimposition an identification methodology on the same level of forensic odontostomatology and molecular genetics; Gordon et al. [18] underline that C/F superimposition is accepted by South African judicial system as a method to identify unknown individuals. Nevertheless, most of the authors state that superimposition should be performed in conjunction with other

traditional identification techniques [16, 18], because of the very low accuracy rates, and may be conducted alone only when the skull is the unique part available [16]. However it is important to emphasize that, among the results obtained by the cranio-facial superimposition, a considerable number of false negatives (superimpositions evaluated as mismatch, despite the skull belongs to the photographed subject) and false positives (superimpositions evaluated as matches, despite the skull doesn't belong to the photographed subject) are still present precluding a certain identification or exclusion.

Therefore the aim of this survey is, first of all, to evaluate the reliability of computer-aided non automatic cranio-facial superimposition technique, using the method explained by Gordon et al. [18]; secondly to examine some aspects of cranio-facial superimposition technique that have never been evaluated in literature, in particular if the presence of the mandible can introduce errors because of its intrinsic mobility, if skulls of a specific sex can match with photo of a subject of opposite sex, and if a selection of skulls by sex can effectively increase positive identifications. We have also evaluated if the use of 3D model of the skull [18, 21, 24, 25] with a "user friendly" software that has never been employed for this purpose, makes the superimposition process easier and increases correct identifications. Finally we checked if the method which uses only landmarks or only morphological characters can provide more positive results compared with the combined one.

Materials and methods

For our survey, 5 skulls (4 females and 1 males) and 10 scanned photographs of faces shoot from different perspectives (7 female and 3 male subjects, including the photos corresponding to the skulls) were used (Fig. 1). The skulls were scanned using a Laser Scanner Minolta Vivid 910 (Konica Minolta

Sensing, Inc. Osaka-Japan). For each skull two 3D model were made: one with jointed mandible and the other without mandible. Superimpositions were done by an operator, who didn't know the real combination between skull and photo, in order to evaluate the difficulty either in the placement of the landmarks and in the execution of the technique, and to test repeatability.

Four different superimposition methods were used: 2D-2D (photo of the subject – image obtained from 3D model of skull), 2D-3D (photo of the subject – 3D model of skull), 2D-2D w/out-m (photo of the subject - image obtained from 3D model of skull, without mandible) e 2D-3D w/out-m (photo of the subject - image obtained from 3D model of skull, without mandible). First we used the 2D-2D methods, that turned out to be long; we then developed a method to superimpose directly the 3D model of skull on the photograph of the subject. Finally we produced 50 superimpositions for each method and therefore 200 total superimposition.

Fig. 1. Ten digital photographs and five 3D models of skulls used in this survey.

Superimpositions images were produced using respectively Adobe Photoshop CS5 for 2D-2D superimpositions and Vam for 2D-3D superimpositions.

For 2D-2D superimposition, first the skull is oriented (with VAM) by trial and error in the same position of the face in the photo and it is converted in JPG format; then the skull image and the photo are opened with Adobe Photoshop CS5. Image borders are cut off in order to focus on the face; the dimension of the obtained image is uniformed (450 pixel length) so to utilize the same target size in all pictures; targets are placed both in skull and photo (in two different colors, dimension 12 pixel). Finally the skull image is overlapped to the photo and sized in order to match orientation landmarks (i.e. right and left Ectocantion, Subnasal point and Nasion [18]), modifying transparency and scale.

For 2D-3D superimposition, 3D skull model is opened with Vam and targets are placed through a specific tool; subsequently the background photo, already modified by Adobe Photoshop (uniformed to 450 pixel of length and with landmarks of dimension 12 pixel already placed), is opened and transparency, size and orientation are adjusted through specific tools in order to match orientation landmarks.

The employed methodology is Gordon's et al. one [18], that combines 12 morphological features illustrated by Austin-Smith [5] and 16 anatomical landmarks (placed both in skull and face); the Superior Incisal point was added as an additional landmark (IS: the most inferior midline point on the lower border of the central superior incisors). After the two images are overlapped, as Gordon et al. [18] recommended, morphological characters are visually assessed, while the correspondent landmarks (bones and soft landmarks) should overlap, touch, or be within a certain distance no longer than the diameter of the dot to be a match. However, unlike Gordon et al.'s methodology that utilized 3D Studio Max

software program to carry out the superimposition, [18] we manually overlap the two images (skull and photo) with Adobe Photoshop CS5 or Vam, and we use together landmarks and morphological features in the same superimposition.

We have established a cut-off value (as we will explain below) in the number of disagreements to obtain a *match*. The threshold for a *match* is 2 disagreements for landmarks (2L) and 2 disagreements for morphological features (2M) in superimposition with complete skull. In other words, a superimposition that gives as result (2L, 2M) or (2L, 1M) is a *match*, but the one that gives as result (3L, 1M) is a *mismatch.* Here below we show respectively an example of *match* (Fig. 2, Table 1) and one of *mismatch* (Fig. 3, Table 2): not visible parameters aren't considered as errors. Whereas for superimpositions with skull without mandible, because of the decreasing number of evaluable parameters (14 landmarks and 10 morphological features), the threshold is 1 disagreements for landmarks and 1 disagreements for morphological features (1L, 1M). In this case to establish if the length of skull is compatible with face length, skull length is evaluated from Bregma to Superior Incisal point, if it is visible in the photo, otherwise from Bregma to Prostion, that corresponds to the medial point in the superior margin of the upper lip [16].

Compared with 50 superimpositions resulting from each methodology the correct combinations (that we will await if the technique produces 100% positive results) are 5 *matches* and 45 *mismatches* (since there are 1 *match* and 9 *mismatches* for each skull superimposed to the 10 photos), that following we call them respectively "real *matches*" the effective correspondences (unknown from the operator) to distinguish them from false positives (FP) and "real *mismatches*" the effective not correspondences to distinguish them from false negatives.Skulls and photos were also divided by sex and the obtained results were

evaluated; division by sex is possible when pelvis is present, because sex diagnostic reliability based on pelvis morphology study (95-97%) is better than skull based diagnosis (80%) [26].

Results were analyzed with Fisher's Exact Test (calculated with the software available on http://www.langsrud.com/fisher.htm [27]) and organized on graphics made by means of Microsoft Office Excel software.

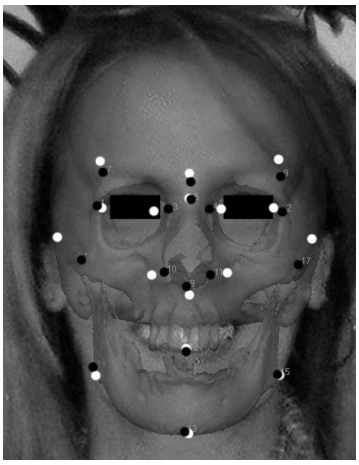

Fig. 2. Example of *match* with 2D-3D method (2L, 1M). Black target are bone landmarks while white target are soft tissue landmarks.

MORPHOLOGICAL FEATURES		LANDMARKS	
Length of the skull compatible with facial length	√	Ectocanthion R	√
Width of the skull fills the forehead	√	Ectocanthion L	√
Correspondence of the temporal line	NR	Subnasal Point	√
Eyebrow follows upper edge of orbit	√	Nasion	√
Eye is contained in the orbit	√	Glabella	√
Correspondence of lacrimal groove	√	Dacryon R	√
Similar breath of nasal bridge	√	Dacryon L	√
Dimensions of nasal aperture within borders of nose	√	Frontotemporale R	√
Anterior nasal spine is superior to the crus	√	Frontotemporale L	√
External auditory meatus is medial to the tragus	√	Gonial angle R	√
Correspondence of oblique line of the mandible	√	Gonial angle L	√
Correspondence of the curve of the mandible	x	Gnathion	√
		Zygion R	x
		Zygion L	x
		Alare R	√
		Alare L	√
		Superior Incisal	√

Table 1. Morphological features and landmarks examined in Fig. 2. "√" indicates the agreements, "x" indicates the disagreements and "NR" indicates a not observable features.

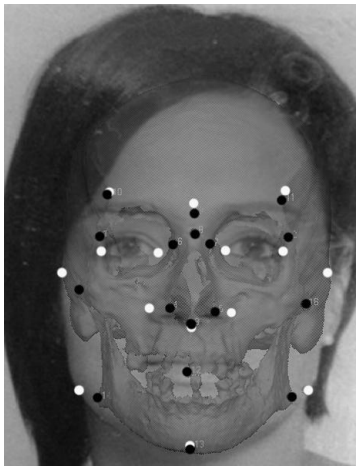

Fig. 3. Example of *mismatch* with 2D-3D method (4L, 2M). Black target are bone landmarks while white target are soft tissue landmarks.

MORPHOLOGICAL FEATURES		LANDMARKS	
Length of the skull compatible with facial length	√	Ectocanthion R	√
Width of the skull fills the forehead	x	Ectocanthion L	√
Correspondence of the temporal line	√	Subnasal Point	√
Eyebrow follows upper edge of orbit	√	Nasion	√
Eye is contained in the orbit	√	Glabella	√
Correspondence of lacrimal groove	√	Dacryon R	√
Similar breath of nasal bridge	√	Dacryon L	√
Dimensions of nasal aperture within borders of nose	√	Frontotemporale R	√
Anterior nasal spine is superior to the crus	√	Frontotemporale L	√
External auditory meatus is medial to the tragus	x	Gonial angle R	NR
Correspondence of oblique line of the mandible	x	Gonial angle L	x
Correspondence of the curve of the mandible	x	Gnathion	√
		Zygion R	x
		Zygion L	x
		Alare R	√
		Alare L	√
		Superior Incisal	NR

Table 2. Morphological features and landmarks examined in Fig. 3. "√" indicates the agreements, "x" indicates the disagreements and "NR" indicates the not observable features.

Results

First, an elaboration of results was needed in order to define the number of disagreements (cut-off) that best divide positive (real *matches*) from negative (real *mismatches*) results. The results of cut-off analysis was respectively 2 disagreements for complete skull and 1 disagreements for skull without mandible: with this thresholds, sensibility and specificity of the test were maximized together (Fig.4).

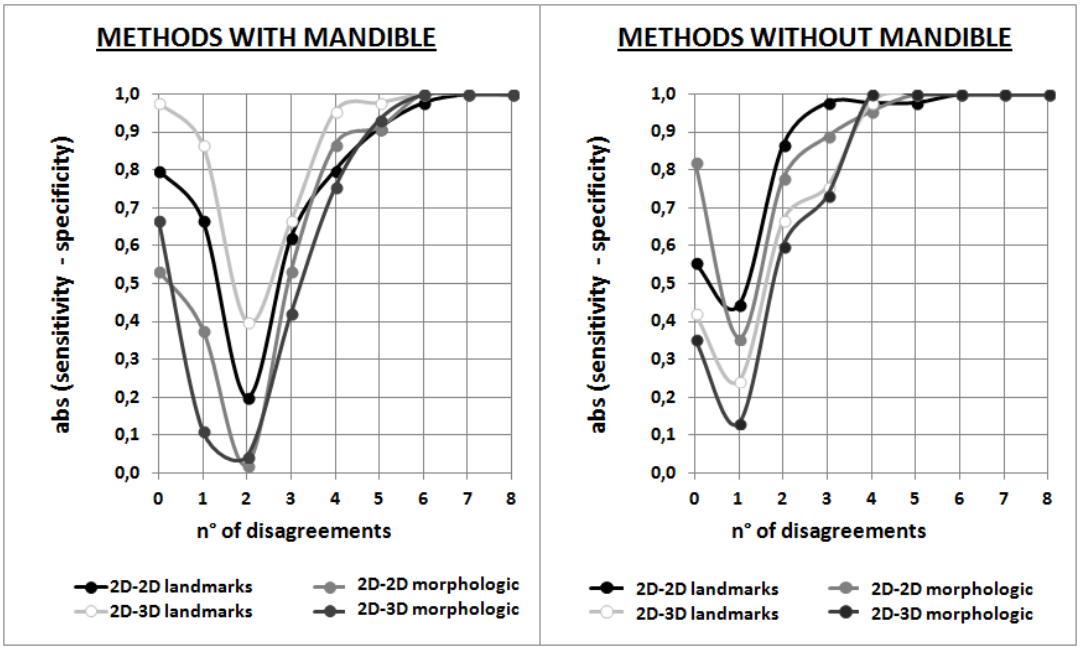

Fig. 4. Graphics show absolute difference between sensitivity (true positive rate) and specificity (true negative rate) as a function of the number of disagreements observed. The minimum of each curve identifies the cut-off point that corresponds to 2 disagreements for methods that utilize complete skull and only 1 disagreement for skull without mandible.

Applying the cut off values, 2D-2D method correctly identified 3 of 5 skulls (i.e. 3 real *matches* and 2 false negatives): in 60% of cases (3/5x100) the correct photo was included among the possible *matches*, while in 40% of cases (2/5x100) the photo belonging to its skull was evaluated as a *mismatch* (false negatives). However in addition to the corrected *matches* it was observed a 17,7% (8/45x100) of False

Positives, i.e. besides correct combination, other photos (from 0 to 3 photos) resulted in a positive *match*. Tab. 3 shows real *matches* and FP obtained with all the techniques analyzed in this study: combined methodology, methodology based only on landmarks and methodology based only on morphological features, both dividing and not dividing the subjects by sex. When taking into consideration subjects divided by sex, only results obtained from female subjects superimpositions (4 skulls and 7 photos) were evaluated, because the availability of male subjects (only 1 skull and 3

photos) was too scarce to reach objective results; so for each methodology 28 superimpositions (4 skulls x 7 photos) were analyzed for a total of 112 superimposition.

Skulls not dividing depending on sex		
METHODS	RM / 5	% FP
2D-2D COMBINED	3 / 5	17,7 %
2D-3D COMBINED	3 / 5	22,2 %
2D-2D w/out-m COMBINED	3 / 5	35,5 %
2D-3D w/out-m COMBINED	2 / 5	17,7 %
2D-2D LANDMARKS	4 / 5	40%
2D-3D LANDMARKS	5 / 5	40%
2D-2D w/out-m LANDMARKS	4 / 5	64,4 %
2D-3D w/out-m LANDMARKS	4 / 5	44,4 %
2D-2D MORPHOLOGIC	3 / 5	37,7 %
2D-3D MORPHOLOGIC	3 / 5	44, 4 %
2D-2D w/out-m MORPHOLOGIC	4 / 5	55,5 %
2D-3D w/out-m MORPHOLOGIC	2 / 5	46,6 %

Skulls dividing depending on sex (only female subjects)		
METHODS	RM / 4	% FP
2D-2D COMBINED	3 / 4	16,6 %
2D-3D COMBINED	3 / 4	25 %
2D-2D w/out-m COMBINED	3 / 4	45,8 %
2D-3D w/out-m COMBINED	2 / 4	16,6 %
2D-2D LANDMARKS	4 / 4	25 %
2D-3D LANDMARKS	4 / 4	33,3 %
2D-2D w/out-m LANDMARKS	3 / 4	54,1 %
2D-3D w/out-m LANDMARKS	3 / 4	33,3 %
2D-2D MORPHOLOGIC	3 / 4	45,8 %
2D-3D MORPHOLOGIC	3 / 4	54,1 %
2D-2D w/out-m MORPHOLOGIC	4 / 4	83,3 %
2D-3D w/out-m MORPHOLOGIC	2 / 4	58,3 %

TABLE 3. Results obtained from different techniques used without dividing skulls by sex (on the left), and dividing skulls by sex (on the right). The number of correct identifications (RM o real matches) obtained respectively from a total of 5 (male and female subjects together) and of 4 skulls (only female subjects) and the percentage of false positives (FP) on a total of respectively 45 (n/45x100) and 24 (n/24x100) real mismatches are indicated.

Analyzing results with Fisher's Exact Test (Tab. 4), and assuming as hypothesis H_0 that the obtained results were due to chance and, on the contrary, as hypothesis H_1 that the obtained results were not due to chance, it happens that, as far as superimpositions done with subjects not divided by sex, the 2D-3D technique which evaluates only landmarks with complete skull is the unique methodology that allows to exclude the hypothesis H_0 because p-value is lower than 0,05 (i.e. there is less than 5% probability that our results are fortuitous). That technique indeed identified all analyzed skulls (0 false negative), with 40% of FP out of 45 real *mismatches* .So considering the total of superimpositions carried out with this methodology the total of 50 superimpositions gave as results 23 *matches* (46%) and 27 *mismatches* (54%); 5 out of 23 obtained *matches* are real *matches,* while the remaining 18 are FP (36%; Fig. 5).

For superimposition carried out dividing skulls by sex, Fisher's Exact Test registered a p-value lower than 0,05; with the 2D-3D

technique based only on landmarks (p-value: 0,02) and with 2D-2D combined technique (p-value: 0,03). The first one (2D-3D) obtained 4 correct identifications out of 4 and 33% of FP out of 24 real *mismatches* (so on a total of 28 superimpositions carried out using only female skulls, resulted 16 *mismatches* and 12 *matches* (of which 4 are real *matches* and 8 are FP) (Fig. 6); the second one obtained 3 correct identifications out of 4 and the 16,67% of FP (Fig. 7).

Superimpositions without dividing skulls depending on sex					
METHODS (50 superimpositions)	RM	FN	FP	RmM	p-value
2D-3D LANDMARKS	5	0	18	27	0,01588
2D-2D COMBINED	3	2	8	37	0,06899
2D-3D COMBINED	3	2	10	35	0,10299
2D-2D LANDMARKS	4	1	18	27	0,10909
2D-3D w/out-m LANDMARKS	4	1	20	25	0,15045
2D-3D w/out-m COMBINED	2	3	8	37	0,25810
2D-2D w/out-m COMBINED	3	2	16	29	0,27486
2D-2D w/out-m MORPHOLOGIC	4	1	25	20	0,29145
2D-2D MORPHOLOGIC	3	2	17	28	0,30997
2D-2D w/out-m LANDMARKS	4	1	28	17	0,40054
2D-3D MORPHOLOGIC	3	2	20	25	0,42211
2D-3D w/out-m MORPHOLOGIC	2	3	21	24	0,77138
REAL VALUE	5	0	0	45	Tot. 50

Superimpositions dividing skulls depending on sex (only female subject)					
METHODS (24 superimpositions)	RP	FN	FP	RmM	p-value
2D-3D LANDMARKS	4	0	8	16	0,02417
2D-2D COMBINED	3	1	4	20	0,03760
2D-3D COMBINED	3	1	6	18	0,08410
2D-2D LANDMARKS	3	1	6	18	0,08410
2D-3D w/out-m LANDMARKS	3	1	8	16	0,15311
2D-3D w/out-m COMBINED	2	2	4	20	0,19145
2D-2D w/out-m COMBINED	3	1	6	18	0,29777
2D-2D MORPHOLOGIC	3	1	11	13	0,29777
2D-3D MORPHOLOGIC	3	1	13	11	0,41709
2D-2D w/out-m LANDMARKS	3	1	14	10	0,48156
2D-2D w/out-m MORPHOLOGIC	4	0	20	4	0,51897
2D-3D w/out-m MORPHOLOGIC	2	2	14	10	0,80390
REAL VALUE	4	0	0	24	Tot. 28

Table 4. P-value obtained with Fisher's Exact Test from superimpositions carry out without dividing skulls by sex (on the left) and from superimpositions carry out dividing skulls by sex (on the right). The value utilized to make contingency tables needing to make Fisher's Exact Test are listed: real *matches* (RM), false negatives (FN), false positives (FP) e real *mismatches* (RmM).

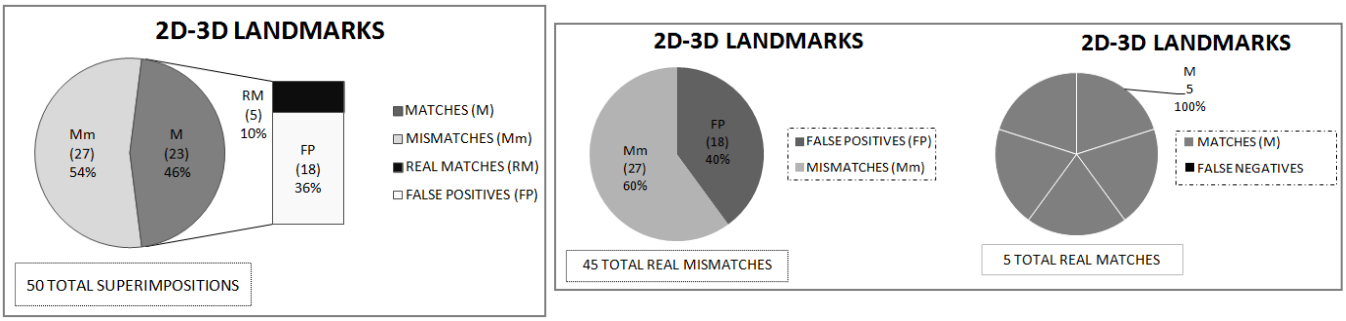

Fig. 5. Graphics show the distribution of results obtained with 2D-3D technique based only on landmarks for superimposition done without dividing skulls by sex. Results refer respectively to a total of 50 superimpositions carried out (Fig. 5a) and on a total of 45

real mismatches and 5 real matches (Fig. 5b). The value of matches (M), mismatches (mM), real matches (RM), false positives (FP) and false negatives (FN) are suggested.

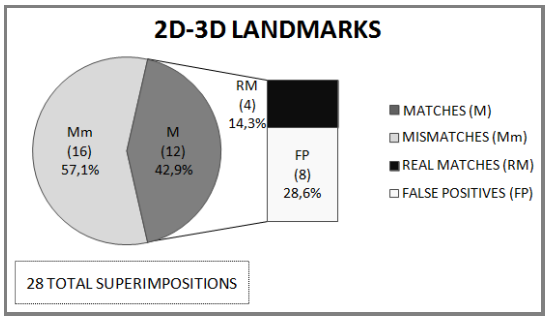

Fig. 6. Graphic shows the results obtained with 2D-3D techniques based only on landmarks for superimposition done dividing subjects by sex. On a total of 28 superimposition (only females subjects) the value of mismatches (mM), matches (M), real matches (RM) and false positives (FP) are suggested.

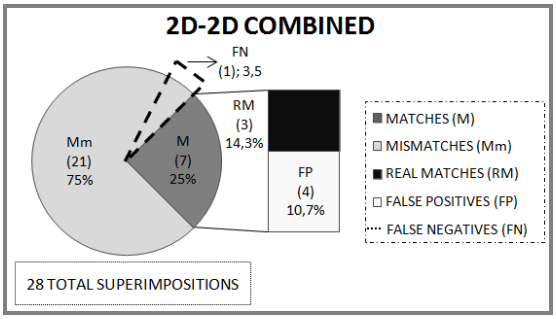

Fig. 7. Graphic shows the results obtained with 2D-2D combined techniques for superimposition done dividing subjects by sex. On a total of 28 superimposition (only females subjects) the value of mismatches (mM), matches (M), real matches (RM), false positives (FP) and false negatives (FN) are suggested.

Discussion

Cranio-facial superimposition has some issues that have been faced and evaluated in this survey.

A common point to all cranio-facial superimposition techniques that use targets proposed in literature, concerns the correct placement of landmarks especially on face (above all some landmarks as Frontotemporale, Gonion and Zygion): the correct apposition of targets, indeed, is affected by operator experience and skill. For this reason in our survey Superior Incisal point was added between landmarks because, if it is visible, it is surely easier and more safe to place if compared with others, since the compared structures (i.e. teeth) are the same both in face and skull [5, 28, 29].

Then we analyzed the number of morphological features and landmarks that should correspond to obtain a *match* between skull and photo. As described in the Results the threshold of 2 and 1 disagreements respectively for complete skulls and skulls without mandible is the one that maximize at the same time sensibility and specificity. If a threshold of 0 disagreements was established, *the methodology would result ineffective,* because the specificity would increase whereas there would be a decrease of sensibility (and so there would be less possibility to identify the positive results or real *matches*): considering all the four techniques, it would occur a drastic decrease both of FP (3,33%, i.e. 6 to 180 real *mismatches*) and of positive identifications (5%, i.e. only 1 to 20 real *matches*).

The use of skulls without mandible was proposed to verify if the intrinsic mobility of this bone could produce a greater number of errors in superimposition results : for instance if a subject laughs or has teeth not in occlusion, the Gnation, and the mandible's curve, moves lower. Mandible absence made results worse (2D-2D combined technique w/out-m and 2D-3D combined technique w/out-m produce respectively 60% and 40% of positive identifications with 35,5% and

17,7% of FP). This is probably due to the fact that without mandible the analyzed parameters are fewer and less peculiar, so there is an increase of FP; furthermore the orientation of skull without mandible is more difficult compared with complete skull.

Because of the restricted number of skulls used for superimpositions, Fisher's Exact Test was performed to verify the reliability of the methods: this test highlighted that when analyzing skulls not divided by sex, the 2D-3D superimposition based exclusively on landmarks was the only reliable technique (p-value 0,01), while if sex of the analyzed subject is known both the 2D-3D technique based only on landmarks (p-value: 0,02) and 2D-2D combined technique (p-value: 0,03) are reliable: the division of subjects by sex, as we expected, improves the results. When considering together male and female subjects, we had some correspondences even between subjects of different sex (FP), resulting in additional errors in the superimpositions.

The methodology that employs 3D model, compared with 2D image of the skull, results convenient from different point of view. Landmark placement and skull orientation are extremely easier with 3D model, therefore the time spent for a superimposition is enormously reduced: with 2D technique it takes on average 1.30 hours to produce a superimposition, while with 3D technique at most 10-15 minutes. It is important to remember that Vam, the stereophotogrammetry software used in this survey, is more user friendly if compared with other software utilized in other survey (as in Gordon et al. [18]), So, considering the 2D-3D techniques based only on landmarks, that is the most reliable technique on Fisher's Exact Test basis (p-value: 0,01), results (5/5 positive identifications; 40% FP) confirm that cranio-facial superimposition isn't still adapted to identify, because of the great percentage of FP; it could rather be utilized to exclude, thanks to the absence of false negatives, even if more researches need to test

this technique with a greater number both of inter-observers and analyzed skulls.

Finally this survey confirms that cranio-facial superimposition has to be used carefully and it shouldn't be utilized to identify for judicial purpose as reliability rate is still too poor.

Furthermore we confirmed that better results can be obtained using complete skulls and dividing them by sex, when it is possible. Finally we proved that the method based only on landmarks is more reliable if compared with that one which employs only morphological features or combined methods.

References

[1] Damas S, Cordon O, Ibanez O, Santamaria J, Aleman I, Navarro F et al. Forensic identification by computer-aided craniofacial superimposition: a survey. ACM Computing Surveys 2001;43(4):1-31.

[2] Dorion RB. Photographic superimposition. Journal of Forensic Science 1983 Jul;28(3):724-34.

[3] Brockleband LM, Holmgren CJ. Development of equipment for the standardization of skull photographs in personal identifications by photographic superimposition. Journal of Forensic Science 1983 Sep;34(5):1214-21.

[4] Maat GJR. The positioning and magnification of faces and skulls for photographic superimposition. Forensic Science International 1989 Jun; 41(3):225-35.

[5] Austin-Smith D, Maples WR. The reliability of skull/photograph superimposition in individual identification. Journal of Forensic Sciences 1994 Mar; 39(2):446-55.

[6] Fenton TW, Heard AN, Sauer NJ. Skull-photo superimposition and border deaths: identification through exclusion and the failure to exclude. Journal of Forensic Sciences 2008 Jan;53(1):34-40.

[7] Bastiaan RJ, Dalitz GD, Woodward C. Video superimposition of skulls and photographic portraits – A new aid to identification. Journal of Forensic Science 1986 Oct;31(4):1373-79.

[8] Iten PX. Identification of skulls by video superimposition. Journal of Forensic Science 1987 Jan;32(1):173-88.

[9] Yoshino M, Imaizumi K, Miyasaka S, Seta S. Evaluation of anatomical consistency in craniofacial superimposition images. Forensic Science International 1995;74:125-34.

[10] Shahrom AW, Vanezis P, Chapman RC, Gonzales A, Blenkinsop C, Rossi ML. Techniques in facial identification: computer-

aided facial reconstruction using laser scanner and video superimposition. International Journal of Legal Medicine, 1996;108(4):94-200.

[11] Yoshino M, Matsuda H, Kubota S, Imaizumi K, Miyasaka S, Seta S. Computer-assisted skull identification system using video superimposition. Forensic Science International 1997 Dec;90 (3):231-44.

[12] Jayaprakash PT, Srinivasan GJ, Amravaneswaran MG. Cranio-facial morphanalysis: a new method for enhancing reliability while identifying skulls by photo superimposition. Forensic Science International 2001;117:121-43.

[13] Pesce Delfino V, Colonna M, Vacca E, Potente F, Introna FJR. Computer-aided skull/face superimposition. American Journal of Forensic Medicine and Pathology 1986 Sep;7 (3):201-12.

[14] Bajnóczky I, Királyfalvi L. A new approach to computer-aided comparison of skull and photograph. International Journal of Legal Medicine 1995;108(3):157-61.

[15] Ghosh AK, Sinha P. An inusual case of cranial image recognition. Forensic Science International 2005 Mar;148(2-3):93-100.

[16] Ricci A, Marella GL, Apostol MA. A new experimental approach to computer-aided face/skull identification in forensic anthropology. American Journal of Forensic Medicine and Pathology 2006;27(1):46-49.

[17] Birngruber CG, Kreutz K, Ramsthaler F, Krähahn J, Verhoff MA. Superimposition technique for skull identification with Afloat software. International Journal of Legal Medicine 2010 Jul;124(5):471-75.

[18] Gordon GM, Steyn M. An investigation into the accuracy and reliability of skull-photo superimposition in a South African sample. Forensic Science International 2012;216:198.e1–198.e6.

[19] Takac S, Pilija V. Exclusion of identification by negative superposition.

Journal of the Antropological Society of Serbia 2012;47:311-16.

[20] De Angelis D, Cattaneo C, Grandi M. Dental superimposition: a pilot study for standardising the method. International Journal of Legal Medicine 2007;121(6):501-6.

[21] Ibanez O, Cordon O, Damas S. A cooperative coevolutionary approach dealing with the skull–face overlay uncertainty in forensic identification by craniofacial superimposition. European Centre for Soft Computing 2012;16:797-808.

[22] Goos MIM, Aberink IB, Ruifrok ACC. 2D/3D image (facial) comparison using

[23] Cattaneo C. Forensic anthropology: developments of a classical discipline in the new millennium. Forensic Science International 2007;165:185-93.

[24] Benazzi S, Stansfield E, Milani C, Gruppioni G. Geometric morphometric methods for three-dimensional virtual reconstruction of a fragmented cranium: the case of Angelo Poliziano. International Journal of Legal medicine 2009 Mar;123:333-44.

[25] Ishii M, Yayama K, Motani H, Sakuma A, Yasjima D, Hayakawa M et al. Application of superimposition-based personal identification using skull computed tomography images. Journal of Forensic Science 2011 Jul;56(4):960-6.

[26] Cattaneo C, Grandi M. Antropologia e odontologia Forense. Guida allo studio dei resti umani. Bologna: Monduzzi Ed, 2004.

[27] http://www.langsrud.com/fisher.htm

[28] Mckenna JJI, Jablonski NG, Fearnhead RW. A method of matching skulls with photographic portraits using landmarks and measurements of the dentition. Journal of Forensic Science 1984 Jul;29(3):787-97.

[29] Al-Amad S, McCullough M, Graham J, Clement J, Hill A. Craniofacial identification by computer-mediated superimposition. The Journal of Forensic Odonto-Stomatology 2006 Dec;24(2):47-52.

CAPITOLO 5

Does cone beam CT actually ameliorate stab wound analysis in bone?

Gaudio D, Di Giancamillo M, Gibelli D, Galassi A,
Cerutti E, Cattaneo C.

International journal of legal medicine (2013 Feb 08)[Epub ahead of print]

Int J Legal Med
DOI 10.1007/s00414-013-0820-0

TECHNICAL NOTE

Does cone beam CT actually ameliorate stab wound analysis in bone?

D. Gaudio · M. Di Giancamillo · D. Gibelli · A. Galassi · E. Cerutti · C. Cattaneo

Received: 2 August 2012 / Accepted: 4 January 2013

Abstract This study aims at verifying the potential of a recent radiological technology, cone beam CT (CBCT), for the reproduction of digital 3D models which may allow the user to verify the inner morphology of sharp force wounds within the bone tissue. Several sharp force wounds were produced by both single and double cutting edge weapons on cancellous and cortical bone, and then acquired by cone beam CT scan. The lesions were analysed by different software (a DICOM file viewer and reverse engineering software). Results verified the limited performances of such technology for lesions made on cortical bone, whereas on cancellous bone reliable models were obtained, and the precise morphology within the bone tissues was visible. On the basis of such results, a method for differential diagnosis between cutmarks by sharp tools with a single and two cutting edges can be proposed. On the other hand, the metrical computerised analysis of lesions highlights a clear increase of error range for measurements under 3 mm. Metric data taken by different operators shows a strong dispersion (% relative standard deviation). This pilot study shows that the use of CBCT technology can improve the investigation of morphological stab wounds on cancellous bone. Conversely metric analysis of the lesions as well as morphological analysis of wound dimension under 3 mm do not seem to be reliable.

Keywords Forensic sciences · Forensic anthropology · Cone beam CT · Sharp force lesions

D. Gaudio · D. Gibelli · E. Cerutti · C. Cattaneo (✉)
LABANOF, Laboratorio di Antropologia e Odontologia Forense,
Sezione di Medicina Legale e delle Assicurazioni,
Dipartimento di Scienze Biomediche per la Salute,
Università degli Studi di Milano, V. Mangiagalli 37,
Milan, Italy
e-mail: cristina.cattaneo@unimi.it

D. Gaudio · A. Galassi
U.O.S. di Medicina Legale, ULSS N. 6 di Vicenza,
Milan, Italy

M. Di Giancamillo
Dipartimento di Scienze Cliniche Veterinarie,
Università degli Studi di Milano, Milan, Italy

Introduction

Sharp force wounds, and especially stab wounds, are among the most common causes of death in cases of homicide [1]; in recent years, several studies have focused on this topic, which involves both forensic pathology and anthropology [2, 3]. The correct interpretation of the morphology of lesions on bone tissue may be crucial for recognizing the tool used and reconstructing the manner of events.

The analysis of the outer morphology of a lesion on bone especially is not always sufficient to reconstruct the type of weapon, its size and shape: analysis of the inner morphology may be needed, especially in cases of knife stab wounds [4], which cannot be completely analysed without destroying the sample or by using casts, difficult to perform on cancellous bone. In recent years, research in digital forensic medicine and osteology has been greatly developed [5–8] and different technologies have been applied to sharp force wounds [9–12]. In 2003, Thali et al. [10] verified Micro-CT technology; in their study, the authors tested the potential of a comparison between the inner morphology of the lesion and the tip of the weapon used. They argued that on the basis of the measured distances and of the angle of injury in a 3D volume dataset, it was possible to determine the size and the shapes of the injury-causing knife blade from the stab wounds. In 2012, Capuani et al. [11] acquired through this technology cut marks made on human clavicles by a hatchet, a serrated and non-serrated knife which were analysed by three different methodologies (light microscopy, SEM, Micro-CT) and these were then compared

with epifluorescence macroscopy. They paid attention to the aspect of walls and floor of the kerf so as to conclude on the nature of the lesion and distinguish between weapons used. The authors argued that Micro-CT allows the analysis of compact bones and spongious trabecular architecture with a very high resolution (in general, isometric voxel went from 10 to 100 μm; however, the resolution depends on the type of Micro-CT), but they concluded that this technology is far from the ideal tool to analyse knife lesions. Another limit of Micro-CT technology is that the samples must be very small and the bone may have to undergo partial destruction (since the gantry of the Micro-CT is very small compared to conventional CT Scan).

In our study we therefore opted for another kind of technology: cone beam CT scan (CBCT). This technology is mainly used in the odontological field for its capability of obtaining excellent resolution images from small and medium sized samples of calcified tissues. This radiological technique can be used in forensics and some applications have already been tested [13, 14]. The aim of the present study was to reproduce digital 3D models of sharp force wounds on bone tissue by the application of CBCT. This study aims at applying such a technology to sharp force wounds on bone tissue and at verifying the reliability of shape and metrical reconstruction, by using different software and with different observers. The experimental project was performed on two samples in order to obtain a 3D representation of the lesions, as well as information concerning the type of weapon, beyond the conventional modes of analysis. Three different software were used, both for visualization of the CT scan, and for reverse engineering in order to test their reliability in the study of sharp force wounds.

Materials and methods

The study was performed on fresh cancellous and cortical bone; bovine vertebrae were chosen as a model for cancellous bone. The spinal process was removed by a saw, and the vertebral body was cut in two halves. The lesions were then produced on the inner side of the vertebral body. The chosen weapons for the experiment were a knife with two cutting edges and a knife with only one cutting edge. On the bovine vertebra six lesions were made, three using a single cutting edge knife, and three with a double cutting edge knife.

A human ulnar diaphysis was chosen as a model for cortical bone. Ten stab wounds were made, five with the single cutting edge knife, and five with the double cutting edge knife. The experimental project was performed accordingly to the local ethical committee regulations.

The details of the lesions are shown in Table 1.

The two bone samples were then acquired by CBCT scan (Newtom 5G), which provides a high resolution thanks to the small isotropic voxels: for the cancellous and cortical bone, 100- and 300-μm slices, respectively, were acquired. The DICOM files were then imported into a software commonly used for the visualization of CT scans (InVesalius 3.0), where the DICOM format was then converted into STL files, and then imported into the software Geomagic 12 (trial version) and Rapidform.

The morphology of each lesion was then analysed using DICOM files by InVesalius 3.0 software and by reverse engineering software. In detail, Geomagic 12 was able to obtain a section of each sample (trim stack), which allows the operator to verify the lesion morphology in different perspectives.

In order to simplify the description of the experimental procedure, the authors did not use the anatomical axes for the analysis of sections, but chose as a reference the lesions themselves, which were divided in different planes as described in Fig. 1.

The morphology of each lesion was analysed according to three transverse planes, called upper transverse section, medial transverse section, lower transverse section.

This procedure delineated two-dimensional outlines of a three-dimensional object where that object intersects a plane and stores the outline(s) in "curved" objects, and therefore allows the operators to compare the morphology of each lesion at different depths within the bone tissue (Fig. 2c,d). The vertebral body underwent a 90° rotation in order to simplify the analysis (the procedure is shown in Fig. 2).

Only the six lesions on cancellous bone were measured by three different software programmes with the available

Table 1 Details of lesions made on cancellous and cortical bone

	Stabbing wounds				
Bone	Single cutting edge	Double cutting edge	Position	Type of bone	No. of lesions
Vertebra		×	Vertebral body	Cancellous	3
	×		Vertebral body	Cancellous	3
Ulna		×	Anterior surface of diaphysis	Cortical	5
	×		Anterior surface of diaphysis	Cortical	5

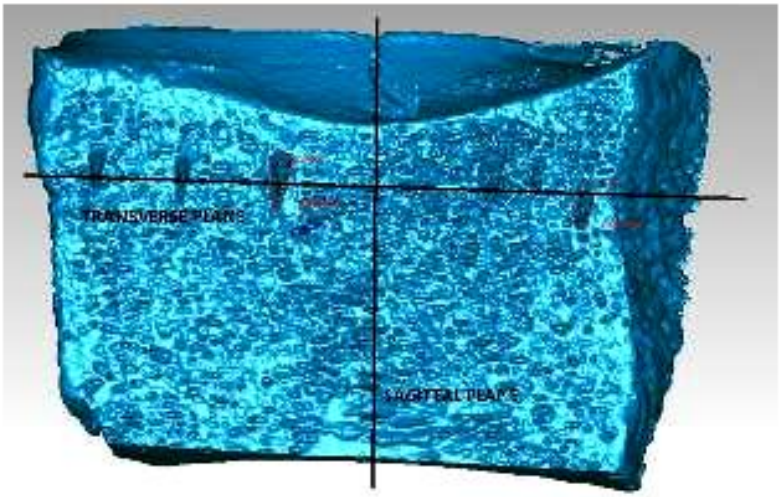

Fig. 1 The vertebral body divided into sagittal and transversal planes

measuring tools. For the lesions made by the single cutting edge weapons, which appeared as "isosceles triangles", the maximum length, the breadth and the depth were measured (Fig. 3). The same measurements were taken on the lesions made by the double cutting edge knife.

In order to evaluate the potential of the chosen measuring tools, two different operators, a forensic anthropologist, with experience in the use of reverse engineering software applied to osteological studies and a forensic pathologist, performed 54 measurements on the six knife stab wounds made on the cancellous bone in order to estimate inter-observer error; in addition, one operator (the anthropologist with experience in using the software) performed a new measurement 15 days after the first one in order to evaluate the intra-observer error. For what concerns the ten stab wounds on the cortical bone of the ulna, metrical assessment was impossible, since all the lesions were very superficial, because of the greater thickness and resistance of cortical bone which prevented the weapon from penetrating deep inside the bone structure. Therefore, because of their small size, the lesions did not show clear cut margins ;this made metrical assessment by reverse engineering and DICOM viewer software impossible (Figs. 4 and 5).

The DICOM files were then converted into STL, and the same lesions were analysed again. In Fig. 6 three stab lesions made by a single cutting edge knife are shown in a transverse section which was created in order to observe the

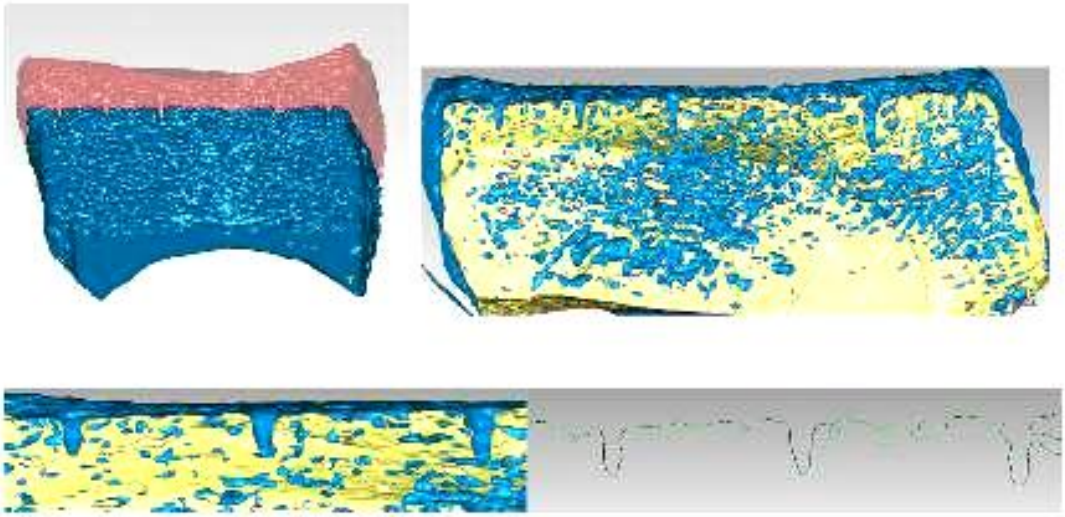

Fig. 2 On the *left*, top the vertebral body in rotation; on the *right* top section of a vertebra which has been rotated at 90° by tool Trim Stack, with section of lesions; below, on the *left* details of three sharp force wounds on cancellous bone; below on the *right* the depth and morphology of the lesion are highlighted by the curved object

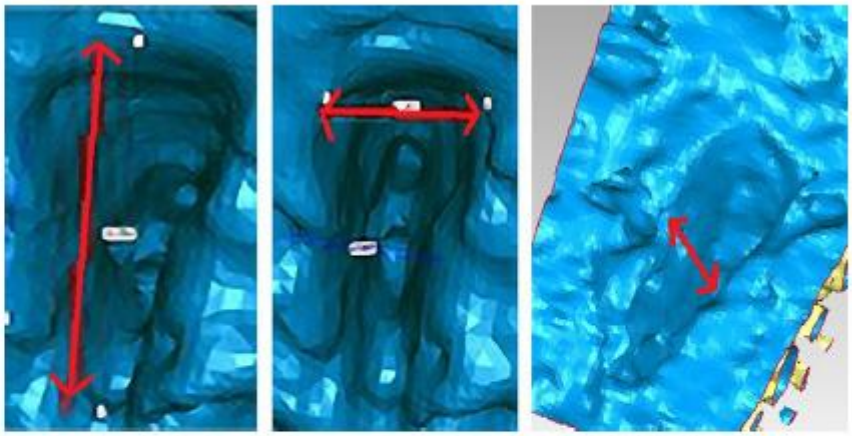

Fig. 3 Measurement of the length, breadth and depth of a lesion made by a single cutting edge knife by reverse engineering software

samples at different depths. The curved objects were then extracted in order to verify the specific morphology.

In order to verify the feasibility of a differential diagnosis of lesions made by single and double cutting edge knives, three transverse sections were created and the specific morphology of each lesion from both the chosen weapons was analysed on cancellous bone.

The same procedure was then repeated for the lesions by the two chosen weapons made on the cortical bone of the human ulna.

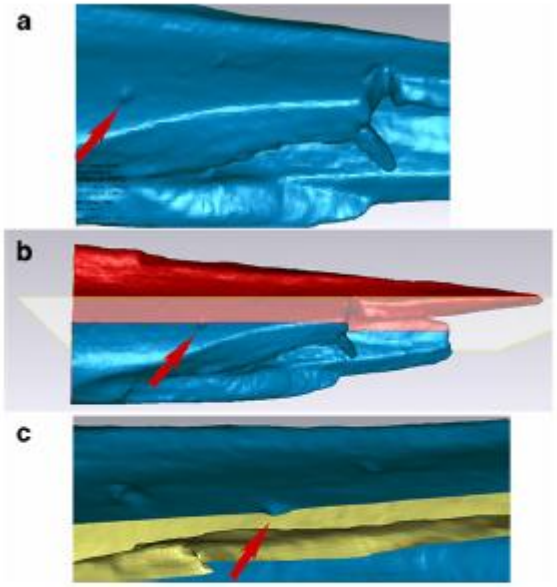

Fig. 4 a Details of a portion of the cortical bone of the ulna with one stab wound indicated by the *red arrow*; it is possible to observe how the lesion is shallow and difficult to detect. b Transverse section of the lesion, always indicated by the *red arrow*, split by an imaginary plane cutting it in half. c The section through the lesion (*red arrow*) shows the scarce definition of detail

In Table 2, the 54 measurements performed on the six lesions made on the cancellous bone are reported; the same measurements were impossible to take on cortical bone and therefore could not be used for metrical analysis.

In order to evaluate the dispersion of the measurements, the mean and standard deviation (expressed in mean percentage, %RSD) were evaluated (Fig. 7); we analysed the

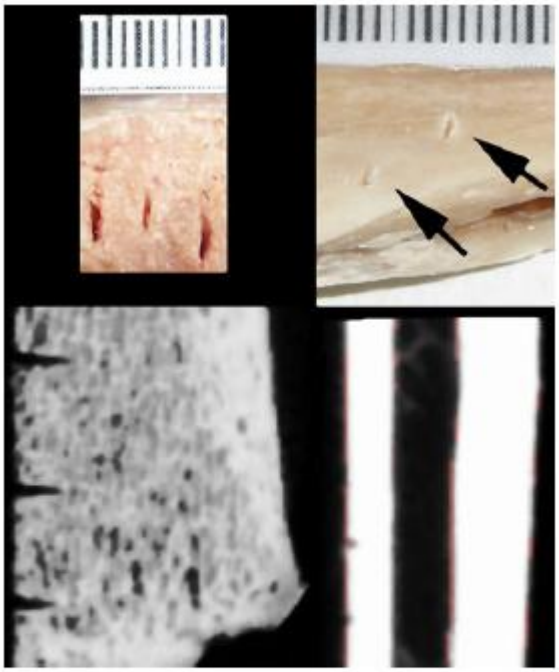

Fig. 5 The original stab wounds in cancellous bone of the bovine vertebra (*left*) and in the cortical bone of human ulna (*right*); below, cross section of cancellous (*left*) and cortical (*right*) lesions both analysed by CBCT: the lesion in the cortical bone is less visible, and the edges are not defined because of the smaller dimensions of the wound

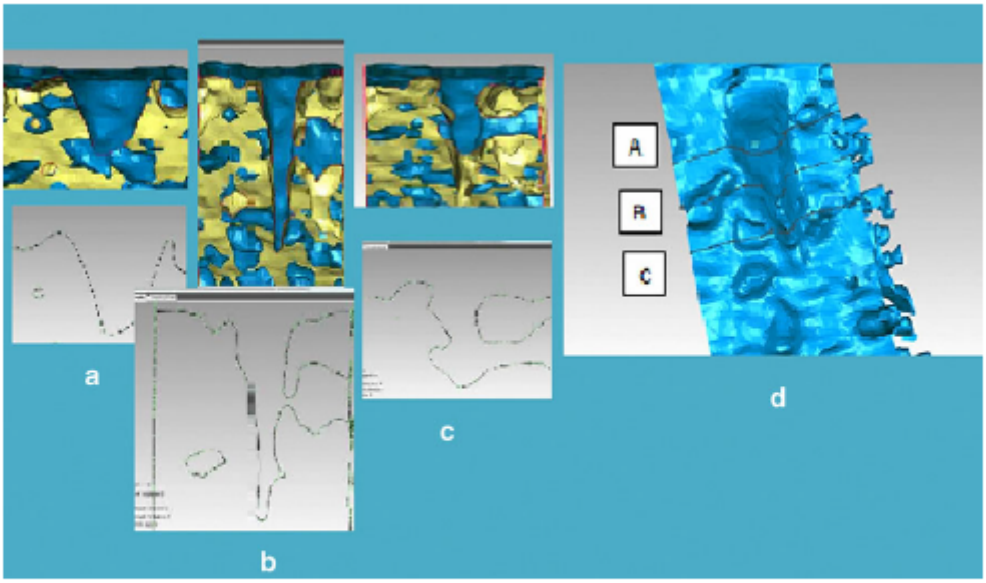

Fig. 6 Section of lesions made by the single cutting edge knife (cancellous bone): a morphology of upper transverse section; b medial transversal section; c lower transversal section; d morphology in the three transversal sections

dispersion of the measurements by three different software (Fig. 8). The same evaluation was made in order to verify the dispersion of the measurements on the three dimensions among different operators (Fig. 9).

Table 2 Details of the three observations: two by Intra Observer (Intra Observer time 0, and after 15 days Intra Observer Time 15 days) and one by Inter observer 2 (Inter Obs.) performed on the six sharp force lesions (From L1 to L6) with three different software (S1: InVesalious 3.0; S2: Geomagic 12 trial version; S3: Rapidform)

Size (mm) vs. lesion		X (length)			Y (breadth)			Z (depth)		
	Method of analysis 3 software vs. 3 observations	S1	S2	S3	S1	S2	S3	S1	S2	S3
L1	Intra Obs.Time 0	3.74	4.01	3.76	1.57	1.27	1.40	5.03	2.77	2.52
	Intra Obs. Time 15 days	3.63	4.21	3.84	1.37	1.45	1.27	3.86	2.60	2.78
	Inter Obs.	3.65	3.35	2.86	0.96	1.05	3.05	2.89	1.12	1.05
L2	Intra Obs. Time 0	3.45	3.00	3.56	1.46	0.96	1.01	5.03	3.03	2.10
	Intra Obs. Time 15 days	3.09	3.72	3.79	0.90	0.95	1.30	3.00	2.94	3.87
	Inter Obs.	3.53	3.50	3.06	0.87	0.84	0.93	2.87	1.91	0.69
L3	Intra Obs. Time 0	4.01	4.02	4.11	1.46	2.02	1.71	5.02	5.04	4.76
	Intra Obs. Time 15 days	4.20	3.81	5.09	1.29	2.31	1.83	4.86	4.97	4.15
	Inter Obs.	4.28	3.52	4.98	1.47	2.18	3.50	5.34	2.84	0.69
L4	Intra Obs. Time 0	4.58	5.25	5.29	1.15	1.78	1.96	3.68	4.03	3.72
	Intra Obs. Time 15 days	4.40	5.07	5.15	1.07	1.85	1.68	3.87	3.92	3.06
	Inter Obs.	4.70	5.16	5.03	1.32	1.93	3.31	3.86	1.93	3.14
L5	Intra Obs. Time 0	3.33	3.82	3.44	1.23	1.27	1.26	2.75	2.93	2.89
	Intra Obs. Time 15 days	3.70	3.96	4.17	0.99	1.40	1.33	2.69	2.66	2.82
	Inter Obs.	3.77	4.08	3.80	1.04	1.40	1.64	2.98	1.97	1.30
L6	Intra Obs. Time 0	3.39	3.28	3.38	1.22	1.14	1.18	2.64	2.99	2.61
	Intra Obs. Time 15 days	3.41	3.99	3.83	1.08	1.44	1.36	2.93	2.33	2.83
	Inter Obs.	3.53	3.87	3.84	1.01	1.59	0.70	2.81	2.66	1.22

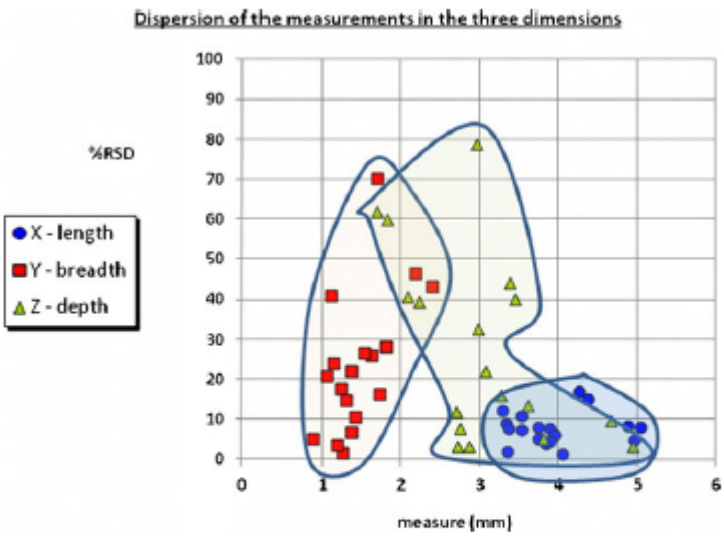

Fig. 7 Dispersion of the measurements in the three dimensions; in *Y*-axis the percentage of relative standard deviation; in *X*-axis the measurement in mm: length shows a limited dispersion over 3 mm

Results

CBCT acquisition easily demonstrated the lesions on the cancellous bone and all the images provided were at high resolution; this allowed us to analyse in depth from a morphological and metrical point of view the lesions in the cancellous bone. The conversion of DICOM files in STL files with reverse engineering software allowed us to obtain an extremely realistic 3D model; in this way, the models could be analysed by defining an infinite number of section planes: such a procedure can be performed only by using 3D image representation techniques, if one aims at preserving the sample integrity.

Results obtained by metrical analysis, divided into length, breadth and depth, are shown in Table 2. The 54 measurements are compared according to the type of parameter, the observer and the type of software. The mean intra-observer error was, considering all the measurements, 0.17 mm (5.8 % of the measurement, SD 0.13); the mean inter-observer error was 0.6 mm (20.5 % of the measurement, SD 0.6 mm).

For what concerns the lesions made by the knife with a single cutting edge, the mean measured length varied between 3.3 and 5.3 mm, the mean breadth between 0.7 and 3.3 mm, the mean depth between 1.2 and 4 mm; for what concerns the lesions made by the knife with two cutting edges, the mean measured length varied between 2.9 and 5.1 mm, the mean breadth between 0.8 and 3.5 mm, the mean depth between 0.7 and 5.3 mm. Differences between software were considered as well: the mean length measured in InVesalious 3.0 was 3.8 mm (SD 0.5 mm), the mean breadth was 1.2 mm (SD 0.1 mm), the mean depth was 3.7 mm (SD 0.8 mm).

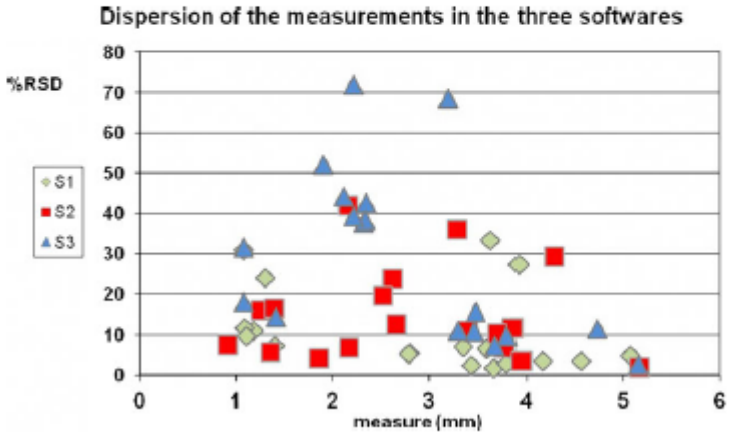

Fig. 8 Dispersion of the measurements in the three software (*S1*: InVesalious 3.0; *S2*: Geomagic 12; *S3*: Rapidform). In *Y*-axis the percentage of relative standard deviation; in *X*-axis the measurement in mm: the highest dispersion values are shown in mean by Rapidform

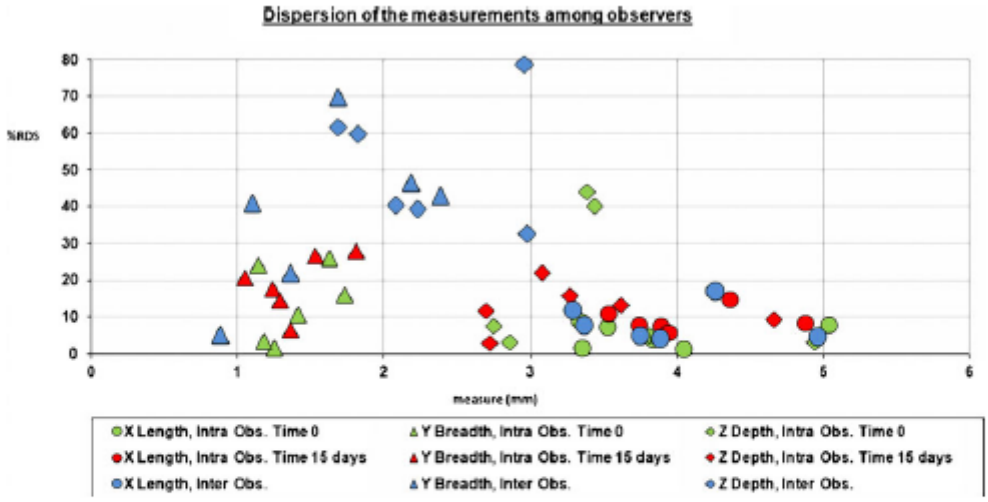

Fig. 9 Dispersion of the measurements among observers (*green*: Intra Observer time 0; *red*: Intra Observer Time 15 days; *blue*: Inter Observer). In *Y*-axis the percentage of relative standard deviation, in *X*-axis the measurement in mm: over 3 mm almost all the measurements show a limited dispersion in both observers

For Geomagic 12 (trial version), the mean length measured was 4.0 mm (SD 0.6 mm), the mean breadth was 1.5 mm (SD 0.4 mm), and the mean depth was 2.9 mm (SD 0.8 mm).

For Rapidform, the mean length measured was 4.1 mm (SD 0.7 mm), the mean breadth was 1.7 mm (SD 0.6 mm), and the mean depth was 2.6 mm (SD 0.5 mm). The degree of dispersion of each parameter is shown in Figs. 7 and 8.

As concerns the real size of the tip of the penetrating tools, the breadth of the two weapons was measured at the mid-depth of the lesions observed in bones. The breadth of the tip of the knife with a single cutting edge at 2.9 mm from the tip was 1.6 mm, whereas the same parameter in the knife with two cutting edges at a distance of 3.3 mm from the tip was 1.3 mm. According to the evaluated parameters of the two weapons, the most reliable software was InVesalious 3.0 for the lesions produced by the knife with two cutting edges (where it shows also the least dispersion of measurements), and Rapidform for the lesions produced by the knife with one only cutting edge (although with the highest dispersion of data among the three software).

Instead, the visibility of the stab marks on the cortical bone, as previously anticipated, was low and not sufficient for metrical assessment.

Discussion

The first results of this pilot study show the potential of CBCT technology in recording sharp force lesions, particularly stab wounds, in bone. The digital elaborations highlighted a high quality which allows the operator to extract sections, curves and linear measurements.

This technology seems to be promising in the documentation of knife stab wounds, and in detail in cases where the traditional casting techniques are more problematic, for example on cancellous bone. The lesions are in fact easily recognizable and their exploration is possible by the DICOM files viewer software.

If the model is imported into an inverse engineering software in the adequate format (in this case, STL files), the morphology of the lesion can be analysed in different transversal planes; this makes it possible to differentiate lesions made by single and double cutting edge knives, since their characteristics seem to be clearly different: in lesions made by the single cutting edge knife the transverse planes describe a trapezoidal shape in the upper section, which then changes into a pyramidal shape with a decreasing depth. In lesions made by a double cutting edge knife, the morphology was homogeneous, and the sections obtained by transversal planes have the shape of isosceles triangles. Therefore the morphological assessment of lesions may be useful for the recognition of the used weapon. The same is not valid for the lesions on cortical bones, where they are less visible and can be measured only with great difficulty. Also the differential diagnosis is less reliable, and in fact a clear difference in morphology between the two types of lesions was not observed in any transverse section. This can be clearly seen in Fig. 4, where the cross section of the lesion shows an indefinite shape.

Differently, Martens et al. [15] observed a higher significance in the detection of a bone lesion in the cortico-trabecular

area in the mandible than in trabecular bone. One problem could be the minimal threshold level, inadequate for the study on long bones; however, further studies would be helpful in supporting this conclusion. On the other hand, in the literature few articles concern the use of CBCT in these conditions and acquisition protocols are not described. Probably a customized resolution protocol must be chosen according to the accuracy needed; however these results need to be confirmed by further analysis on a larger sample.

The limited number of measurements prevents us from drawing any statistical conclusion, but the preliminary results highlight interesting suggestions for what concerns the dispersion of measurements for the three dimensions, the three software and the error among operators; in the former case, the same measurements show a high error range, which may be caused by the scarce precision of the applied procedures by the different observers. However, the higher the measurement the less the error range; in detail, above 3 mm the precision of each measurement considerably increases (Fig. 7).

For what concerns the measurements by the three chosen software, although the scarce precision of the measuring procedure is confirmed, the preliminary results show that InVesalius software is affected by a lower dispersion of data, probably because it allows the operator to choose the correct reference points with less difficulty (in fact, a high dispersion of measurements in all the three observations was verified). This result seems to suggest that DICOM files are more adequate for metrical analyses, although further studies based on a larger sample are needed in order to confirm this conclusion. In addition, InVesalious (which works with DICOM files) was the most precise among the three software in measuring the breadth of lesions produced by the knife with two cutting edges, whereas Rapidform (which, in this study, instead works with STL files) was the most precise in measuring lesions produced by the knife with one only cutting edge (these evaluations were performed using as reference the breadth of the tip of knives used for the experiment).

Furthermore, the high dispersion of the intra and interobserver errors on measurements obtained (% relative standard deviation) (Fig. 9) raises doubts about the reliability of measurements seen with this software. In detail, the highest precision of measurements shown by the forensic anthropologist in comparison with the second observer suggests that the experience in 3D image elaboration software somehow is important in defining the edge of each lesion and therefore brings about greater accuracy and precision. This information therefore points out the role of adequate training in reverse engineering technologies for adequate metrical assessment.

Some considerations concerning the inapplicability of such measuring techniques on the cortical lesions should be made. For what concerns the ten stab wounds on the cortical bone of the ulna, as previously mentioned, metrical assessment could not be performed since the lesions were very superficial due to the greater thickness of the bone which prevented the weapon from further penetrating into the bone structure. The stab wounds on cortical bone in fact seem to be in mean only 1 mm deep, whereas the same lesions in the vertebral body show a depth of up to 4 mm (Table 1). The depth of the lesions in the ulna therefore is only slightly greater than the resolution of CBCT technology applied in the present article (0.3 mm circa). The lesion can therefore be roughly "seen" but not accurately measured. In addition, the visualization of these lesions by 3D image software and DICOM viewers are affected by a variable resolution which depends upon the type of images, software, mode of analysis all factors whose influence cannot be easily pinpointed and defined. In this case, the application of 3D software was not able to detect the lesions in ulnar cortical bone with enough resolution. As a consequence the entire analysis was not able to detect the edge and shape of lesions probably because of the metrical and graphic limits which translate into an insufficient resolution. In the case of the vertebral body, the greater penetration of the weapon produced a lesion with greater length and breadth and thus the lesion was more clearly detectable.

All these considerations suggest that the application of CTCB to bone lesions is not an automatic procedure, but requires a precise evaluation of advantages which may derive from such an approach; in addition, experience in 3D image elaboration is needed in order to obtain the best results. Further studies are needed in order to verify the applicability of such technology to stab wound analysis. At the moment, the preliminary results recommend great caution in the choice of the software for the metrical analysis and in extrapolating metrical and morphological data in general from small osseous stab wounds.

Conclusion

In conclusion, the first results of this pilot study verified the potential of the reproduction of knife stab wounds by CBCT technology, which is very good in case of cancellous bone. The available measuring tools of an inverse engineering software (Geomagic 12 trial version) allowed the authors to verify the exact morphology of the lesions within the bone tissue, and to assess a method for differential diagnosis between single and double cutting edge weapons. All this with a technology that does not require reduction of the sample and which is relatively cheaper than microCT.

The morphological analysis, however, is more reliable than the metrical assessment, which was performed by different observers and by three different software, in every case with high percentual standard deviations for measurements below 3 mm. On the basis of this preliminary study, metric data taken through the use of 3D software from different operators has a

strong dispersion. The results obtained by means of these methodologies must therefore be treated with great caution.

Acknowledgments The authors thank Dr Nicola Guercini, Human Genetic Unit, S.Bortolo Civil Hospital of Vicenza

References

1. Martin IR (1999) Identifying osseous cut mark morphology for common serrated knives. MA thesis, Department of Anthropology, University of Tennessee Knoxville
2. Houck MM (1998) Skeletal trauma and the individualization of knife marks in bones. In: Reichs KJ (ed) Forensic osteology: advances in the identification of human remains. Charles C. Thomas Publisher, Springfield, pp 410–421
3. Symes SA, Smith OC (1998) It takes two: combining disciplines of pathology and physical anthropology to get the rest of the story. Proc Am Acad Forensic Sci 4:208
4. Symes S et al (2002) Taphonomical context of sharp trauma in suspected cases of human mutilation and dismemberment. In: Haglund WD, Sorg MH (eds) Advances in forensic taphonomy: method, theory and archaeological perspectives. CRC Press, New York, pp 403–434
5. Thali MJ, Braun M, Dirnhofer R (2003) Optical 3D surface digitizing in forensic medicine: 3D documentation of skin and bone injuries. Forensic Sci Int 137(2–3):203–208
6. Thali MJ, Braun M, Buck U et al (2005) Virtopsy—scientific documentation, reconstruction and animation in forensic: individual and real 3D data based geometric approach including optical body/object surface and radiological CT/MRI scanning. J Forensic Sci 50 (2):428–442
7. Verhoff MA, Ramsthaler F, Krähahn J et al (2008) Digital forensic osteology—possibilities in cooperation with the Virtopsy® project. Forensic Sci Int 174(2–3):152–156
8. Fourie Z, Damstra J, Gerrits P, Ren Y (2011) Evaluation of anthropometric accuracy and reliability using different three-dimensional scanning systems. Forensic Sci Int 207(1–3):127–134
9. Jackowski C, Bolliger S, Thali MJ (2009) Sharp trauma. In: Thali MJ, Dirnhofer J, Vock P (eds) The Virtopsy approach 3D optical and radiological scanning and reconstruction in forensic medicine. CRC Press, New York, pp 493–497
10. Thali MJ et al (2003) Forensic microradiology: micro-computed tomography (Micro-CT) and analysis of patterned injuries inside of bone. J Forensic Sci 48(6):1336–1342
11. Capuani C et al (2011) Deciphering the elusive nature of sharp bone trauma using epifluorescence macroscopy: a comparison study multiplexing classical imaging approaches, Int J Legal Med [Epub ahead of print]
12. Pounder DJ et al (2011) Virtual casting of stab wounds in cartilage using micro-computed tomography. Am J Forensic Med Pathol 32 (2):97–99
13. Von See C et al (2009) Forensic imaging of projectiles using cone-beam computed tomography. Forensic Sci Int 190(1–3):38–41
14. Murphy M et al (2012) Accuracy and reliability of cone beam computed tomography of the jaws for comparative forensic identification: a preliminary study. J Forensic Sci [Epub ahead of print]
15. Martens S et al (2009) Radiographic detection of artificial bone lesions in an *in vitro* mandible. Presented at the 17th International Congress of Dentomaxillofacial Radiology, Amsterdam

CAPITOLO 6

Application of high resolution pQCT analysis to forensic cases for the assessment of bone trauma: a technical note

Rubinacci A, Tresoldi D, Villa I, Rizzo G, Gaudio D, De Angelis D, Gibelli D, Cattaneo C.

To be submitted International Journal of Legal Medicine

Technical note

Application of high resolution pQCT analysis to forensic cases for the assessment of bone trauma: a technical note

Rubinacci A[1],MD, Tresoldi D[2], Villa I[1], PhD, Rizzo G[2], Gaudio D[3] ,BSc De Angelis D[3] MD. PhD MD, Gibelli D[3] MD PhD Cattaneo C[3], MD, PhD

[1]Bone Metabolism Unit
Scientific Institute San Raffaele, Milano

[2]Institute of Molecular Bioimaging and Physiology,
CNR, Segrate (Milan), Italy

[3]LABANOF, Laboratorio di Antropologia e Odontologia Forense
Sezione di Medicina Legale
Dipartimento di Scienze Biomediche per la Salute
Università degli Studi di Milano

Abstract

The evaluation of bone trauma has been considerably improved by the introduction of the most recent technologies; in the last years the peripheral quantitative computed tomography (pQCT) has found new fields of application in clinical medicine, but none of them concerns the forensic practice.

This study exposes the potential of pQCT applied to forensic scenario throughout a real case, concerning a mummified corpse of a 16 year old girl. The autopsy pointed out several sharp force wounds at the chest. Among the others, a specific penetrating lesion affected the body of the first thoracic vertebra, deepening within the underlying cancellous bone. A pQCT scanner was used for the measurements (Research SA+; Stratec Medizintechnik GmbH, Pforzheim, Germany). A more precise reconstruction of the path of the lesion within the trabecular bone was reached, with more details concerning the morphological characteristics of the lesion inside the vertebral bone and the elaboration of a 3D model was created, which allowed the operator to define the volume of the lack of tissues related to the lesion. The application of pQCT scan proved to be a potentially useful tool for assessment of bone trauma, although further studies are needed in order to verify its reliability.

Keywords: forensic anthropology; pQCT; bone trauma, sharp force

Introduction

An accurate analysis of bone fractures is crucial for determining cause and manner of death; the accurate fracture interpretation is essential for identifying the location of impact sites, establishing multiple impact sites, sequence of blows and the characteristics of the weapon (1). From this point of view the study of bone lesions is one of the main topic in forensic anthropology and pathology. In particular the analysis of Sharp force wounds, and especially stab wounds, is as crucial as problematic: the correct interpretation of the morphology of lesions on bone tissue may be fundamental to recognize the tool used and reconstructing the way of inflicting trauma, however the small dimensions of lesions often don't allow an exhaustive interpretation about the weapon that produced them.

This topic has known in the last years a crucial development by the application of most advanced technologies such as scanning electron microscopy coupled with X-ray energy dispersive spectrometry (SEM-EDS) (2,3) and traditional CT scan and NMR technologies (4,5,6,7), and the application of new techniques which allow the operator to draw a more precise visualization of bone structure, such as cone beam computed tomography (8,9).

So what are the radiological technologies more effective to document and investigate very small lesions, but fundamental in order to reconstruct manner of death, like sharp wounds? The Micro-CT technology allows us to reach very high in resolution compared to conventional CT (in general isometric voxel was from 10 to 100 microns, the resolution depends of the type of Micro-CT), however bones may have to undergo partial destruction. Cone Beam technology (used in the odontological field) can also be used on middle or little size samples, without causing their distruction. The first studies concerning the employment of this technology for the documentation of Sharp Wounds on spongy bones seem to lead to promising results (9).

The natural history of forensic sciences is characterized by the progressive implementation in the forensic practice of the most advanced technologies, usually previously developed with clinical purposes, with a consequent improvement of morphological and metrical details of bone structures. This has led in some cases to the "blind" application of such techniques to the forensic cases, without a preliminary evaluation concerning the specific issues which can be adequately and specifically evaluated by the new technologies, usually determined by the idea that technology means more information. This point of view was denied in the last years by different authors which underlined the existence of specific factors of variability which affect the analysis of corpses and define the complementary nature of the new techniques with regards to

the classical morphological autoptical and forensic anthropological approaches (10).

On the other hand, some methods may bring about relevant improvements in the field of bone assessment, since they may meet specific limits which cannot be faced by other methodologies or the traditional morphological analysis. This is the case of the morphological evaluation of signs of trauma on trabecular bone, which is usually difficult to assess by the macroscopic, microscopic (SEM-EDX) and radiological methods because of the most irregular disposition of bone trabeculae and the absence of the compact structure of the cortical bone (moreover the traditional casting techniques are problematic on cancellous bone). The recent introduction of Peripheral Quantitive Computerized Tomography (pQCT) may give some help in this sensitive field of research: it is a tomographic technique able to assess quantitatively the densitometric properties of bone. In addition, current pQCT scanners have a sufficient resolution (70 µm) to visualize the trabecular network of human bone in the three spatial dimensions (11), and therefore allow the operator to reconstruct an accurate geometrical and densitometric model of bone which takes into account both macro and microstructural components (12). The use of specific developed software can provide a 3D model of the bone specimen, based on the information obtained by the scanner. In this way, this technology allows the observer to obtain a virtual model of the bone sample which can be analysed in three dimensions; in addition, the specific properties of the pQCT make easier the analysis of the trabecular bone, which is traditionally difficult to assess by the classic radiological methods.

At the moment, pQCT has been applied to different field of research, especially for the evaluation of osteoporosis and bone distribution, thanks to its accuracy in analysis of trabecular bone (13-14, 15). In addition, recently it has been used for investigating the anatomy of dental root canals and canal volumes changes after instrumentation (16). However, at the moment no study has been yet still performed concerning the possible application of such technology to the forensic scenario, for example for assessing bone trauma in trabecular bone.

This study aims at providing the first example of application of pQCT to a real forensic case in order to highlight the advantages which may derive from the use of such modern technique.

Case report

In 2010 a mummified corpse of a 16 year old girl was found in a church; the subject was seen alive for the last time in 1993. The autopsy pointed out several sharp force wounds at the chest. Ribs, cervical and thoracic vertebrae and the scapulae were recovered and cleaned by mummified tissues in order to analyse in depth the bone lesions. Among the others, a specific penetrating lesion affected the body of the first thoracic

vertebra (Fig. 1), deepening within the underlying cancellous bone. The morphology of the lesion and its position inside a bone rich in trabecular bone required more detailed radiological tests, among which a conventional TC scan which gave general indications concerning the depth and breadth of the lesion.

A pQCT scanner was therefore used for the measurements (Research SA+; Stratec Medizintechnik GmbH, Pforzheim, Germany). This translation rotation scanner works with a specially developed X-ray tube with a 50-lm spot size (high voltage 50 kV, anode current <0.3 mA, mean X-ray energy 37 keV, energy distribution after filtration 18 keV full width half maximum [FWHM]). The detector-system consists of 12 miniature semiconductor crystals with amplifiers. The precision error supplied by the manufacture for density measurement in vivo is around 1.5%. All images were obtained with 360 projections, with a section thickness of 100 µm and at in-plane pixel size of 100 x 100 µm. The thoracic vertebra was positioned in the centre of a perspex container made for this purpose and total scanning time was 4 hours.

A more precise reconstruction of the path of the lesion within the trabecular bone was reached (Fig. 2), with more details concerning the morphological characteristics of the lesion inside the vertebral bone. In addition, a 3D reconstruction and visualization of the structure of interest was created. Briefly the procedure consisted in the following steps: 1) slice by slice bone contour extraction using an already validated algorithm to divide bone tissue from background [13, 14]; 2) definition of the area characterized by lack of tissues due to the lesion and its contour; 3) starting from these contours (bone and lesion area), generation of a 3D model as a polygonal mesh structure; 4) 3D rendering of the mesh model, characterizing, each structure of interest with specific colour, brightness and transparency (Fig. 3). In this way, the visualization of the inner walls of the lesion was also possible with the chance of taking measurements of the linear and volume parameters (Fig. 4).

Discussion and conclusion.

In the last year the forensic practice has seen a constant and progressive increase of application of the most modern technologies, usually implemented from the clinical context. The recent introduction of pQCT has considerably increased the precision of analysis of the trabecular bone, which is usually difficult to assess by traditional microscopic or radiological techniques. From this point of view the present case study has shown an increased definition of one lesions within the spongeous bone; in addition, the details of the 3D models provide an improved evaluation of the morphology and metrical parameters of bone lesions, with respect to the conventional CT scan which fails in defining the lesions edges within the trabecular bone. In addition, the 3D

reconstruction of the volume showing lack of tissue allows the operator to extrapolate relevant information concerning the metrical parameters of the lesion, with a clear amelioration for what concerns the reconstruction of the used weapon.

Finally, the pQCT technology allows to obtain a good resolution (70 µm, more high of CT Cone Beam)

This first example of the application of such technology to a forensic case shows the potential of pQCT for the assessment of bone trauma, although, as observed for other modern technologies applied to the forensic field, some points of criticism need to be overcome, especially for what concerns the correct evaluation of the lesion path within the trabecular bone. Further studies are therefore needed in order to correctly define the limits of such technology.

Fig. 1: detail of the sharp force lesion on the first thoracic vertebra (in the red square) with details of the same lesion by stereomicroscopy

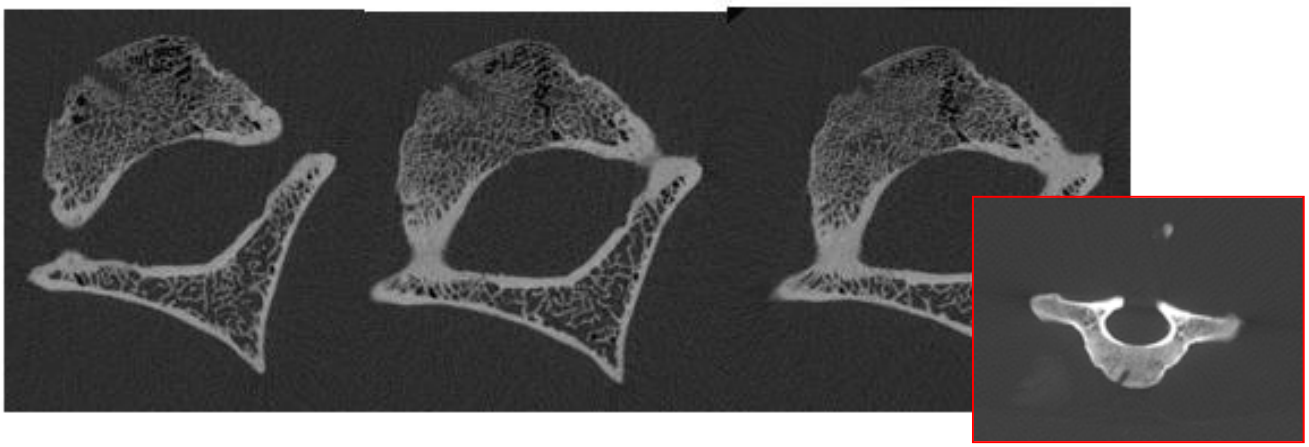

Fig. 2: visualization of the vertebral lesion by use of pQCT; in the red square, image of the same lesion by conventional CT scan

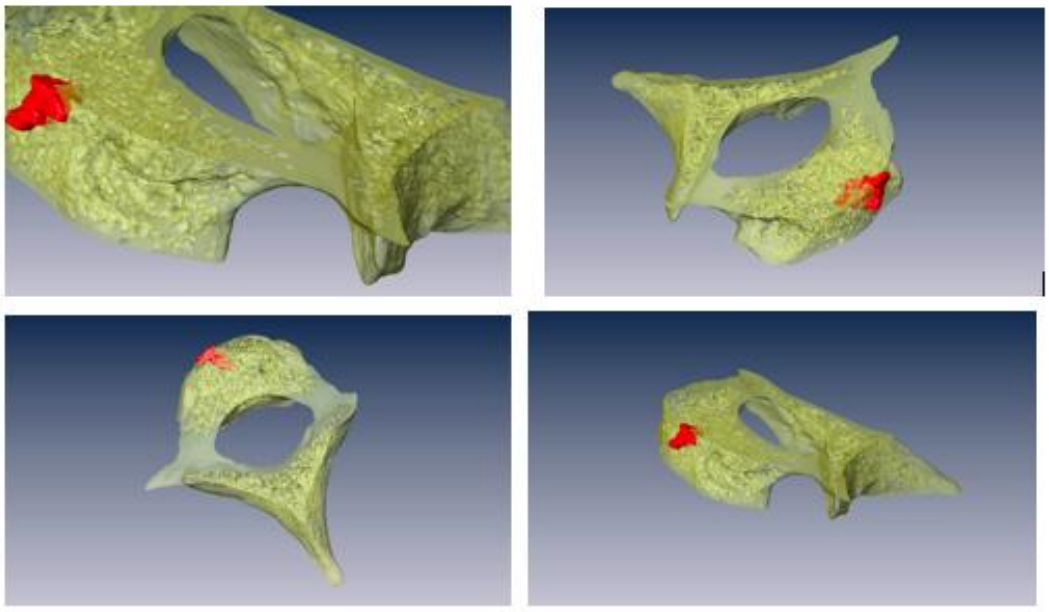

Fig. 3: rapresentative 3D rendering of the model of the first thoracic vertebra acquired by pQCT; the bone is coloured in yellow and shown in transparency, the bone lesion is in red.

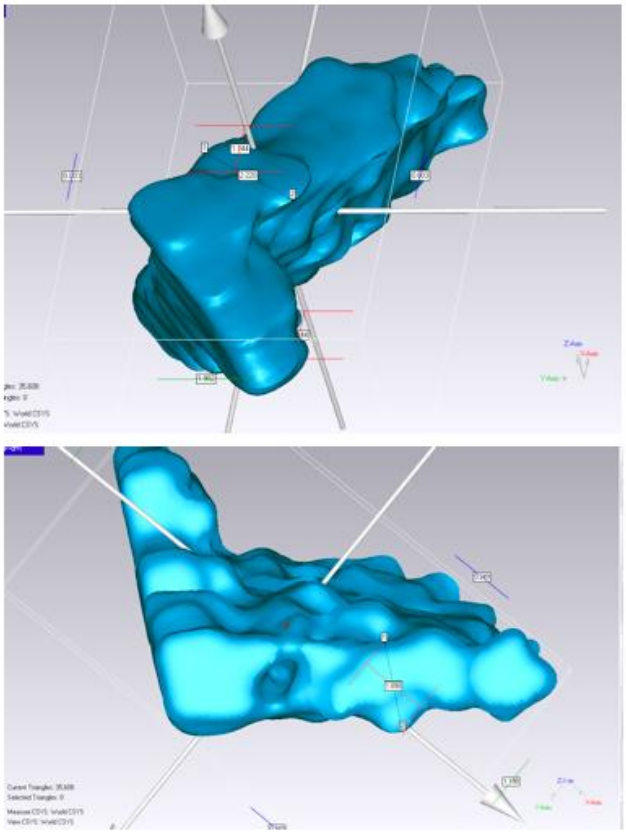

Fig. 4: extrapolation of the volume and inner morphology of the bone lesion by the 3D model acquired by the pQCT

References

1) Burd DQ, Gilmore AE, Individual and class characteristics of tools, J Forensic Sci 2001;46(2):228-33
2) Pechnikovà M, Porta D, Mazzarelli D, Rizzi A, Drozdova E, Gibelli D, Cattaneo C, Detection of metal residues on bone using SEM-EDS. Part I: blunt force injury, Forensic Science International, 2012, in press
3) Gibelli D, Mazzarelli D, Porta D, Rizzi A, Cattaneo C, Detection of metal residues on bone using SEM-EDS – Part II: sharp force injury, Forensic Sci Int 2012, in press
4) Buck U, Christe A, Naether S, Ross S, Thali MJ, Virtopsy - noninvasive detection of occult bone lesions in postmortem MRI: additional information for traffic accident reconstruction. Int J Legal Med. 2009;123(3):221-6
5) Thali MJ, Taubenreuther U, Karolczak M, Braun M, Brueschweiler W, Kalender WA, Dirnhofer R, Forensic microradiology: micro-computed tomography (Micro-CT) and analysis of patterned injuries inside of bone, J Forensic Sci. 2003;48(6):1336-42
6) Capuani C et al (2011) Deciphering the elusive nature of sharp bone trauma using epifluorescence macroscopy: a comparison study multiplexing classical imaging approaches, Int J Legal Med [Epub ahead of print].
7) Pounder DJ et al (2011) Virtual Casting of Stab Wounds in Cartilage Using Micro-Computed Tomography. Am J Forensic Med Pathol 32(2):97-99
8) Von See C, Bormann KH, Schumann P, Goetz F, Gellrich NC, Rücker M, Forensic imaging of projectiles using cone-beam computed tomography, Forensic Sci Int. 2009;190(1-3): 38-41.
9) Gaudio D, Di Giancamillo M, Gibelli D, Galassi A, Cerutti E, Cattaneo C., Does cone beam CT actually ameliorate stab wound analysis in bone? International Journal of Legal Medicine (2013) (In press).
10) Cattaneo C, Marinelli E, Di Giancamillo A, Di Giancamillo M, Travetti O, Vigano' L, Poppa P, Porta D, Gentilomo A, Grandi M, Sensitivity of autopsy and radiological examination in detecting bone fractures in an animal model: implications for the assessment of fatal child physical abuse. Forensic Sci Int. 2006;164(2-3):131-7
11) MacNeil JA, Boyd SK, Accuracy of high-resolution peripheral quantitative

computed tomography for measurement of bone quality, Med Eng Phys 2007(29):1096-1105

12) Boutroy S, Bouxsein ML, Munoz F, Delmas PD, In vivo assessment of trabecular bone microarchitecture by high-resolution peripheral quantitative computed tomography, J Clin Endocrinol Metab 2005(90):6508-6515

13) Rizzo G, Tresoldi D, Scalco E, Mendez M, Bianchi AM, Moro GL, Rubinacci A, Automatic segmentation of cortical and trabecular components of bone specimens acquired by pQCT, 30th Annual Internatonal IEEE EMBS Conference, Vancouver, British Columbia, Canada, August 20-24 2008

14) Rizzo, G, Scalco E, Tresoldi D, Villa I, Moro GL, Lafortuna CL, Rubinacci A, An automatic segmentation method for regional analysis of femoral neck images acquired by pQCT, Ann Biomed Eng 2011;39(1):172-84

15) Rubinacci A, Tresoldi D, Scalco E, Villa I, Adorni F, Moro GL, Fraschini GF, Rizzo G, Comparative high-resolution pQCT analysis of femoral neck indicates different bone mass distribution in osteoporosis and osteoarthritis, Osteoporos Int 2012:23:1967-75

16) Sberna MT, Rizzo G, Zacchi E, Capparè P, Rubinacci A, A preliminary study of the use of peripheral quantitative computed tomography for investigating root canal anatomy, Int J Endodontic J 2009;42:66-75

CAPITOLO 7

The application of cone-beam CT in the aging of bone calluses: a new perspective?

Cappella A, Amadasi A, Gaudio D, Gibelli D, Borgonovo M, Di Giancamillo M, Cattaneo C.

International journal of legal medicine (2013) 127:1139–1144

Int J Legal Med (2013) 127:1139–1144
DOI 10.1007/s00414-013-0824-9

TECHNICAL NOTE

The application of cone-beam CT in the aging of bone calluses: a new perspective?

A. Cappella · A. Amadasi · D. Gaudio · D. Gibelli · S. Borgonovo · M. Di Giancamillo · C. Cattaneo

Received: 16 October 2012 / Accepted: 14 January 2013 / Published online: 7 February 2013

Abstract In the forensic and anthropological fields, the assessment of the age of a bone callus can be crucial for a correct analysis of injuries in the skeleton. To our knowledge, the studies which have focused on this topic are mainly clinical and still leave much to be desired for forensic purposes, particularly in looking for better methods for aging calluses in view of criminalistic applications. This study aims at evaluating the aid cone-beam CT can give in the investigation of the inner structure of fractures and calluses, thus acquiring a better knowledge of the process of bone remodeling. A total of 13 fractures (three without callus formation and ten with visible callus) of known age from cadavers were subjected to radiological investigations with digital radiography (DR) (conventional radiography) and cone-beam CT with the major aim of investigating the differences between DR and tomographic images when studying the inner and outer structures of bone healing. Results showed how with cone-beam CT the structure of the callus is clearly visible with higher specificity and definition and much more information on mineralization in different sections and planes. These results could lay the foundation for new perspectives on bone callus evaluation and aging with cone-beam CT, a user-friendly and skillful technique which in some instances can also be used extensively on the living (e.g., in cases of child abuse) with reduced exposition to radiation.

Keywords Forensic science · Forensic pathology · Forensic anthropology · Fracture repair · Bone callus · Fracture healing · CBCT

A. Cappella · A. Amadasi · D. Gaudio · D. Gibelli · C. Cattaneo (✉)
Laboratorio di Antropologia ed Odontologia Forense (LABANOF), Sezione di Medicina Legale, Dipartimento di Scienze Biomediche per la Salute, Sezione di Medicina Legale e delle Assicurazioni, Università degli Studi di Milano, V. Mangiagalli 37, Milan, Italy
e-mail: cristina.cattaneo@unimi.it

S. Borgonovo · M. Di Giancamillo
Facoltà di Medicina Veterinaria, Dipartimento di Scienze Cliniche Veterinarie, Sezione di Radiologia Veterinaria Clinica e Sperimentale, V. Celoria 10, Milan, Italy

Introduction

The analysis of skeletal trauma is a crucial task in forensic anthropology. The age of a bone fracture which occurred during life is usually reflected in an active or well-established callus. Needless to say, the age of a callus is crucial both for identification purposes as well as for reconstructing the history of violent trauma suffered by a victim. As concerns identification, it is for example of extreme importance to assess whether a bone callus of an unidentified decedent is 2 or 10 years old: this in fact may be crucial in searching among hospitals for possible victims of accidents who correspond to a specific biological profile. Aging calluses is also crucial when assessing if the person was tortured or beaten weeks or months before death, for example during imprisonment.

This however may not be a simple task, especially when dealing with dry bone. Most research in the area of the timing of bone reparation and of callus formation has focused on clinical studies (mostly in the orthopedic field), both with classic radiological techniques and digital radiography [1–3], as well as with more advanced technologies like computed tomography or magnetic resonance imaging [4–10]. Radiological investigations of fracture healing are routinely used also in the forensic field for the assessment of

child abuse [11–15] and more generally for aging fractures and calluses. The same issues have been investigated with sporadic histological and biochemical studies on humans and animals [16, 17]. The in vivo follow-up of the mechanical stability of fracture repair and mineralization due to production of trabecular bone within the fracture gap is a necessary tool for an objective evaluation of the course of a successful healing. But once a certain stage of healing has been achieved, not many further observations exist.

Up to six stages of bone healing have been described in radiology [18, 19]. This staging, based mostly on the features of the fracture line, fracture gap, and inner structure of the newborn callus, has several limitations: firstly, the entire process is basically evaluated with a combination of subjective assessments. This is performed by a visual and subjective evaluation of radiographs, using criteria such as the presence of bridging or obscuration of the fracture line (lucent, sclerotic, or invisible), fracture margin (that can be sharp, blurred, or invisible), visible bridging activity (starting, partial, or complete), and the deposition of new tissue inside the callus and its mineralization. It is clear that a grading of the fracture repair and callus from an objective and quantitative point of view can hardly be performed with current radiological approaches. Moreover, from an osteological point of view, it is difficult to pinpoint where and at what different stages different parts of a callus are. Some anthropological studies have marginally investigated the morphological appearance of bone remodeling in the skeleton [20, 21] with a rough evaluation of features like osteoblastic/osteoclastic activity and line of demarcation to the surrounding bone. Some other studies have concerned macroscopic analysis in cases of child abuse [12, 22]. However, the general blurriness of radiological images in vivo does not allow us to evaluate the particular evolution of the calcified tissues during healing.

The present study therefore wishes to investigate if the use of more sensitive and specific radiological tools can help us gain knowledge in this field and lead the way towards a more accurate analysis of the degree of fracture healing, which is a necessary prerequisite for aging trauma. In particular, we wish to explore the potential of cone-beam CT technology with a pilot study in the analysis of calluses/fractures of known age, aimed at visualizing different levels of bone callus mineralization.

Materials and methods

Bone calluses

Thirteen bone fractures (with or without evident formation of bone callus) of known age were taken according to Police Mortuary Regulation from eight individuals upon autopsy (Table 1). Samples were taken during autopsies and the flesh was mechanically removed. In three cases (cases 1, 2, and 3), calluses were too young for mineralization to be present, whereas in the other ten samples, the presence of the callus was clearly visible: the more regular and smooth, the older the lesion. Each lesion was subjected to radiological investigation with digital radiography (DR) and cone-beam CT (CBCT), in order to evaluate any difference in DR and CT images and any additional information this new technology can provide in the analysis of bone fractures. The evaluation of the bone healing degree by DR was based on the description and outlines of the following six stages [18, 19]: stage 1 is designated as "fracture event" and the radiographic characteristic is the absence of visible bone healing; stage 2 is defined as "granulation" with signs of initial visible healing such as the widening of the fracture gap due to resorption, blurring of the fragment edges, and appearance of faintly mineralized buds of callus ("cloudy," "fluffy," or "immature callus"); stage 3 is the "mature callus" that appears radiopaque and is indicated by new bone growth of similar density as normal bone and the clear demarcation of the fracture line is still clearly delineated; stage 4 shows partial bridging and represents the moment when the callus is connected across the fracture gap in some points; and stage 5 classifies the fracture as clinical union because the mature callus has nearly bridged the fracture completely and the fracture line remains faint and characterized by almost "complete bridging" and almost "complete obscuration." Stage 6 represents the complete bridging and complete eradication of a fracture line that is no longer visible on the X-ray.

DR investigation

Digital radiographs were performed in an anteroposterior projection. DRs were performed with a triple-phase X-ray tube with fixed plant and rotating anode (power 72 kV, inherent filtration 3.5 mm of Al) with a double localized spot (1.2×1.2 and 2×2 mm) and a distance of 100 cm from fire to film. The tool has a CR Agfa Compact® system, put together with the same radiological tube.

Cone-beam CT

Samples were subjected to radiological investigation with cone-beam CT, using the Newtom 5G Cone Beam CT QR System (Verona, Italy) with high resolution, thanks to the small isotropic voxels. The medium time of reconstruction of the image is 45 s. The acquisition of the images is reached with a rotation of 360° around the samples.

DR and cone-beam images were then evaluated in blind by an expert in the field of radiology, and every callus was

Table 1 Differentiation in stages with DR and further detectable features with cone-beam CT

Number	Site of fracture	Presence of callus	Age of the fracture	DR stage	Additional information with cone-beam CT
1	Distal radius	No	5 days	1	No additional information if compared with DR
2	Rib	No	10 days	1	No additional information if compared with DR
3	Cranial vault	No	18 days	1	•Fracture more easily detectable •Fracture course clearly detectable in the cortical and spongy bone
4	Supraspinous fossa of the scapula	Yes	20 days	4	•Detection of fracture line (with DR, it is almost undetectable) •Outer outline of the callus ("blurred" in DR images) •Inner structure of the callus ("blurred" in DR images)
5a	Rib	Yes	28 days	3	•Detection of the inner line of fracture ("blurred" and incomplete in DR images) •Evaluation of the outer outline of the callus: continuous on one side and patchy on the other (not assessable with DR) •Different deposition of mineralized tissue inside the callus (with DR, no differences in the gray scale are detectable)
5b	Rib	Yes	28 days	4	•Detection of the course of the fracture line (not assessable in 2D images with DR) •Outer outline of the callus ("blurred" in DR images) •Organization and disposition of different layers inside the callus (not assessable with DR) •Different deposition of mineralized tissue inside the callus (with DR, no differences in the gray scale are detectable)
5c	Rib	Yes	28 days	4	•Detection of the course of the fracture line (not assessable in 2D images with DR) •Outer outline of the callus ("blurred" in DR images) •Organization and disposition of different layers inside the callus (not assessable with DR) •Different deposition of mineralized tissue inside the callus (with DR, no differences in the gray scale are detectable)
5d	Rib	Yes	28 days	3	•Detection of the fracture line (not assessable with DR) •Outer outline of the callus: patchy on both sides (with DR, this feature cannot be assessed) •Inner organization in layers and different deposition of mineralized tissue (uniform gray aspect in DR)
6a	Rib	Yes	2 years	6	•Degree of mineralization of the surface of the callus (not assessable with DR) •Outer outline of the callus ("blurred" in DR images) •Smoothness of the surface of the callus (not assessable with DR) •Inner organization of the different layers of the callus (not assessable with DR)
6b	Rib	Yes	2 years	6	•Degree of mineralization of the surface of the callus (not assessable with DR) •Outer outline of the callus ("blurred" in DR images) •Smoothness of the surface of the callus (not assessable with DR) •Inner organization of the different layers of the callus (not assessable with DR)
6c	Rib	Yes	2 years	6	•Degree of mineralization of the surface of the callus (not assessable with DR) •Outer outline of the callus ("blurred" in DR images) •Smoothness of the surface of the callus (not assessable with DR) •Inner organization of the different layers of the callus (not assessable with DR)
7	Sternotomy	Yes	2 years	6	•Detection of the course of the fracture line (not assessable in 2D images with DR) •Detection of different stages of mineralization around the fracture line and inside the callus (not assessable with DR)
8	Femural head and acetabulum	Yes	14 years	6	•Different deposition of mineralized tissue ("blurred" in DR images) •Organization of the different layers of the callus (not assessable with DR)

scored according to the six stages of bone healing stated by Hendrix [18] and Toal and Mitchell [19] and previously described. These standards were used in the evaluation of DR images; for the CBCT images, a case by case description was provided since the previous classification was difficult to apply in a comparative manner.

Results

Table 1 shows the results of the classification of the DR images in six stages and the comparison between DR and cone-beam images. Regarding DR, the increase in the stage evaluation roughly follows the increase in the age of the fracture: the older the fracture, the higher the stage, up to the last stage (sixth) of fracture healing. Beyond this threshold, when the bone callus unites the two margins of the fracture and is easily detectable, both with macroscopic and radiological analyses, DR images show similar patterns. Conventional radiography, because of the lack of definition and magnification, led to a superimposition in the evaluation of the middle stages of fracture healing and to a sort of "smoothing out" of any lesion into stage 6 when it was beyond a certain age; CT images, instead, allowed the observer to gain a more precise and defined knowledge of the inner and outer structures of the callus, thus recognizing different kinds and stages of mineralization (Figs. 1, 2, and 3), a clear identification of the fracture line (when still present and detectable), and a vision of the inner organization of the callus in 3D (Fig. 4). In detail, in very "young" fractures, CT images do not add important information to radiographs (fracture numbers 1 and 2), especially when the fracture line is the only feature one can detect in the radiological images: in these cases, CBCT gave in fact no additional information. On the other hand, things change when the fracture is older: the greater the age of the fracture, the more information CT images added in detecting features that can help in the evaluation of the process of fracture healing. The great potential of CBCT is proven by the additional information listed in the last column of Table 1: the enormous amount of information that such tomographic images can provide to the observer is evident. The greater the stage of fracture healing, the more useful and informative features increase on the radiological images: fracture lines become more visible, with the outer and inner layers of the callus become clearer for example. Moreover, different and more subtle levels of bone mineralization become assessable and distinguishable, as well as the inner morphologic organization. Many of these features were clearly not visible with more conventional methods even to the trained eye of the radiologist. To sum up, cone-beam CT imaging gave us a clearer image of the inner and outer structures of the callus, fracture line, inner organization of the different layers of the callus, and different stages of mineralization.

Discussion

The task of aging bone fractures in skeletal remains is still a crucial and tricky issue in the forensic field both in the case of the living and of cadavers. One only has to think of the hundreds of cases every year of child maltreatment in which aging a fracture correctly may make the difference in diagnosing child abuse and thus contribute to ensuring the child's safety, or of war crime scenarios where properly establishing the age of a bone callus on a skeleton may reveal torture during imprisonment. At the moment, particularly on dry bone, very few studies have investigated the morphological features of bone remodeling [20–22] beyond standard radiology, giving only a rough evaluation mostly on single cases. Moreover, the clinical standards one can make use of are not always in complete agreement (especially on the intermediate stages of fracture healing), and they do not give further information on what happens beyond the last stage (what every clinician defines as "complete recovery") [1–10, 18, 19]. On one side, this radiological study demonstrated the problems a trained observer has to face when evaluating fracture healing with conventional radiography: the low definition and bidimensionality of the images lead to a superimposition of some stages, thus leading to observer-dependent observations, without a clear and common concordance, most of all in the intermediate stages like stage 3, stage 4, or stage 5. Concerning all fractures falling into stage 6, the DR images were essentially similar in every case. The major aim of the study was, however, to test for the first time the skills of CBCT in the analysis of the structure of bone calluses on dry bone, a feature every anthropologist has to cope with quite frequently. CBCT was chosen because it is considered as the most valuable tool in the

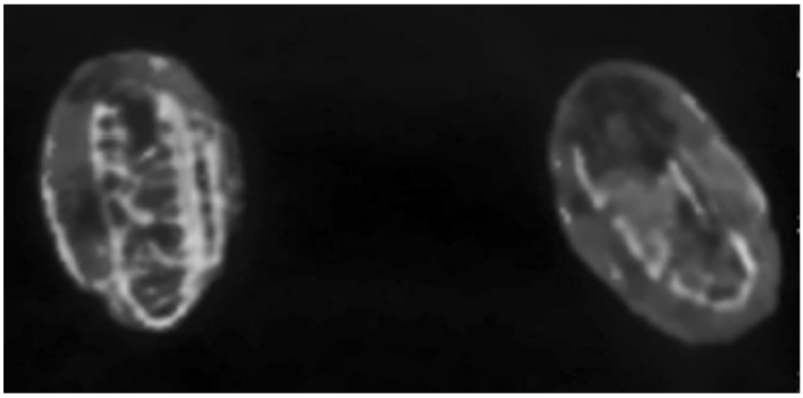

Fig. 1 Different features in the inner structure of calluses with the same age (28 days) in cases 5c (*left*) and 5d (*right*). On the *left*: high mineralization and regular outline of the callus; on the *right*: poor mineralization and disorganized structure of the callus

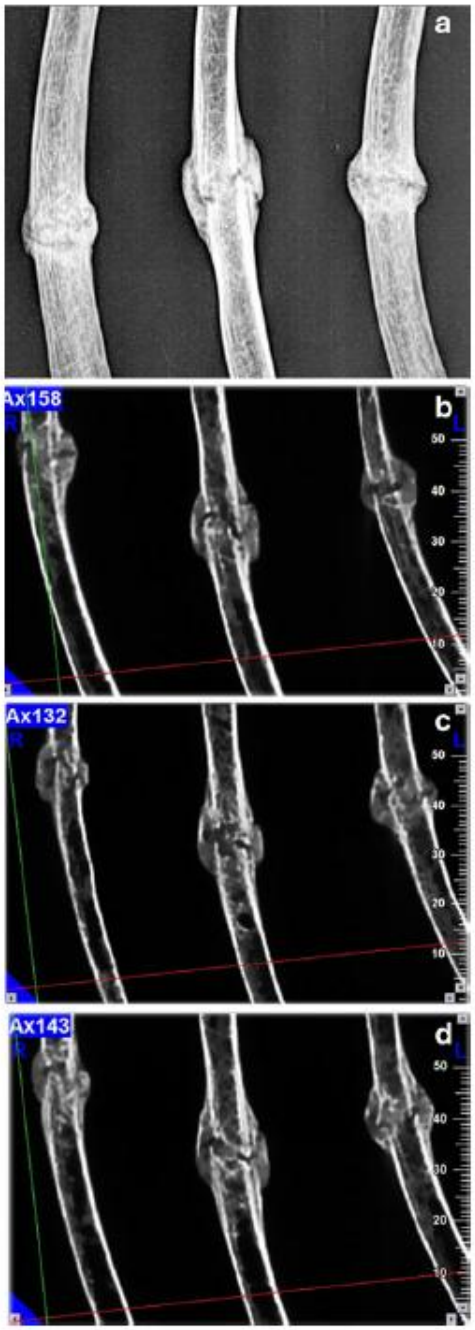

Fig. 2 Comparison of DR (a) and cone-beam CT images (b–d) of three coeval calluses (age 28 days). The callus evaluation resulted to be more precise with CBCT due to its high resolution and its possibility to give subsequent slices on different planes, providing more information on the inner structure of the callus. The rib on the right (a) shows a stage 4 healing (the fracture hidden by new bone formation) in the DR image; the same rib view in CBCT images (b–d) clearly shows more detail

evaluation of hard tissues for in vivo evaluations (particularly bone and teeth of the maxillofacial area). Firstly, in the earliest

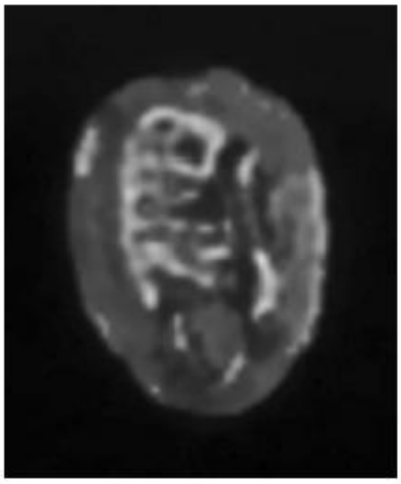

Fig. 3 Inner organization of the callus (age 28 days) and different stages of mineralization. Cone-beam CT image (case 5b)

stages of fracture healing, when the presence of initial callus formation is macroscopically and radiologically (with DR) undetectable, CBCT seemed to bring no significant advantages, since any sign of early changes in the fracture pattern seemed to be undetectable. On the other hand, CBCT provided much more information concerning the different stages of mineralization of specific areas of the callus and other possibly useful features such as the different disposition of bone and cartilage inside the fracture gap, the sequence of new formation, the inner and outer structures, and the characteristics of bone remodeling after the callus has been formed and strengthened. The skills of this kind of radiological investigation are clearly visible in the two cases where coeval fractures on

Fig. 4 Old callus (2 years) in case 6b, cone-beam CT image. The inner part of the fracture line is still detectable, while the outer outline of the callus is smooth and continuous

different ribs were investigated: on one hand, the stages in which the bone calluses fell with DR were substantially similar because of similar features of the radiological images; on the other hand, the high definition of the CT images led to a precise view of the inner structure of the callus, with different dispositions of the layers inside the callus, several degrees of mineralization, different features of the fracture line, and characteristics of the surface of the callus. This clear aspect of the inner structure in coeval calluses can be at first sight misleading: if the stage assessed with DR is the same for every callus, the different features of the inner structure with CBCT can lead to a different stage evaluation. However, the results of this study have to be read as a key element for the future: the clearer features of the structures or the pattern of the fracture line can provide an easier definition of the stages of bone healing. To our knowledge, a radiological technique like cone-beam CT can be a helpful and valuable tool by which to begin a novel classification of bone healing.

The interest in radiological techniques has been rapidly developing in the forensic field [23–26] and in our opinion cone-beam CTs can be particularly helpful: sensitivity is frequently higher than the standard CT technology and the sample does not need to be as small as in the case of micro CT and pQ CTs. Furthermore, the skills of a radiological technique like cone-beam CT must be taken in serious consideration in another crucial forensic field like that of child abuse: one only has to think of the low amount of radiation and the quick acquisition time of the images (CBCT usually needs seconds when a traditional CT needs minutes), provided the lesion is in small parts of the body (like upper or lower limbs) which will fit into the gantry.

Such a technique could thus open up the possibility of making a concrete progress in this field, aiming at correctly evaluating injuries and fracture healing processes. Therefore, cone-beam CT, already known in the forensic field for gunshot and sharp force trauma, can be a helpful and reliable tool for the final purpose of a clear and defined view of bone fractures and calluses, thus trying to make the stages of fracture healing more clear and to create a new classification of bone remodeling.

References

1. Aro H, Eerola E, Aho AJ (1985) Determination of callus quantity in 4-week-old fractures of the rat tibia. J Orthop Res 3(1):101–108
2. Eastaugh-Waring SJ, Joslin CC, Hardy JR, Cunningham JL (2009) Quantification of fracture healing from radiographs using the maximum callus index. Clin Orthop Relat Res 467(8):1986–1991
3. Lujan TJ, Madey SM, Fitzpatrick DC et al (2010) A computational technique to measure fracture callus in radiographs. J Biomech 43(4):792–795
4. Augat P, Merk J, Genant HK, Claes L (1997) Quantitative assessment of experimental fracture repair by peripheral computed tomography. Calcif Tissue Int 60(2):194–199
5. Den Boer FC, Bramer JA, Patka P et al (1998) Quantification of fracture healing with three-dimensional computed tomography. Arch Orthop Trauma Surg 117(6–7):345–350
6. Lynch JA, Grigoryan M, Fierlinger A et al (2004) Measurement of changes in trabecular bone at fracture sites using X-ray CT and automated image registration and processing. J Orthop Res 22(2):362–367
7. Schmidhammer R, Zandieh S, Mittermayr R et al (2006) Assessment of bone union/nonunion in an experimental model using microcomputed technology. J Trauma 61(1):199–205
8. Nyman JS, Munoz S, Jadhav S et al (2009) Quantitative measures of femoral fracture repair in rats derived by micro-computed tomography. J Biomech 42(7):891–897
9. Morgan EF, Mason ZD, Chien KB et al (2009) Micro-computed tomography assessment of fracture healing: relationships among callus structure, composition, and mechanical function. Bone 44(2):335–344
10. Hayward LN, de Bakker CM, Lusie H et al (2012) MRT letter: contrast-enhanced computed tomographic imaging of soft callus formation in fracture healing. Microsc Res Tech 75(1):7–14
11. Islam O, Soboleski D, Symons S et al (2000) Development and duration of radiographic signs of bone healing in children. AJR Am J Roentgenol 175(1):75–78
12. Klotzbach H, Delling G, Richter E et al (2003) Post-mortem diagnosis and age estimation of infants' fractures. Int J Legal Med 117(2):82–89
13. Cattaneo C, Marinelli E, Di Giancamillo A et al (2006) Sensitivity of autopsy and radiological examination in detecting bone fractures in an animal model: implications for the assessment of fatal child physical abuse. Forensic Sci Int 164(2–3):131–137
14. Halliday KE, Broderick NJ, Somers JM, Hawkes R (2011) Dating fracture in infants. Clin Radiol 66(11):1049–1054
15. Malone CA, Sauer NJ, Fenton TW (2008) A radiographic assessment of pediatric fracture healing and time since injury. J Forensic Sci 56(5):1123–1130
16. Schindeler A, McDonald MM, Bokko P, Little DG (2008) Bone remodeling during fracture repair: the cellular picture. Semin Cell Dev Biol 19(5):459–466
17. Vetter A, Epari DR, Seidel R et al (2010) Temporal tissue patterns in bone healing of sheep. J Orthop Res 28(11):1440–1447
18. Hendrix RW (2002) Fracture healing. In: Rogers LF (ed) Radiology of skeletal trauma, vol 1, 3rd edn. Churchill Livingstone, Philadelphia
19. Toal RL, Mitchell SK (2002) Fracture healing and complications. In: Thrall DE (ed) Textbook of veterinary diagnostic radiology, 4th edn. Saunders, Philadelphia
20. Barbian LT, Sledzik PS (2008) Healing following cranial trauma. J Forensic Sci 53(2):263–268
21. Wieberg DA, Wescott DJ (2008) Estimating the timing of long bone fractures: correlation between the postmortem interval, bone moisture content, and blunt force trauma fracture characteristics. J Forensic Sci 53(5):1028–1034
22. Walker PL, Cook DC, Lambert PM (1997) Skeletal evidence for child abuse: a physical anthropological perspective. J Forensic Sci 42(2):196–207
23. Yang F, Jacobs R, Willems G (2006) Dental age estimation through volume matching of teeth imaged by cone-beam CT. Forensic Sci Int 159(1):78–83
24. von See C, Bormann KH, Schumann P et al (2009) Forensic imaging of projectiles using cone-beam computed tomography. Forensic Sci Int 190(1–3):38–41
25. Lee WJ, Wilkinson CM, Hwang HS (2012) An accuracy assessment of forensic computerized facial reconstruction employing cone-beam computed tomography from live subjects. J Forensic Sci 57(2):318–327
26. Murphy M, Drage N, Carabott R, Adams C (2012) Accuracy and reliability of cone beam computed tomography of the jaws for comparative forensic identification: a preliminary study. J Forensic Sci 57(4):964–968

CAPITOLO 8

Indagini preliminari e materiale in elaborazione.

8.1 Age estimation from canine volumes.

De Angelis D., Gaudio D., Cipriani F., Guercini N., Cattaneo C.

Introduction.

Biological age estimation techniques are constantly evolving and they find daily application not only in the clinical field such as dismetabolic diseases diagnosis or orthodontic therapies, but also in the forensic field in cases concerning the determination of the chronological age of a corpse or a living subject.

Unidentified bodies age estimation is a crucial step in the biological profile reconstruction and it is often needed before personal identification is performed. Age estimation on a living person is a less known field, but more and more approached by the forensic communities as, for example, immigration to Europe of people without information from a civil registry is increasing.

Teeth and bone development are frequently used in sub adults age estimation giving back more precise results if compared with methods commonly used for adult age estimation. Dental methods are also often used because teeth are very resistant to chemical and physical factors (Cattaneo 2004). Moreover, pathologic and environmental factors have less influence on teeth development if compared to skeletal ones. Teeth are made up by dentin, that contain the pulp chamber, enamel, that cover the crown dentin and cementum that cover the root. Enamel, once formed, do not change; modifications are due just to external factors such as decalcification, fractures, abrasions and habits that could lead to a permanent enamel modification. Conversely, dentin and pulp chamber changes during the entire life of a person, not only in subadults. With age, dentine formation continues slowly: the formation of secondary dentine produces the pulp chamber decrement in size. Starting from this consideration, various authors developed age estimation methods based on pulp chamber contraction.

In 1950 Gustafson published a method that takes into consideration pulp chamber contraction among other factors; one of the main limitation of the method consists in the fact that dental features are observed on a thin tooth slice, so the tooth has to be destroyed to apply it.

Thanks to the use of radiography less invasive approaches can be followed, and, most of all, applicable on living subjects. These methods are based upon the correlation between chronological age and some ratios between linear measurements on a tooth radiograph (Tadokoro, 1959; Itagaki, 1974, Ikeda et al.1985, Andrea et al., 1995; Kvaal et al. 1995). Other methods take into consideration the ratio between the radiographic image of the pulp chamber area and the entire tooth area (Itoho 1972, Shinozaki 1975, Cameriere et al. 2004, 2007). These methods are therefore

based on mono or bi dimensional measurements performed on a radiograph of three-dimensional structures.

The use of CT allow a precise quantitative volume evaluation of all the dental tissues. Vandevoort et al. (2004) were the first to use a micro-CT on 43 monoradicular teeth to asses the correlation between chronological age of a subject and the ratio between the pulp chamber volume and the entire tooth volume; they used a specifically developed software to evaluate all the volumes. Even if it turned out to be a time consuming method and the correlation coefficient was moderate (r= - 0,57; R2 = 0.31), authors gave a great impulse to the following researches.

Aboshi et al. (2005) used 100 lower premolars to develop an age estimation method based on the ratio between the pulp chamber volume and the entire tooth volume determined via a micro-CT and 3D reconstruction via TRI/3D-BON software (Ratoc System Engineering, Japan).

Someda et al. (2009) performed micro CT on 155 sound central inferior incisors with closed apices. With the aid of a commercial software (TRI/3D-BON, Ratoc System Engineering, Japan) they calculated enamel, dentine and pulp chamber volumes. Regression formulae were then calculated taking into consideration the ratio between the pulp chamber volume and the entire tooth volume except the enamel.

Yang et al. (2006) found a moderate correlation coefficient from a linear regression (r= - 0,54; R^2= 0.29) using the ratio between volumes of pulp chambers and of entire teeth of 28 monoradicular teeth. They used a CBCT and a specifically developed software.

Tardivo et al. (2011) evaluated volumes of 133 canine via a CBCT. They chose canines as they usually survive to other teeth regardless of age, they are less subjected to wear and they have the biggest pulp chamber among monoradicular teeth. Volumes were calculated using a CBCT and the commercial software MIMICS (Materialise NV, Leuven, Belgium). Authors published three regression formulae with a correlation coefficient of -0,62 and a coefficient of determination of 0,38 regarding male and females together, r = - 0,68 and R2 0.47 for males and r = - 0,57 e R2 = 0.32 for females.

Star et al. (2011) adopted the software Simimplant Pro to calculate volumes from 111 teeth CBCT; they found a better correlation between volume ratios and chronological age in females than in males (R^2=0.37 females; R^2=0.30 males) and a better correlation using incisors (r= - 0,27) if compared to canines. The lower correlation found using canines could be due to the little number of canines (32).

Jagannathan et al. (2011) made 188 canines CBCT and calculated pulp chamber and teeth volumes via a software by GE Systems, USA; they elaborated a regression formula with a lower error (r= -

0,63) of Yang's (2006). Authors suggest then that correlations may vary in different populations and that specific formulae should be applied for the age estimation.

Finally, Sakuma et al. (2013) used a MDCT and the commercial software Synapse (Fujifilm Medical Co., Ltd., Tokyo, Japan) to determinate the volumes of 136 inferior premolars. Correlation coefficients between volumes ratios and chronological age are r= - 0, 43 and R2= 0,186 for females, r = -0,772 and R2 = 0,596 for males.

The literature review shows that the research in the field of correlation between teeth volume ratios and chronological age is still at the beginning and deserves deepening. Teeth commonly used by authors are monoradicular ones, often canines; radiographic images come from micro-CT (Vandevoort et al., 2004; Aboshi et al., 2005; Someda et al., 2008), MDCT (Sakuma et al.,2013) and CBCT (Fan Yang et al., 2006; Tardivo et al. 2011; Star et al.,2011; Jagannathan et al.,2011); volumes are calculated via commercial license software. From the review it also come out that the proposed regression formulae are different among authors, maybe because of the different geographic origin of the population, maybe because of the different population age distribution. The present study starts from these considerations, with the aim of proposing new regression formulae using:

- CBCT images, as cone beam tomographs are nowadays quite common in dentistry,
- canines as they usually survive to other teeth regardless of age, they are less subjected to wear, they have the biggest pulp chamber among monoradicular teeth,
- a freeware, open source software to calculate volumes.

Materials and methods.

CBCT from 91 subjects, 42 males and 49 females aged 17 to 77 were used to determinate pulp chamber volumes and entire teeth volume of the upper right canines. All the CT were performed because of clinical reasons that had nothing to do with upper right canines. Only sound teeth were taken into consideration. The machine used was an i-Cat Next Generation (Imaging Sciences International, Hatfield, Pa) with the following setting: voxel size: 0,4 mm, scan time: 8,9 sec, mA: 5, mAs: 19, kV: 120, Scan width: 23,2 cm, Scan height: 17 cm. DICOM files were then elaborated via the freeware and open source software OsiriX (22).

AGE RANGES	15 20	20 25	25 30	30 35	35 40	40 45	45 50	50 55	55 60	60 65	65 70	70 75	75 80	80 85	85 90	TOTAL
ALL	10	7	8	6	8	6	6	8	5	10	7	8	1	1	0	91
MALES	5	2	2	4	5	3	3	4	1	4	5	3	1	0	0	42
FEMALES	5	5	6	2	3	3	3	4	4	6	2	5	0	1	0	49

Tab1: population age distribution.

Pulp chamber and entire tooth volumes were calculated highlighting on assail slices the tooth and the pulp chamber perimeters via the tool ROI (Region Of Interest). OsiriX can automatically generate ROIs on slices between two manually created ROIs, so, via the tool “pencil” ROIs were generated every 3-4 slices, from the tooth apex to the most occlusal point of the crown.

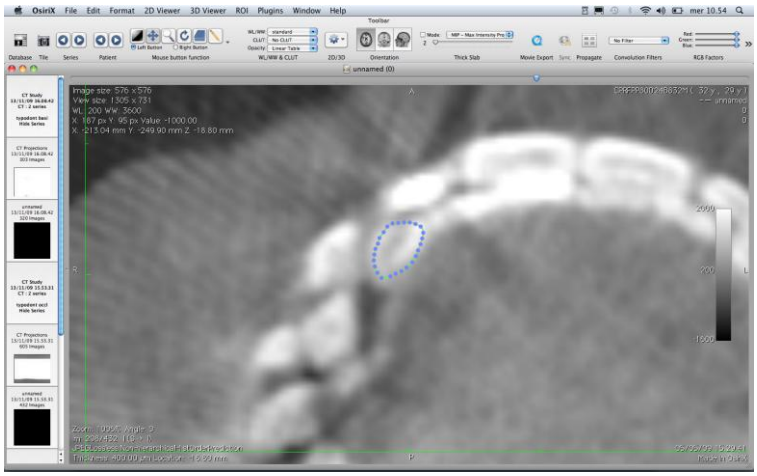

Fig.1 the ROI delimitation

Missing ROIs are then automatically generated by the software via the function “generate missing ROIs” and verified analyzing each assail slice to correct them if necessary. Volumes ROIs are calculated by the OsiriX function “ROI Volume – Compute Volume”.

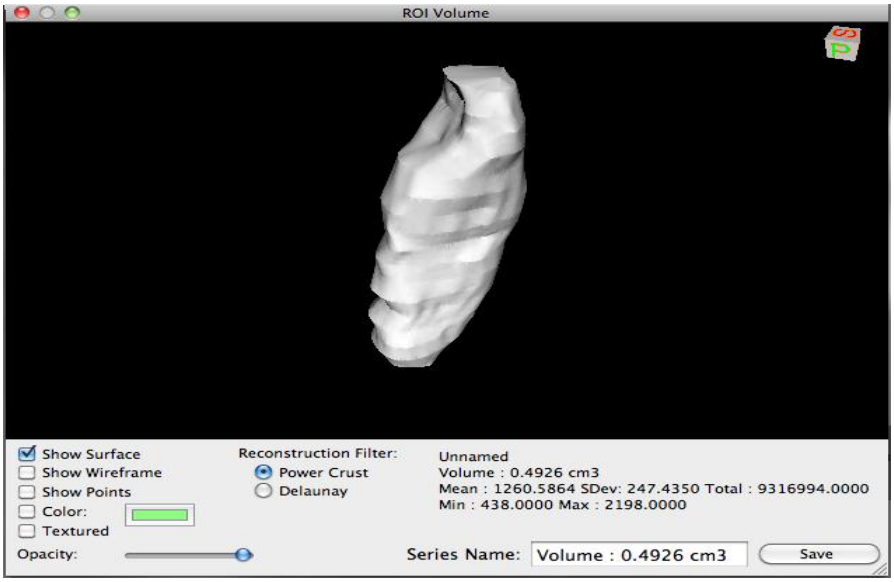

Fig.2 the software generated tooth volume

Via this algorithm, teeth volumes (DV), pulp chamber volumes (PV) and their ratios (PV/DV) were calculated.

Results.

Teeth volumes have a continuous distribution with a maximum modal from 0,4 cm^3 and 0,5 cm^3 in the female group and from 0,7 cm^3 to 0,8 cm^3 in the male group (fig.3) Pulp chamber distribution is uniform in both sex with the exception of the lower interval from 0,005 cm^3 e 0,01 cm^3 (fig.4). The PV/PD ratios distribution is uniform, with the exception of the upper interval from 0,07 cm^3 and 0,08 cm^3.

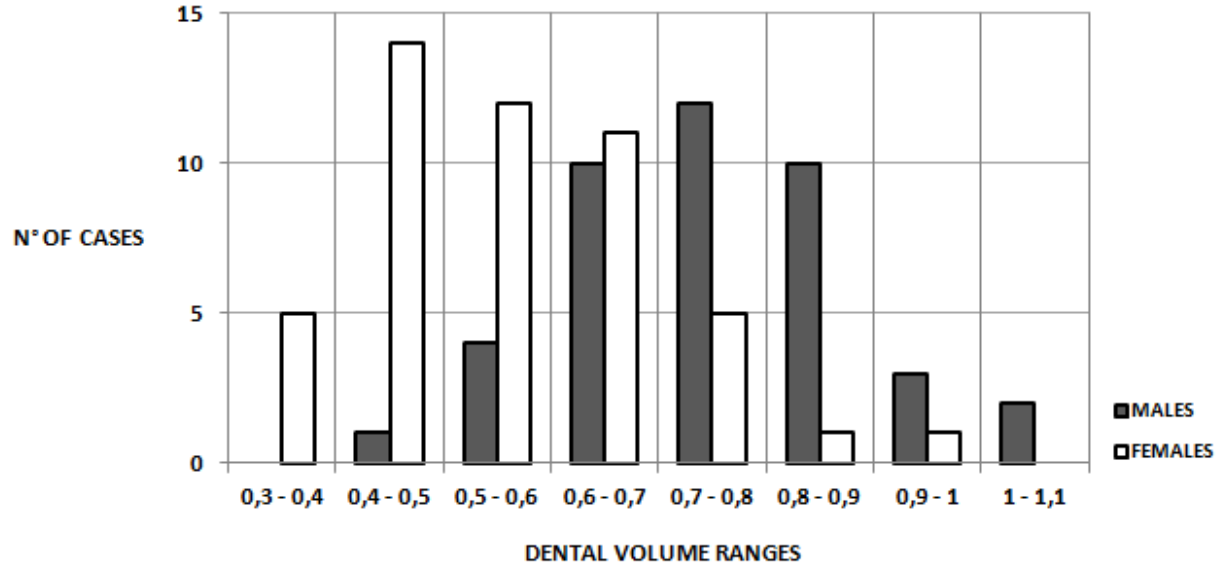

Fig.3: dental volumes distribution in both sex

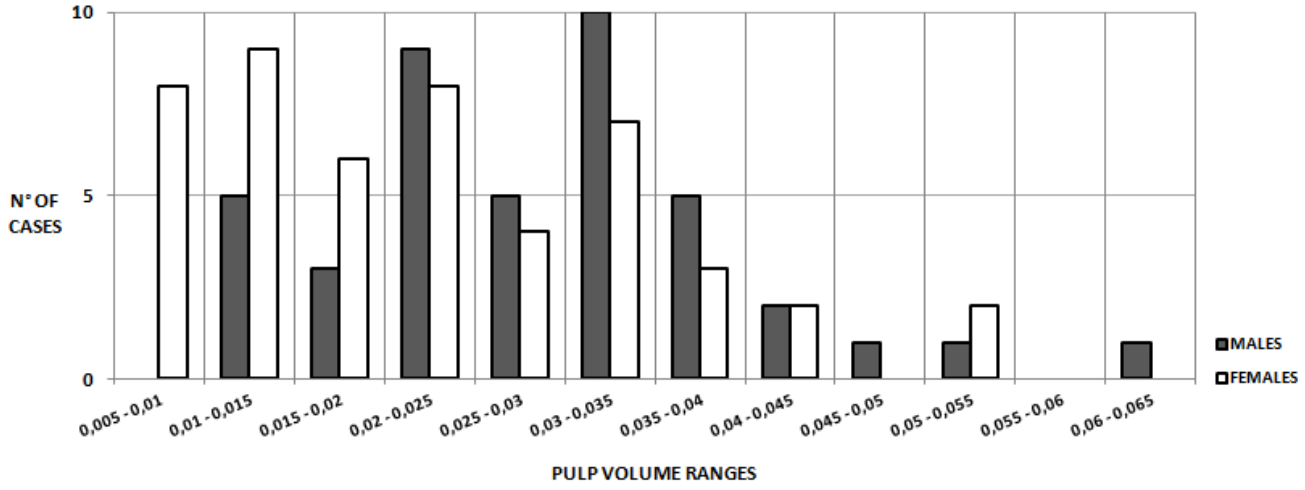

Fig. 4: pulp distribution in both sex

As data distribution do not show any abnormal or significantly eccentric element, all 91 teeth were included for the regression analysis

P/D ratio turned out to be correlated to chronological age with linear function for the female group and less correlated, but significantly, for the male and the whole group. The correlation degree is calculated on "r" parameters (correlation coefficient or Pearson product moment correlation coefficient) and "R2" (coefficient of determination).
The correlation is moderate for the female group **(regression formula: Y = -774,8 X + 74,4 r= - 0,696 R2 = 0,485)**, moderate for males **(regression formula: Y = -795,3 X + 75,5 r=-0,513 R2 = 0,263)** and moderate as well when considering both sex **(regression formula: Y = -780,9 X + 74,7 r= - 0,624 R2 = 0,389).**

A comparison between two regression lines for males and females by Student's test does not detect a significant difference (2-tailed p-value for slope is 0.93 and 0.92 for intercept) thus making it likely a common regression line to all samples.
The better correlation in the female group is probably due to the more steady distribution in the higher P/D values (>0,5) while in the male group there's a higher density in intermediate values (0,03-0,04).
Prediction intervals, defined by desired confidence intervals and defined as observed data variance function, were calculated to describe prevision accuracy. (Tab.2, Fig.5).

	ESTIMED AGE by linear regression	CONFIDENCE ESTIMATION	PREDICTION INTERVAL (years)
ALL	Y = -780,9 X + 74,7	95%	± 29
		90%	± 24
		80%	± 19
		70%	± 15
		60%	± 12
MALES	Y = -795,3 X + 75,5	95%	± 32
		90%	± 27
		80%	± 21
		70%	± 17
		60%	± 14
FEMALES	Y = -774,8 X + 74,4	95%	± 28
		90%	± 23
		80%	± 18
		70%	± 15
		60%	± 12

Tab.2: prediction interval with different confidence

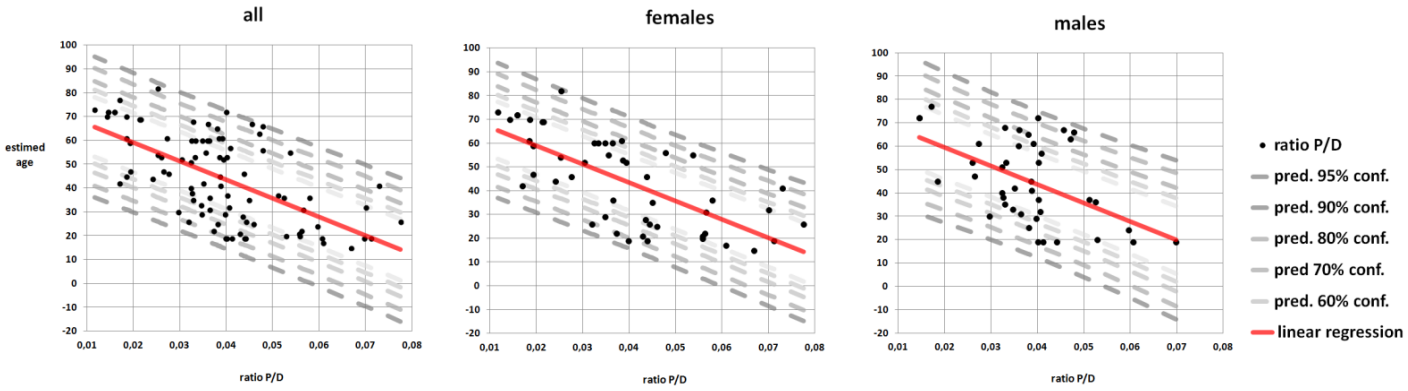

Fig. 5: Confidence and prediction interval graphs

Age estimation using linear regression formulae from the studied population are not very precise: prediction interval is around ± 30 with 95% confidence for males and females. Different intervals with a lower excursion (higher precision) are therefore listed, but they are obviously associated to a higher uncertainty (lower accuracy): with 60% confidence there is a prevision interval of ±12years in the female group and ±14 for males.

Discussion.

Chronological age estimation on a cadaver is often a crucial step in the biological profile reconstruction and a precious aid in personal identification; age estimation is as well important when applied in living subjects for civil, criminal or social issues. Methods developed for sub adults subjects are indeed much more reliable than the ones used when bones and teeth are completely developed. Among adult methods, the ones that take into consideration the formation of secondary dentine, in other words the pulp chamber contractions, are well known by the forensic community and widely adopted. In the last few years different authors studied the correlation between chronological age and the ratio between the volume of the pulp chamber of a tooth and its entire volume adopting images from micro-CT, MDCT e CBCT processed via commercial software.

In this study CBCT of sound upper canines from living subjects were used to evaluate the correlation between the patient's age and the volume ratio between pulp chamber and tooth with the aid of a freeware, open source software. CBCTs were used because nowadays they are quite common between dental practitioner; canines were chose because already used in previous studies and because are frequently found more sound than other teeth in dental arches; lastly a freeware,

open source software was used to allow affordable reproducibility of the proposed method and formulae.

Linear models published by Star et al. (2011) and by Tardivo (2011), authors that studied the correlation between canines volumes and age, have correlation indices (r) that go from a minimum of 0.27 to a maximum of 0,68. Correlation coefficients from the present study are similar to Tardivo's (2011). Comparing the results from the present study to Star's, a better correlation can be noticed in the present study, probably because of the lower number of canines used by Star (32) if compared to this one (91).

Determination index R2 for females is 0,485; 0,263 for males and 0,389 when considering both sex. The female group better correlation is probably due to a steadier distribution even in higher values of P/D (> 0,05) while in the male group we have a higher density in intermediate values.

Age estimation adopting the proposed regression formulae have a prediction interval of ±12 years with 60% confidence; however, with 95% confidence, the prediction interval is ±30 years. This last consideration makes the proposed regression formulae not jet very useful in the forensic field. More studies focused on bigger population, characterized by a steady age distribution and maybe the use of other teeth together with canines, are indeed needed to evaluate the possibility of an age estimation reliable method based on pulp chamber volume contraction.

References

1) Cattaneo C, Grandi M.,(2004). Antropologia e Odontologia Forense. Guida allo studio dei resti umani. Testo atlante. Monduzzi Editore, Bologna.
2) Gustafson G., Age determination on teeth. J. Amer. Dent. Assoc., 41,45, 1050
3) Bang G, Ramm E. Determination of age in humans from root dentin transparency. Acta Odontol Scand 1970; 28(1):3–35.
4) Lamendin H, Baccino E, Humbert JF, Tavernier JC, Nossintchouk RM, Zerilli A. A simple technique for age estimation in adult corpses: the two criteria dental method. J Forensic Sci 1992;37(5):1373–9.
5) M. Tadokoro, Study of age related changes in tooth (I)—morphological changes of dental canal in anterior teeth, Dental Outlook 16 (1959) 83–100.
6) M. Itagaki, An age estimation based on the chronological changes in the pulp cavity, with reference to the ratio between length of the teeth and pulp cavity,Nihon Univ. Dent. J. 48 (1974) 700–706.
7) N. Ikeda, K. Umetu, S. Kashimura, T. Suzuki, M. Oumi, Estimation of age from teeth with their soft x-ray findings, Nihon Houigaku Zatushi 39 (1985) 244–250.

8) G.D. Andrea, T. Oriella, R. Cristina, The coronal pulp cavity index: a biomarker for age determination in human adults, Am. J. Phys. Anthropol. 103 (1997) 353–363.
9) S.I. Kvaal, K.M. Kolveit, I.O. Tomsen, T. Solheim, Age estimation of adults fromdental radiographs, Forensic Sci. Int. 74 (1995) 175–185.
10) S. Itoho, Research on age estimation based on teeth, Nihon Houigaku Zatushi 26 (1972) 31–41.
11) J. Shinozaki, An age estimation from the ageing of dental pulp cavity based on surface area index, Nihon Univ. Dent. J. 49 (1975) 666–678.
12) R. Cameriere, L. Ferrante, M. Cingolani, Variations in pulp/tooth area ratio as an indicator of age: a preliminary study, J. Forensic Sci. 49 (2004) 317–319.
13) Cameriere R, Ferrante L, Belcastro MG, Bonfiglioli B, Rastelli E, Cingolani M. Age estimation by pulp/tooth ratio in canines by peri-apical X-rays. J Forensic Sci 007;52(1):166–70.
14) F.M. Vandevoort, L. Mebergans, J.V. Cleynenbreugel, D.J. Bielen, P. Lambrechts, M. Wevers, A. Peirs, G. Willems, Age calculation using X-ray microfocus computed tomographical scanning of teeth. A pilot study, J. Forensic Sci. 49 (2004) 787–790.
15) H. Aboshi, T. Takahashi, T. Komuro, Y. Fukase, A method of age estimation based on the morph metric analysis of dental pulp in mandible first premolars by means of three-dimensional measurements taken by micro CT, Nihon Univ. Dent. J. 79 (2005) 195–203.
16) Someda H, Saka H, Matsunaga S, Ide Y, Nakahara K, Hirata S, et al. Age estimation based on three-dimensional measurement of mandibularcentral incisors in Japanese. Forensic Sci Int 2009;10:110–4.
17) Yang F, Jacobs R, Willems G. Dental age estimation through volumematching of teeth imaged by cone-beam CT. Forensic Sci Int 2006;15: S78–83.
18) Tardivo D, Sastre J, Ruquet M, Thollon L, Adalian P, Leonetti G, et al. Three-dimensional modeling of the various volumes of canines to determine age and sex: a preliminary study. J Forensic Sci 2011;56766–70.
19) H. Star; P. Thevissen, R. Jacobs, S.Fieuws, T. Solheim; G. Willems. Human Dental Age Estimation by Calculation of Pulp–Tooth Volume Ratios Yielded on Clinically Acquired Cone Beam Computed Tomography Images of Monoradicular Teeth J Forensic Sci, January 2011, Vol. 56.
20) N. Jagannathan, P. Neelakantan, C. Thiruvengadam, P. Ramani,P. Premkumar, A. Natesan, J.S. Herald, H. U. Luder. Age Estimation in an Indian Population Using pulp/tooth Volume

Ratio of Mandibular Canines Obtained from Cone Beam Computed Tomography; J Forensic Odontostomatol. 2011;29:1:1-6

21) Sakuma, H. Saitoh, Yoichi Suzuki,Yohsuke Makino, Go Inokuchi, Mutsumi Hayakawa, Daisuke Yajima, Hirotaro Iwase. Age Estimation Based on Pulp Cavity to ToothVolume Ratio Using Postmortem Computed Tomography Images

22) Rosset A, Spadola L, Ratib O. OsiriX: An Open-Source Software for Navigating in Multidimensional DICOM Images. J Digit Imaging. 2004 Sep;17(3):205-216.

8.2 A preliminary study of virtual facial reconstruction by means of 3D models acquired by Laser Scanner and a new facial reconstruction software.

Gaudio D., Guyomarc'h P., Cattaneo C.

Introduction.

Facial reconstruction is the last step in the developing of a biological profile of a subject. Of course it is an operation possible only in the presence of a cranium and although it is mainly used in forensic, sometimes it shows to be useful in archaeology too [1,2,3,4]. Nevertheless it is important to make clear that the final goal, judicially speaking, is not to obtain the face of the studied subject as it was, but to give a relatively alike, highly effective, which, correctly diffused, can lead to the recognition by relatives or simple acquaintances [5].

To produce this resemblance, reconstructing techniques are based on the assumption the cranium morphology influences the morphology of the surrounding soft tissues (in other words: face).

On the original cranium a cast takes place; then this cast is used as basis for the reconstruction, which can be operated by hand (Manual) or, as we'll see, by computer. The manual reconstruction is generally conducted following what is known as "Manchester Protocol", which mixes two different techniques, the Russian method and the American. The first is mainly based upon anatomy, through a detailed reconstruction of the whole muscle tissues of head and neck, using clay or plasticine. The second method uses tissue thicknesses, gathered along the years through different ways – from the usage of pin run into corpses' faces to more modern ultrasound technologies; these thicknesses are signalled on the cranium by rubber or timber pieces which mark the extreme borders of the face. These must be connected each other by clay (or others materials) stripes. The average tissue values are gathered up in tabs, divided by sex and physical constitution. With the Manchester protocol (1973) the facial reconstructor first runs the thicknesses on the cast, then anatomically reconstructs the face. This protocol takes part in binding the artistic freedom of the reconstructor: in fact, in 1910 through Eggelin counter-test it was proved that several reconstructors, even using the same thicknesses, can produce great differences with the original sample and among the casts themselves. Therefore, introducing the Manchester technique points to limit mistakes by the executors. Nevertheless, even with this protocol, the variety in execution is still the main limit in the manual technique.

The use of new cranium acquisition technologies and the diffusion of 3D modelling softwares may lead to improvements in facial reconstructing: for example, by means of 3D models and of tools of quick prototipation (3D print) it is possible to get a copy of the cranium without accessing the original sample [6].

One of the first works in using computer graphics in facial reconstruction belongs to 1989 [7], in which a cranium was acquired by a "primitive" model of Laser Scanner (then elaborated by a medical graphic software, UCL for 3D surface). The result, even if approximate, put basis to develop this combination of means [8]. After that followed various works which goal was to reproduce the manual method of reconstructing tissues in virtual context [9]. For some of these works systems of 3D animation softwares was expected [10,11,12,13]. For others, systems of virtual sculpturing was expected [14]. A different approach was the trying to adapt a virtual face with "average" tissue samples, "forcing" (distortion) and modelling it on the cranium examinated [15].

During this study a 3D Laser Scanner has been used in order to acquire crania on which operate the facial reconstruction. This has then been developed by the use of a software still under exam (TIVMI – AFA3D). This software has been tested to import DICOM files (coming from CT) but in this preliminary study it has been verified the possibility to import models obtained by the Laser Scanner and to examine advantages and drawbacks of these kind of models for the use of the new software. The final goal was not just verifying the actual resemblance to the real subject, but also the effective possibility for different operators to reproduce the same reconstruction, in order to understand whether this method can limit differences between operators.

Materials and methods.

Four crania have been acquired, of which we might dispose of images when alive (3 females and 1 male). The acquisition has been operated through Minolta Vivid 910 Laser Scanner (Konica Minolta Sensing, Inc. Osaka – Japan). For every subject separate acquisitions of cranium and mandible have been carried out, linking them virtually by Autodesk 3ds Max software. This kind of procedure has been elected to get the most complete 3D model possible. The four 3D models have been saved in OBJ format and subsequently imported into the TIVMI software (for treatment and Inscreased Vision for Medical, developed in the PACEA laboratory, UMR 5199 of CNRS, University of Bordeaux). In the TIVMI software it has been developed the AFA3D module, allowing for the estimation of face shape based on skull landmark coordinates. It has been developed in the Université de Bordeaux, between the UMR5199 PACEA (Anthropologie des Populations Passées et Présentes) and the UMR5800 LaBRI (Laboratoire Bordelais de Recherche en Informatique). This software applies a huge quantity of tissue thicknesses (78) in as many craniometrical points, obtained by a research oh tissue values executed on a large sample of CTs (500 individuals of French nationality). Once the model has been imported the procedure to the reconstruction sees:

- The manual positioning (lead by the operator) of 78 landmarks on the cranium 3D model (fig.1).
- The input of generic information about the subject, that is sex (male/female/unknown), age (<40; >/= 40; unknown) and the constitution (normal, overweight, unknown) (fig.2).

Now the software gives, by means of a mesh, a synthetic skin to the cranium, on the basis of a thicknesses database. Soft tissue depths are estimed using regression formulae, and landmarks of facial organs (eyes, nose, mouth and ears) are independently estimated with regression of PC scores extracted after procrustes superimpositions of the datasets in R [16].

Facial reconstructions of the four subjects have been carried out by two different operators and compared to the real faces. The four couples of reconstructions have then compared each other through the function generated color-coded mapping of the differences of Amira® software (multifaceted 3D software platform for visualizing, manipulating, and understanding biomedical data).

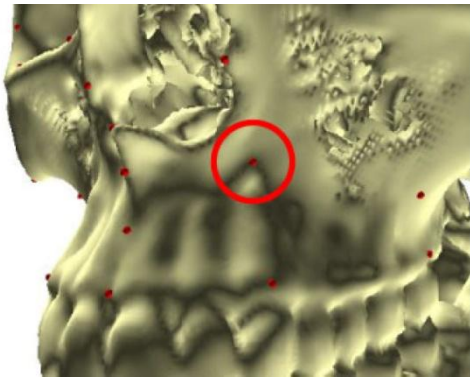

1) Porion (left)
2) Porion (right)
3) Orbitale (left)
4) Orbitale (right)
5) Nasion
6) Glabella
7) Rhinion
8) Mid-nasal
9) Nasomaxillofrontale (left)
10) Nasomaxillare (left)
11) Mid-nasomaxillare (left)
12) Apertion (left)
13) Nasomaxillofrontale (right)
14) Nasomaxillare (right)
15) Mid-nasomaxillare (right)
16) Apertion (right)
17) Nasospinale superior
18) Spinale
19) Sub-spinale
20) Maxillofrontale (left)
21) Ectoconchion (left)
22) Zygoorbitale (left)
23) Supraconchion (left)
24) Superciliare (left)
25) Frontomalare orbitale (left)
26) Frontomalare temporale (left)
27) Jugale (left)
28) Zygotemporale superior (left)
29) Maxillofrontale (right)
30) Ectoconchion (right)
31) Zygoorbitale (right)
32) Supraconchion (right)
33) Superciliare (right)
34) Frontomalare orbitale (right)
35) Frontomalare temporale (right)
36) Jugale (right)
37) Zygotemporale superior (right)
38) Frontotemporale (left)
39) Frontotemporale (right)
40) Zygion (left)
41) Zygion (right)
42) Mastoidale (left)
43) Mastoidale (right)
44) Condylion (left)
45) Midcranius (left)
46) Gonion (left)
47) Condylion (right)
48) Midcranius (right)
49) Gonion (right)
50) Zygomatic (left)
51) Zygomaxillare (left)
52) Zygomatic (right)
53) Zygomaxillare (right)
54) Midphiltrum
55) Prosthion
56) Infradentale
57) Labiomentale
58) Pogonion
59) Gnathion
60) Supragnathion
61) Sub-maxillar curvature (left)
62) Ectomolare (left)
63) Supracanine (left)
64) Canine fossa (left)
65) Infracanine (left)
66) Mental foramen (left)
67) Inframolare (left)
68) Midmandibular body (left)
69) Sub-maxillar curvature (right)
70) Ectomolare (right)
71) Supracanine (right)
72) Canine fossa (right)
73) Infracanine (right)
74) Mental foramen (right)
75) Inframolare (right)
76) Midmandibular body (right)
77) Midmandibular border (left)
78) Midmandibular border (right)

Fig.1: positioning of a landmark in correspondence of the canine fossa. On the right the complete list of 78 landmarks.

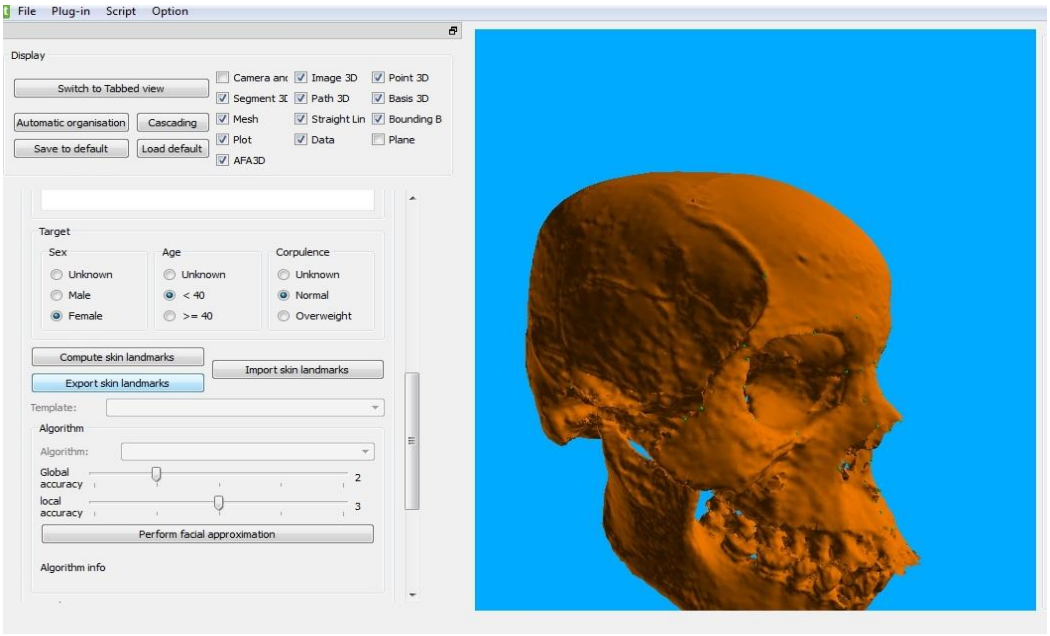

Fig. 2: The input of generic information about the subject, that is sex, age and the constitution.

Results.

The importing of 3D models of crania acquired by Laser Scanner in OBJ format has given an excellent visualization of the anatomic characteristics useful for a correct placing of landmarks; some difficulties have still been noticed in correspondence to Nasomaxillofrontale and Zygomaxillare.

The faces obtained by the discussed method have produced little resembling reconstructions (an example in fig. 4). Nevertheless in all four the cases a quite trustworthy reproduction of the nose pyramid have been noticed, both if observed in frontal way and in lateral way. Also the overall shape of the faces has result coherent with the original, when observed in frontal way. The orbit region has resulted as little resembling, and so did the buccal region. In detail, in the first case it has been observed a wrong reconstruction of the morphology of the eyes, with constant production (present in all of the four cases) of "drop shaped" with side-tip of the eye, bent towards the lower side. Even by using four landmarks the shape of the lips seems to be standardized and therefore little resembling to the original samples.

The color-coded mapping of the differences between couples of facial reconstruction lead on the same crania by different operators (therefore representing the inter-observator mistake), shows a good homogeneity in terms of morphology on precise regions of the face: we refer to the facial massif, particularly the nose, cheeks (between Zygion and Alare), temples (in coincidence to the frontotemporal) and to the region set between Subspinal and Prosthion. In two case (3,4, see fig. 4)

it has been observed a discrepancy larger than 2 mm in the frontal and epifrontal regions, and around the ear.

Fig. 3: an example of facial reconstruction of a subject (on the left).

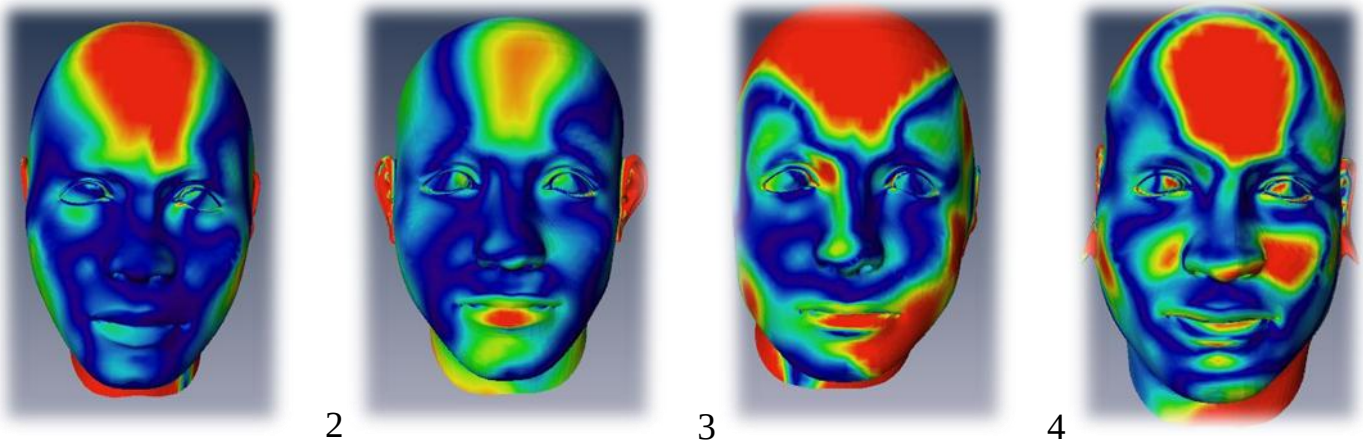

Fig. 4: color-coded mapping of the differences between the four couples of facial reconstruction
The larger distances are marked by red color (>2 mm); in the blue regions there is no difference metric (0 mm).

Discussions and conclusions.

The study, developed combining Laser Scanner acquisition method combined with the experimented tool AFA3D of TIVMI software must be deepen through a statistic analysis of morphometric differences between the two operators and an enlarging of the number of crania analyzed.

Anyway this preliminary study has given some methodical indication of particular relevance: the test testifies the possibility to import 3D models obtained by means of Laser Scanner into the software, converting the model into OBJ format. Using Laser Scanner, mobile and transportable, seems to be more comfortable than conventional CT, because of the possibility to acquire data directly wherever the sample is kept (the anthropology laboratory itself, a museum, etc.). Nevertheless the major advantage has been seen in the quality of the model, excellently reproduced in every detail, particularly the cranium sutures. This detailed reproduction of the bone surface allows a better and more comfortable placing of landmarks, fundamental for the experimented software: a lot of them are situated in the very correspondence of the sutures (i.e. Mid-nasal,Zygo-maxillare, Frontomalare orbitale/temporale, MId-nasomaxillare, etc.). The same good quality resolution can be obtained also with new generation CT (CBCT for example) anyway and Laser Scanner is not the best solution when studying archaeological subject with no direct access to the cranium, such as mummified corpses [6].

Even though some regions of the face have shown to be well represented (particularly the nose pyramid), the final result of the reconstruction of the four subject is little resembling to the original, in an overall view. This even an extremely high number of landmarks have been used (78).

It has already be discussed that facial reconstruction does not aim to reproduce perfectly a face, but just to give a "probable" result, that is because the experimented computerized method is based, just like manual method, on tissue thicknesses that are nothing else than average values, calculated on a sample. The very contrary of what a face is, that is a gathering of peculiar characteristics. It's very important to say that the discussed methodology excludes the individuality of the operator, which can influence the result of the reconstruction only through the input of the particulars of the subject (sex, age, constitution) and the correct/incorrect placing of landmarks.

The major limits spotted in the experimented method is the impossibility to show subjects' teeth, fundamental in the process of identification, because of their certain reliability, teeth which are instead part of the manual methodology; furthermore there's the wrong output of the eyes morphology. An advantage of the experimented technology lies instead in the possibility to verify the reproducibility of the result: as above mentioned the variability in execution among reconstructors is still one of the major limits of the manual method. Again it is difficult to conduct

inter-operators studies when two manual reconstructors are working on the same cranium. The manual method is time consuming (it takes several days for the complete execution) and it must be conducted by staff with particular anatomical knowledge of anatomic and of instruments to be used. The experimented process has shown to be instead relatively quick (the Laser Scanner acquisition of cranium and mandible can be accomplished in about an hour; preliminary elaboration with Autodesk 3ds Max takes half an hour and the virtual reconstruction with AFA3D takes about 3 hours more), the operator needs to have ostheologic and antropometric basal knowledge but a good experience in softwares for 3D modeling.

As result the computerized technique shows to be more repeatable because of its quickness and because it can be executed by operators with less specific tasks (and fast to be acquired as well). The possibility to work on a virtual reconstruction in a format that can be imported and exported on and from softwares for the analysis of 3D data allows to compare quickly morphometric of the face obtained, operation that has been carried out during the course of this preliminary study by the use of color-coded maps obtained by Amira. The results show quite a remarkable difference (of some millimeters) among the pairs of facial reconstructions. The most relevant (>2 mm) have been observed in the frontal, epifrontal and ear regions. No difference (0 mm) has been noticed in the region of the facial massif for 2 couples of 4. These first result are considered to be promising, even though it is critical to deepen some causes of discrepancies: as the software automatically generates the thicknesses on which landmarks are placed, it is evident that 1) discrepancies between couples of reconstructions are due partly to the different placing of some landmarks accomplished by the two operators. It will therefore be necessary to assess this discrepancy. Observing the color coded maps it is already possible to get in the mandible landmarks the craniometrical points which show more issues in terms of repeatability. 2) Frontal, epifrontal and ear zone discrepancies are not due to different positioning of the landmarks (in fact it has been observed an excellent correspondence of glabella and frontotemporals landmarks) as much as the lacking of landmarks themselves in those very regions. Of course they will need to be implemented.

The possibility to conduct the above mentioned evaluations, with the aid of 3D analysis softwares, constitutes a great advantage itself in the study and in the development of the method here discussed which, given the exposed limits of facial reconstruction, present improvement margins.

References

1. Cesarani F, Martina MC, Grilletto R, Boano R, Roveri AM, Capussotto V, Giuliano A, Celia M, Gandini GAJR, (2004). Facial reconstruction of a wrapped Egyptian mummy using MDCT. *Am J Roentgenol.* **183**(3):755-758.
2. Nedden D, Knapp R, Wicke K, (1994). Skull of a 5300-year-old mummy: reproduction and investigation with CT-guided stereolithography. *Radiology* **193**: 269-272.
3. Benazzi S, Fantini M,. De Crescenzio F, Mallegni G,'Mallegni F, Persiani F, Gruppioni G, (2009). The face of the poet Dante Alighieri reconstructed by virtual modelling and forensic anthropology techniques. *Journal of Archaeological Science* **36** (2): 278–283.
4. Tyrrell AJ, Evison MP, Chamberlain AT, Green MA, (1997). Forensic three-dimensional facial reconstruction: historical review and contemporary developments. *Journal of Forensic Sciences*, **42**(4):653-661)
5. Cattaneo C, Grandi M,(2004). Antropologia e Odontologia Forense. Guida allo studio dei resti umani. Testo atlante. Monduzzi Editore, Bologna.
6. (http://medialab.di.unipi.it/Project/Mummia/Tesi/Cap_1_FR.htm).
7. Vanezis P, Blowes RW, Linney AD, Tan AC, Richards R, Neave R(1989) Application of 3-D Computer Graphics for facial reconstruction and comparison with sculpting techniques. *Forensic Science International*, **42**: 69-84.
8. Vanezis P, Vanezis M, McCombe G, Niblett T, (2000). Facial reconstruction using 3-D computer graphics. *Forensic Science International*, **108:** 81-95.
9. Wilkinson CM, (2005). Computerized Forensic Facial Reconstruction: A Review of Current Systems. *Forensic Science, Medicine, and Pathology,* **1:** 173-177.
10. Buhmann D, Bellman D, Kahler K, Haber J, Seidel HP,WilskeJ, (2003). Computer-aided soft tissue reconstruction on the skeletonised skull. Proceedings of the first International Conference on Reconstruction of Soft Facial Parts (RSFP), 37–39. Potsdam, Germany.
11. Eliasova H, Dvorak D, Prochazka IO, (2003). Facial three-dimensional Reconstruction. Proceedings of the first International Conference on Reconstruction of Soft Facial Parts (RSFP), 45–48. Potsdam, Germany.
12. Kindermann K, (2003). Innovative approaches to facial reconstruction using digital technology. Proceedings of the first International Conference on Reconstruction of Soft Facial Parts (RSFP). 127–132. Potsdam, Germany.
13. Kahler K, Haber J, Seidel HP, (2003). Reanimating the dead: reconstruction of expressive faces from skull data. *Computer Graphics Proceedings*. **22**:554–567

14. Wilkinson CM, (2003). “Virtual” sculpture as a method of computerized facial reconstruction. Proceedings of the first International Conference on Reconstruction of Soft Facial Parts (RSFP), 59–63. Potsdam, Germany.
15. Michael SD, Chen M, (1996). The 3-D reconstruction of facial features using volume distortion. Proceedings of 14th Annual Conference of Eurographics, 297–305. UK.
16. Guyomarc'h P, (2011). Reconstitution Faciale par Imagerie 3D : Variabilité morphométrique et mise en oeuvre informatique. Université Bordeaux 1, UMR5199 PACEA (A3P). Dissertation (downloadable at www.theses.fr/2011BOR14354).

CONCLUSIONI

Il lavoro di tesi qui presentato ha indagato l'applicazione delle tecnologie tridimensionali su numerose tematiche nell'ambito dell'antropologia fisica e forense. Per affrontare tali tematiche è stato necessario selezionare gli strumenti e i software, acquisire digitalmente la più ampia varietà di materiale possibile e quindi concentrarsi sulle linee di ricerca che apparivano più promettenti. Si è elaborato un modello acquisito (tramite laser scanner a tempo di volo) nel corso di uno scavo di archeologia forense **(Capitolo2)**, che ha permesso la riproduzione tridimensionale del luogo di giacenza producendo una rappresentazione "immersiva", che consente all'operatore di esplorare e analizzare lo scavo in tutti suoi aspetti geometrici.

È stato altresì acquisito materiale in diverse condizioni tafonomiche rilevando come la tecnologia laser scanner sia poco adatta a registrare materiale carbonizzato (poiché il laser è assorbito dal colore scuro dell'osso) e materiale riflettente, come ad esempio i denti (che riflettono il laser producendo "rumore", ovvero nuvole di punti ridondanti intorno alla superficie) ma che la stessa tecnologia risulti molto adatta ad acquisire le superfici di soggetti viventi (e cadaveri non in stato di decomposizione) e dei reperti scheletrici non alterati gravemente da eventi tafonomici. I reperti scansionati costituiscono un importante archivio virtuale, utilizzato per diversi studi: tra il materiale scansionato vi sono 24 calchi di sinfisi pubiche e 19 superfici auricolari di una collezione archeologica che sono stati utilizzati per verificare la riproducibilità delle scansioni con l'utilizzo di 3 diversi tipi di Laser Scanner **(capitolo 3)**. È importante sottolineare che le performance dei Laser non sono comparabili esclusivamente dall'accuratezza indicata dal costruttore in quanto vi sono variabili (dalla luce nel momento dell'acquisizione, all'angolo di ripresa, alla distanza tra oggetto e scanner) che possono influire sulla qualità della scansione. Lo studio condotto ha dimostrato la riproducibilità delle aree acquisite con differenti Laser che, se sovrapposte, differiscono di una percentuale che varia tra lo 0.3% e il 2.4%.

La tecnologia Laser Scanner si è rilevata la più adatta e veloce per acquisire crani e mandibole sui cui condurre studi relativi al profilo biologico e all'identificazione personale. I modelli 3D acquisiti tramite Laser Scanner sono stati utilizzati per testare una tecnica di sovrapposizione cranio-facciale computer-assistita non automatica **(capitolo 4)**. I risultati ottenuti indicano che l'uso del modello 3D del cranio facilita il processo di sovrapposizione rendendolo molto più veloce, tuttavia, per quanto concerne l'affidabilità del metodo, la persistenza di un'alta percentuale di falsi positivi rivela che la tecnica di sovrapposizione cranio-facciale non deve essere utilizzata per identificare ma è più idonea come tecnica di esclusione.

I modelli di cranio e mandibola 3D acquisiti con Laser Scanner sono stati testati come base per condurre ricostruzioni facciali in ambiente virtuale **(capitolo 8.2)** Attraverso l'utilizzo di un nuovo software in fase di sperimentazione (TIVMI-AFA3D) si è valutata l'effettiva capacità del software di riprodurre volti a partire da modelli 3D e si è testata la riproducibilità della ricostruzione facciale ottenuta tra due inter-operatori su quattro crani, di cui si era in possesso dell'immagine del soggetto in vita. Le ricostruzioni facciali compiute dagli inter operatori sono state confrontate tramite una mappa colorimetrica che ha rilevato buona omogeneità in termini morfometrici su regioni del volto precise (massiccio facciale, guance e tempie), ma discrepanze in corrispondenza dei rami mandibolari e nella regione frontale, epifrontale e dell'orecchio. Le discrepanze tra le coppie di ricostruzioni facciali sono dovute in parte alla diversa collocazione di alcuni landmarks operata dai due operatori, in parte alla carenza di landmarks nella regione frontale e dell'orecchio. L'impossibilità di condurre ricostruzioni di volti che mostrano i denti (elementi di grande importanza identificativa) risulta il principale limite della metodica sperimentata; testare la riproducibilità del metodo attraverso software dotati di mappe colorimetriche che confrontino i modelli 3D dei volti ottenuti costituisce un vantaggio oggettivo per controllare e quindi migliorare la metodica virtuale.

Nel corso di questa ricerca si è potuto riscontrare come la tecnologia Laser Scanner sia adatta per condurre acquisizioni sia su scavo e sia singoli reperti scheletrici in laboratorio grazie alla trasportabilità dello strumento unito all'alta qualità delle acquisizioni che esso produce. Tuttavia tale tecnologia ha il limite "intrinseco" di poter acquisire solamente superfici, non può rivelare nulla di ciò che è all'"interno" dell'elemento che si sta acquisendo. Nello studio condotto per la determinazione dell'età a partire da volumi dentari (**capitolo 8.1)** era necessario acquisire sia il volume esterno del dente sia il volume della camera pulpare, ci si è rivolti pertanto a una recente tecnologia TAC in grado di acquisire l'esterno e la struttura interna di reperti di piccole dimensioni (con accuratezza sub millimetrica): la CT Cone Beam. Tramite l'utilizzo di un software gratuito (OsiriX) è stato possibile ottenere i volumi necessari per poter calcolare il rapporto tra i due volumi e svolgere lo studio della regressione. Il coefficiente di correlazione e di determinazione sono paragonabili a quelli condotti da altri autori con strumentazioni più costose (in particolare con software a pagamento), l'equazione ricavata mostra tuttavia ancora scarsa precisione nella stima dell'età.

La CBCT è una metodologia che si è rilevata utile anche nell'ambito dell'indagine di lesività, ambito in cui il Laser Scanner si rivela non idoneo se utilizzato per acquisire lesioni che intaccano in profondità la superficie ossea (lesioni d'arma bianca) e lesioni pregresse e in via di guarigione (lesioni antemortem). È stato condotto uno studio su lesioni da punta e taglio prodotte in laboratorio

su osso spugnoso e corticale acquisite con CBCT **(Capitolo 5)**. Benché su osso corticale non siano stati conseguiti risultati soddisfacenti, su osso spugnoso sono state ottenute ottime riproduzioni tridimensionali delle lesioni ed è stato proposto un metodo per l'analisi differenziale tra lesioni monotaglienti e bitaglienti.
In un caso reale di antropologia forense, in cui la vittima è stata attinta con un colpo d'arma bianca sul corpo della prima vertebra cervicale, è stata invece testata per la prima volta in ambito forense la Tomografia Computerizzata Quantitativa periferica (peripheral Quantitative Computed. Tomography, *pQCT*), ottenendo la ricostruzione tridimensionale della lesione e della porzione "mancante" dell'osso, ricostruzione, questa, che permette di risalire alla forma della lama **(capitolo 6)**. Per quanto concerne la lesività antemortale la tecnologia CBCT è risultata efficace nella valutazione della struttura interna dei calli ossei **(capitolo 7),** valutazione utile nella datazione di una frattura pregressa.

In conclusione, la ricerca condotta ha confrontato tecnologie tridimensionali diverse cercando di verificarne le potenzialità e i limiti, proponendo una "guida" utile alla scelta delle metodiche 3D disponibili in base all'ambito antropologico a cui ci si rivolge, nella consapevolezza che le tecnologie digitali sono comunque in continuo, e vivace, sviluppo. Nella consapevolezza, infine, che le metodiche illustrate non possono in alcun modo sostituire il giudizio critico dell'operatore: come disse qualcuno, il telescopio non avrebbe scoperto nulla, se non c'era Galileo a guardarci dentro.

Appendice

Lista delle pubblicazioni

Riviste nazionali NON –ISI:

"Le indagini antropologiche alta mortalità infantile e popolazione disagiata"

Mazzucchi, Sguazza, Steffenini, Gaudio, Cattaneo

In "Il Capitolium di Brescia. Mille anni di storia (II seca.c-VII sec d.C); pp 487-495

Riviste internazionali ISI:

Does high tech ct actually ameliorate stab wound analysis in bone?"
Gaudio D , Digiancamillo M, Gibelli D., Galassi A, Cattaneo C.
International Journal of Legal Medicine
127 Volumes 604 Issues, 2013.

The application of cone-beam CT in the aging of bone calluses: a new perspective?
A. Cappella, A. Amadasi, D. Gaudio, D. Gibelli, S. Borgonovo, M. Di Giancamillo, C. Cattaneo
International Journal of Legal Medicine
127 Volumes 604, 2013

"Excavation and study of skeletal remains from a World War I Mass Grave."
Gaudio D., Betto A., Vanin S., De Guio A., Galassi A., Cattaneo C.
International Journal of Osteoarchaeology
(In stampa, pubblicazione online: 8 Aug 2013)

The difficult task of assessing perimortem and postmortem fractures on the skeleton: a blind test on 210 fractures of known origin.
Cappella Annalisa, Amadasi, Alberto, Castoldi Elisa, Mazzarelli Debora, Gaudio Daniel, Cattaneo Cristina;
Journal of Forensic Sciences (Accettato Settembre 2013)

Monografie:

-"L'archeologia forense: il corretto recupero dei corpi sepolti"
Gaudio, Gibelli, Poppa, Galassi, Sala, Salsarola, Cattaneo.
-"La ricostruzione delle dinamiche"
Galassi, Gaudio, Sgrenzaroli Vassena,.
In: Le investigazioni sulla Scena del Crimine, di Curtotti e Saravo, G.Giappichelli Editore, Torino, 2013.

Ringraziamenti

Il primo ringraziamento è rivolto alla Prof. Cattaneo per il costante appoggio in questi tre anni ma anche negli anni precedenti. Per avermi lasciato libertà e indipendenza. Ringrazio anche il Dottor Galassi per l'elasticità che ha dimostrato nel primo anno, in cui non era facile far incastrare i vari impegni. Grazie a tutta la vecchia guardia del Labanof che ho ritrovato (Porta, Pas, Danilo, Mazzu, Gibi) e la nuova guardia, che ho conosciuto, nella convinzione che siete il presente ma anche il futuro (Mazza, Sguazza, Annalisa, Magli, Alberto,Valentina). Grazie alle varie persone con cui mi sono confrontato e incrociato numerose volte in questi anni (Nicola Guercini, Chiara Villa, Analia, Pierre, Marco Caccianiga, Chiara Compostella e tutti quelli che sto dimenticando). Grazie anche a Lara, Lisa e Marco. Agli amici che mi hanno supportato e sopportato (Marco Dell'Aquila, ancora Nicola, Mauro, Mel, Paolo, Barbara Wanda,Vito, Matteo, Erika, Manuel, Q, Nilo). Grazie alla mia vecchia auto per non avermi mai abbandonato in A4, ma grazie soprattutto ai miei per il costante supporto, nonostante le grandi difficoltà di questi ultimi anni. Infine grazie a Elena per tutto quello che fai, per aver pazientato nel corso delle mie assenze, per avermi incoraggiato in tutti i modi, per la stabilità che mi hai dato, e che spero un giorno potrò ricambiare.